Fluid-Mineral Interactions: A Tribute to H. P. Eugster
© The Geochemical Society, Special Publication No. 2, 1990
Editors: R. J. Spencer and I-Ming Chou

Normative analysis of groundwaters from the Rustler Formation associated with the Waste Isolation Pilot Plant (WIPP), southeastern New Mexico

MARC W. BODINE, JR.† and BLAIR F. JONES
U.S. Geological Survey, MS 432 National Center, Reston, Virginia 22092, U.S.A.

Abstract—Salt norms and simple salt assemblages have been calculated for 124 water analyses from the three aquifers of the Ochoan Series of the Rustler Formation of Permian age (plus four analyses from overlying strata) at and near the Waste Isolation Pilot Plant (WIPP) in southeastern New Mexico. The results indicate that Rustler Formation waters range from hypersaline, primitive-diagenetic fluids, probably synsedimentary, to meteoric recharge waters. The distribution of normative halite in the aquifer fluids is compatible with zones that describe the extent of halite dissolution in the Rustler Formation. Recharge waters have entered the Rustler aquifers through overlying strata and/or laterally. Their norms reflect negligible to extensive resolution of Rustler or Permian Age Salado Formation halite, pervasive resolution of calcium sulfate in the Rustler Formation throughout the region, and silicate hydrolysis of framework minerals in clastic sediments within and above the Rustler.

The salt norms indicate (1) small, apparently isolated areas of the Culebra and Magenta Dolomite aquifers in the Rustler Formation contain primitive-diagenetic fluid residuals because of very low formational transmissivity; (2) within most areas of the Rustler Formation that are not overlain by halite, extensive infiltration of recharge waters into the Magenta, Culebra, and Rustler-Salado contact zone aquifers is correlative with normative sulfate content; (3) much of the halite resolution effected by Rustler-Salado contact zone waters has taken place in uppermost Salado Formation halites; (4) mixtures of primitive-diagenetic solutes with alkali sulfate-bearing recharge can produce NaCl-rich norms without halite dissolution; and (5) normative alkali sulfate content can be related to the ground-water flux from overlying continental (siliciclastic) sediment.

The large variation in hydrologic properties of the extensively studied Culebra Dolomite aquifer is emphasized by the diversity in normative results. In addition, the flow field simulations presented by DAVIES (1989) are reflected in the areal distribution of normative compositions. Interpretation of the norms is consistent with the north-to-south flow direction and velocities in the model, and is compatible with paleo-recharge from the Nash Draw area to the north and west of the WIPP site.

INTRODUCTION

AN UNDERSTANDING of the evolution and hydrodynamics of ground waters in salt beds at the Waste Isolation Pilot Plant (WIPP) in the Delaware Basin in southeastern New Mexico is essential for developing the technology to assure effective containment of long-lived nuclear waste. The groundwaters occur in several geologic horizons above and below the waste facility and exhibit a wide range of compositions, origins, and flow regimes that are currently being investigated by a variety of techniques in several laboratories.

We propose that recasting a water's chemical composition into a "salt norm" (BODINE and JONES, 1986) is a useful diagnostic tool in this effort. The salt norm is the idealized equilibrium assemblage of mineral salts at surficial conditions that is quantitatively equivalent to the solute concentrations in the water. The salt norm can be envisioned as the assemblage of salts that would have precipitated from the evaporated water sample and would be in equilibrium with the last vestage of remaining water. The normative assemblage yields a diagnostic chemical-mineralogical characterization of the water, aids in the interpretation of the origin of the water's solutes, is indicative of the character of water-rock interaction in subsurface environments, and may contribute to determining the evolutionary path of the water chemistry.

In this report, after a brief review of the calculation of the salt norm and the criteria for its interpretation, we present salt norms for 124 analyses of groundwaters from the Rustler Formation and 4 analyses of groundwaters from overlying strata from the WIPP-site region and discuss their use in characterizing the waters and indicating their origin and evolution.

THE SALT NORM

Presenting a water's dissolved constituents as neutral salt abundances is not new. In the nineteenth century it was the accepted practice to report water compositions in terms of abundances of simple salts. As HEM (1970) pointed out, this practice predated acceptance of the Arrhenius concept of dissociated ions, and although it also attempted to express water compositions in terms of the salts produced upon evaporation, it was actually more closely related to classical gravimetric analytical procedures

† Deceased.

with minimal regard to salt speciation and association. It is not surprising then, that this form of expressing water composition diminished in the twentieth century with only occasional use for specific purposes in the more recent literature either by forming assemblages of simple salts (RANKAMA and SAHAMA, 1950, p. 318) or attempts at forming reasonable associations of mineral salts (LAMBERT, 1978).

The striking differences in salt mineral assemblages in marine and nonmarine evaporite deposits are clearly indicative of both lithologic origin and subsequent geochemical evolution for the dissolved constituents (EUGSTER and JONES, 1979; EUGSTER *et al.*, 1980). Thus it is informative to reconstruct solute content of a natural water into the equilibrium salt assemblage to be obtained if the water evaporated to dryness under earth surface conditions.

The salt norm is analagous to the CIPW norm (CROSS *et al.*, 1902) which is an idealized equilibrium assemblage of igneous minerals that is calculated from the rock's chemical composition. The CIPW norm has proved useful in igneous petrology not only for characterizing and classifying igneous rocks but for providing invaluable quantitative data for rigorous interpretation of the origin and evolution of an igneous complex. We suggest similar advantages for the salt norm in characterizing natural waters and interpreting their chemical evolution. Characterization of a water composition as a salt norm is more detailed and more suggestive of solute origin and subsequent interaction than major cation-anion predominance that is currently the most commonly utilized system of hydrochemical classification.

Calculation of the salt norm

The salt norm is calculated with the computer program SNORM (BODINE and JONES, 1986) and this discussion will be limited to the program's major features. The program computes the norm by quantitatively assigning up to 18 solutes (Table 1) into the equilibrium assemblage of salts obtained from a list of 63 normative salts (Table 2). SNORM computes the normative assemblage directly from the solute matrix without proceeding along a succession of reaction paths. The salt norm characterizes a natural water's composition and indirectly indicates solute source

Table 1. Solutes in water analyses assigned to normative salts

	Cations		Anions	
Major	Mg^{2+}	Na^{+}	Cl^{-}	HCO_3^{-}
	Ca^{2+}	K^{+}	SO_4^{2+}	CO_3^{2-}
Minor	Li^{+}	Sr^{2+}	Fl^{-}	NO_3^{-}
	NH_4^{+}	Ba^{2+}	*Br^{-}	†B
			*I^{-}	PO_4^{3-}

* Assigned as solid solution to chloride normative salts.

† Recast as borate with assignment of a preliminary charge of $-^{7}/_{12}$ per boron, that is, the artificial borate ion $(BO_{1.79})^{-7/12}$; if feasible, reassigned the charge per boron appropriate for the borate stoichiometry of the borate salt in the normative assemblage (see BODINE and JONES, 1986).

Table 2. Chemical formula of the normative salts

Ammonia niter	NH_4NO_3
Anhydrite	$CaSO_4$
Antarcticite*	$CaCl_2 \cdot 6H_2O$
Aphthitalite*	$K_3Na(SO_4)_2$
Arcanite*	K_2SO_4
Barite	$BaSO_4$
Bischofite*	$MgCl_2 \cdot 6H_2O$
Bloedite*	$Na_2Mg(SO_4)_2 \cdot H_2O$
Borax	$Na_2B_4O_7 \cdot 10H_2O^{+}$
Burkeite*	$Na_6CO_3(SO_4)_2$
Calcite*	$CaCO_3$
Carnallite*	$KMgCl_3 \cdot 6H_2O$
Celestite	$SrSO_4$
Dolomite*	$CaMg(CO_3)_2$
Epsomite*	$MgSO_4 \cdot 7H_2O$
Fluorapatite	$Ca_5(PO_4)_3F$
Fluorite	CaF_2
Glauberite*	$Na_2Ca(SO_4)$
Gypsum	$CaSO_4 \cdot 2H_2O$
Halite*	$NaCl$
Hydroxyapatite	$Ca_5(PO_4)OH$†
Indirite	$Mg_2B_6O_{11} \cdot 15H_2O$**
Inyoite	$Ca_2B_6O_{11} \cdot 13H_2O$**
Kainite*	$KMgClSO_4 \cdot 3H_2O$
Kalicinite*	$KHCO_3$
Kieserite*	$MgSO_4 \cdot H_2O$
Leonite*	$K_2Mg(SO_4)_2 \cdot 4H_2O$
Magnesite*	$MgCO_3$
Mascagnite	$(NH_4)_2SO_4$
Mirabilite	$Na_2SO_4 \cdot 10H_2O$
Niter	KNO_3
Nitrobarite	$Ba(NO_3)_2$
Nitrocalcite	$Ca(NO_3)_2$
Nitromagnesite	$Mg(NO_3)_2$
Picromerite*	$K_2Mg(SO_4)_2 \cdot 6H_2O$
Pirssonite*	$Na_2Ca(CO_3)_2 \cdot 2H_2O$
Polyhalite*	$K_2Ca_2Mg(SO_4)_4 \cdot 2H_2O$
Salammoniac	NH_4Cl
Sellaite	MgF_2
Soda niter	$NaNO_3$
Strontionite	$SrCO_3$
Sylvite*	KCl
Syngenite*	$K_2Ca(SO_4)_2 \cdot 2H_2O$
Tachyhydrite*	$Mg_2CaCl_6 \cdot 12H_2O$
Teschemacherite	NH_4HCO_3
Thenardite*	Na_2SO_4
Trona*	$Na_3H(CO_3)_2 \cdot 2H_2O$
Ulexite	$NaCaB_5O_9 \cdot 8H_2O$**
Villiaumite	NaF
Wagnerite	Mg_2PO_4F
Witherite	$BaCO_3$
—	$BaCl_2 \cdot H_2O$
—	$BaCl_2 \cdot 2H_2O$
—	$LiCl \cdot H_2O$
—	Li_2CO_3
—	LiF
—	$LiNO_3 \cdot 3H_2O$
—	$Li_2SO_4 \cdot H_2O$
—	$Mg_3(PO_4)_2$
—	Na_3PO_4
—	$SrCl_2 \cdot 2H_2O$
—	$SrCl_2 \cdot 6H_2O$
—	$Sr(NO_3)_2$

*Diagnostic major cation and anion salt (gypsum and mirabilite omitted because their respective hydration equilibria preclude chloride or nitrate in the water).

† Normative hydroxyapatite calculated as $Ca_{4.75}(PO_4)_{3.17}$ in order to preserve charge balance.

** Stoichiometry of borate salts modified if norm calculated with average borate charge of $-^{7}/_{12}$ per boron (see BODINE and JONES, 1986).

and chemical evolution of the water; no direct information on reaction paths or extent of mineral saturation for an individual water sample is given by SNORM.

Solutes

The solutes (Table 1) were selected to comply with two criteria: (1) the solute, at least occasionally, occurs in natural waters in more than negligible (trace) concentrations; and (2) the solute forms its normative salt(s) through direct combination with other solutes in the analysis without interacting with the aqueous environment or requiring any chemical or charge modification. Thus, neither pH nor redox enter directly into the SNORM calculations. Only boron, which is reported as the element in conventional water analyses, fails to comply with these criteria. In SNORM boron is recalculated as borate and contributes to the total anion charge of the analysis.

Total cation equivalency must equal total anion equivalency in order to assign all solutes to neutral salt species. This is accomplished in SNORM by proportioning all cation and anion concentrations in the analysis to yield neutral charge balance. The deviation of the cation and anion proportionation factors from unity is a measure of the completeness and accuracy of the water sample analysis.

Normative salts

SNORM forms the salt norm from a list of 63 permissable normative salts (Table 2). Most of the salts occur as minerals and are thermodynamically stable at 25°C, 1 bar total pressure, and atmospheric partial pressure of carbon dioxide ($10^{-3.5}$ bars) at the water activity imposed by the salt assemblage.

After SNORM establishes the maximum number of phases in the assemblage with the Gibbs phase rule, the salt norm is calculated by assigning the solutes to the single assemblage that quantitatively consumes all solutes and contains no unstable salt associations. The unstable salt associations have been determined with free energy minimization reactions. Where thermodynamic data were lacking, mineral associations in surficial assemblages and analogy with relations in similar equilibria were used to estimate unstable associations.

Interpretation of the salt norm

Characterization and interpretation of the salt norm relies almost exclusively on the major cation-major anion salts in the norm (those salts denoted with an asterisk in Table 2) although salts of minor solutes are included in the norm. Throughout this report we express normative salt relative abundances as their *anhydrous weight percentages* in the salt norm. Anhydrous weight percentage of the normative salt excludes waters of hydration in the salt's formula from the salt's weight in calculating relative abundance and such normative abundances more closely reflect solute proportions.

Because the salt norm relates water composition to the relative abundances of both cations and anions, one or more of the key salts in the salt norm more fully characterizes water composition than does cation or anion predominance. Thus, the designation of a water sample as a "tachyhydrite water" is more explicit than its designation as a "chloride-rich water." Even more importantly, the norm, both qualitatively and quantitatively, is indicative of solute source and the character of water-rock interactions that occurred during the water's evolution.

To that end BODINE and JONES (1986) developed a diagnostic chart (Fig. 1) relating the occurrence of normative salts to solute source and chemical evolution of the water. Three major categories of solute sources are recognized: a meteoric source in which the waters derive their solutes through surficial weathering processes; a marine source that, with or without modification, reflects a dominant sea water origin; and a diagenetic source in which the solutes reflect substantial rock-water interaction. In Table 3 we have compiled a representative group of salt norms from BODINE and JONES (1986) that illustrate the major features of Fig. 1.

Meteoric norms

Norms for meteoric waters characteristically contain alkali-bearing sulfate or carbonate normative salts (Fig. 1). Dissolution of soluble minerals (such as calcite and other carbonates, gypsum, and halite), contamination by anthropogenic constituents, or introduction of aerosol often contribute an appreciable fraction of the solutes in meteoric waters. However, it is the hydrolysis reactions involved in the weathering of silicate rocks that generate the most diagnostic features in the norms of meteoric water. Alkali-bearing carbonate salts in the norm reflect atmospheric carbon dioxide-water interaction forming carbonic acid and accompanying hydrolysis of silicate minerals. Alternatively, alkali-bearing sulfate salts in the norm reflect sulfide mineral oxidation forming sulfuric acid with consequent hydrolysis of silicate minerals.

Salt speciation and abundance in the norm frequently permits more detailed interpretation (Fig. 1). Although the norms in Table 3 include but four of the many examples comparing the character of the norm of meteoric waters with the weathering processes and host lithologies that are in BODINE and JONES (1986), they illustrate some important diagnostic features. The trona-burkeite abundance in the Arizona norm (Table 3, no. 1) illustrates extensive carbonic acid hydrolysis during the weathering of an Na-rich silicate host. Anhydrite-epsomite-bloedite in the Sudbury norm (Table 3, no. 3) reflect sulfuric acid hydrolysis of mafic rocks, whereas thenardite-glauberite in the Virginia norm (Table 3, no. 2) characterize similar weathering of a granite rock. The abundant halite in the Yilgarn norm (Table 3, no. 4) most likely reflects halite dissolution that practically overwhelms but does not obliterate the indicators (polyhalite-leonite) of sulfuric acid hydrolysis.

Marine norms

Sea water has a characteristic halite-bischofite-kieserite-carnallite-anhydrite norm (Table 3, no. 5) with the magnesium chloride association as represented by the bischofite-carnallite pair in the norm as the single unique diagnostic feature. It is difficult to attribute this association ultimately to any other than a marine source, though there may have been subsequent continental recycling (BODINE and JONES, 1986).

Only a few subsurface waters (other than those in the immediate vicinity of a marine source) yield norms quantitatively similar to that for sea water. This is not unex-

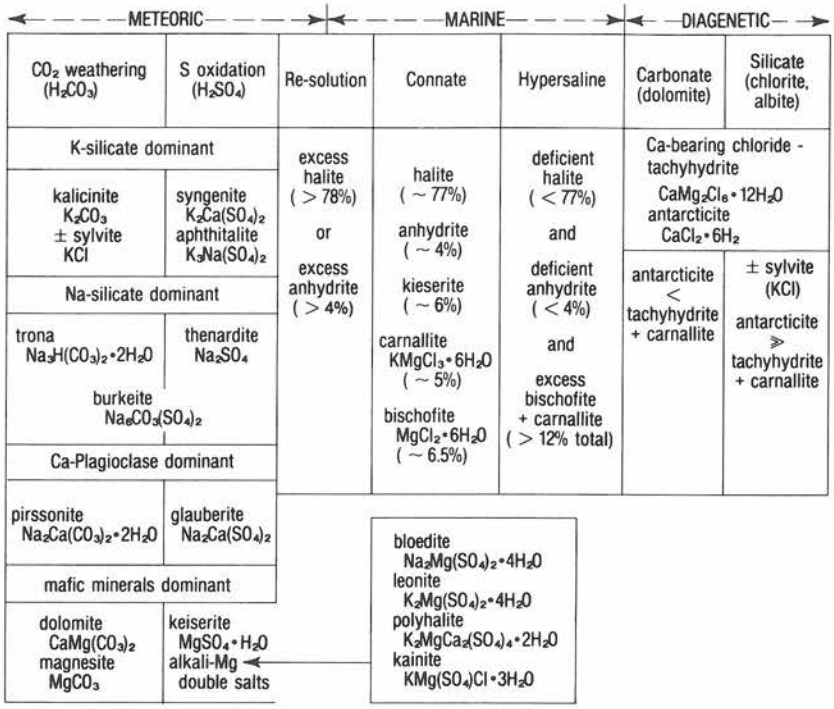

FIG. 1. Diagnostic chart for normative salts from BODINE and JONES (1986).

pected. Mixing, continental cycling, and water-rock interaction, including resolution of marine evaporite salts, can be expected not only to produce quantitative variations among the sea water normative minerals but to qualitatively modify the normative mineralogy, as in many cases reviewed by BODINE and JONES (1986). As one example of the latter, a connate marine groundwater mixing with a meteroic water bearing normative alkali sulfates can eliminate bischofite and generate sylvite or kainite in the norm as magnesium becomes associated with sulfate rather than chloride. The presence of polyhalite in an otherwise marine-like norm provides an even stronger indication of marine-meteoric water mixing.

Surface brines that have evolved through fractional precipitation of calcium sulfate, halite, or even the bitter salts yield norms qualitatively identical to sea water but quantitatively distinct (Fig. 1). The salt norm of a Black Sea evaporite brine sampled at the early states of magnesium sulfate deposition (Table 3, no. 6) illustrates the pronounced relative enrichment of bischofite, carnallite, and kieserite in the norm with a corresponding decrease of halite. Subsurface waters from a marine evaporite source are subject to similar modifications as subsurface marine waters; however, elimination of the bischofite or bishofite-carnallite signature from the norm becomes less likely.

Diagenetic norms

The presence of calcium-bearing chloride minerals, tachyhydrite and antarcticite (Table 2), in the salt norm is indicative of solute diagenesis (Fig. 1). Nearly all such norms in BODINE and JONES (1986) were obtained from subsurface fluids associated with deep sedimentary basins, highly saline strata, or crystalline shield areas, and are most readily interpreted as evolving through the exchange of magnesium and sodium in solution for calcium in the solid phase. Because of the relatively low solubility of calcium sulfate, the abundance of normative sulfate salts becomes vanishingly small as calcium-bearing chlorides increase.

In carbonate rocks the exchange of magnesium in solution for calcium in the solid phase primarily reflects dolomitization. The extent of the exchange is limited by the Ca/Mg concentration ratio for the calcite-dolomite equilibrium. Although affected by aqueous calcium and magnesium ion activity coefficients, temperature, and mineralogy of the carbonate species, the Ca/Mg ratio, reflected in the norm by the antarcticite to tachyhydrite ratio, is not expected to greatly exceed unity (maximum of about 4?) due to dolomitization alone. For example, the norm of a marine evaporite brine associated with extensive recent dolomitization from the north Sinai (Table 3, no. 7) contains abundant tachyhydrite with only minor antarcticite.

Alternatively, in silicate rocks the exchange of magnesium and sodium in solution for calcium in plagioclase and Ca-bearing mafic minerals, reflecting albitization and chloritization, can proceed much farther than similar exchanges accompanying dolomitization, particularly because of the decrease in solubility of magnesium silicate at moderately elevated temperatures. For example, magnesium salts are nearly absent in the halite-antarcticite norm of a Sudbury mine water in crystalline rocks (Table 3, no. 8).

Graphic representation of the salt norm

A simplified representation of the salt norm for graphic display on maps has led to the definition of the "simple-

Table 3. Examples of salt norms (anhydrous weight percent) of waters representing various paths of solute evolution selected from BODINE and JONES (1986)

	1	2	3	4	5	6	7	8
TDS	477 mg/kg	905 mg/kg	4,280 mg/l	227,000 mg/l	35,150 mg/kg	309,200 mg/kg	275,500 mg/kg	241,000 mg/l
Salt norm								
Calcite	—	7.4	—	—	—	—	—	—
Dolomite	0.9	4.5	—	—	—	—	<0.1	—
Magnesite	0.4	—	3.4	<0.1	0.3	—	—	—
Trona	60.2	—	—	—	—	—	—	—
Burkeite	31.4	—	—	—	—	—	—	—
Anhydrite	—	—	40.8	—	4.0	—	0.2	0.1
Kieserite	—	—	—	—	6.1	26.1	—	—
Epsomite	—	—	28.6	4.7	—	—	—	—
Polyhalite	—	—	4.5	2.2	—	—	—	—
Leonite	—	—	—	2.5	—	—	—	—
Syngenite	—	4.7	—	—	—	—	—	—
Bloedite	—	—	18.8	—	—	—	—	—
Glauberite	—	24.9	—	—	—	—	—	—
Aphthitalite	0.3	—	—	—	—	—	—	—
Thenardite	—	52.9	—	—	—	—	—	—
Kainite	—	—	—	1.8	—	—	—	—
Halite	6.5	4.7	3.7	88.7	78.1	30.8	35.0	19.0
Sylvite	—	—	—	—	—	—	—	0.1
Carnallite	—	—	—	—	4.9	19.3	0.1	<0.1
Bischofite	—	—	—	—	6.5	23.7	—	—
Tachyhydrite	—	—	—	—	—	—	58.9	—
Antarcticite	—	—	—	—	—	—	5.8	79.7

1. Meteoric groundwater evolved chiefly through carbonic acid hydrolysis of sodium-rich silicate rocks, Navaho Sandstone, Mexican Water, Arizona (WHITE *et al.*, 1963).

2. Meteoric groundwater evolved chiefly through sulfuric acid hydrolysis of Paleozoic granite, Chester, Virginia (WHITE *et al.*, 1963).

3. Meteoric groundwater evolved chiefly through sulfuric acid hydrolysis of mafic igneous rocks, Sudbury area, Ontario (FRAPE *et al.*, 1984).

4. Meteoric groundwater evolved chiefly through resolution of marine solutes (halite) diluting sulfuric acid hydrolysis effects, Yilgarn Block, Western Australia (MANN, 1983).

5. Normal sea water (RILEY and CHESTER, 1971).

6. Marine evaporite brine at initial deposition of magnesium sulfate, Black Sea pond, Ukraine (ZHEREBTSOVA and VOLKOVA, 1966).

7. Diagenetic water resulting chiefly from dolomitization of calcarenite, Hayareah Sabka, Bardawil Lagoon region, north Sinai (LEVY, 1977).

8. Diagenetic water most likely resulting chiefly from albitization and chloritization of crystalline rocks, North Mine, Sudbury District, Ontario (FRAPE and FRITZ, 1982).

salt assemblage" (BODINE and JONES, 1986). The simple-salt assemblage is constructed by SNORM from the salt norm through separation of each major-ion normative salt into its simple-salt components (all salts with minor solutes are omitted). For example, one mole of polyhalite (Table 2) in the norm is recalculated as 2 moles of $CaSO_4$, 1 mole of K_2SO_4, and 1 mole of $MgSO_4$. The abundance of each simple salt from its respective normative-salt sources is summed and normalized to its weight and molar percentage in the simple-salt assemblage. Each simple salt is defined with an anion charge of −2 to maintain consistency throughout an array of simple salts; this results in molar units of the alkali chlorides being expressed as Na_2Cl_2 and K_2Cl_2. Twelve different simple salts are recognized: the carbonates (bicarbonate in normative salts is recast as carbonate), the sulfates, and the chlorides (chloride includes any bromine and iodine as if in solid solution) of each major cation, including calcium, magnesium, potassium, and sodium.

Graphic display of the sample salt abundances is formatted as a rose diagram in which the circle is divided into twelve 30 degree segments with each segment representing a specific simple salt (Fig. 2A). We have arranged the simple salts on the diagram with the sulfates occupying the upper third of the circle, the carbonates occupying the lower left third, and the chlorides occupying the lower right third. The three anion groups are separated by radial boundary lines on the rose diagram. The salts within each anion group are sequentially arranged in terms of their respective relative solubilities. For example, calcium sulfate, the least soluble of the sulfates, occupies the rightmost segment in the sulfate area and is followed from right to

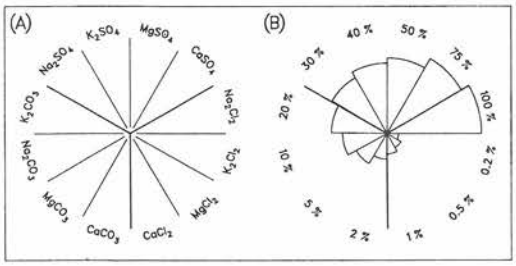

FIG. 2. The simple-salt rose diagram: A. Location of simple-salt segments on the rose diagram. B. Relative scale of segment radii as a function of the cube root of the salt's weight or mole fraction in the assemblage.

left by Mg_2SO_4, then K_2SO_4, with Na_2SO_4, the most soluble of the sulfates, in the leftmost segment of the sulfate group.

The radius of each segment of the rose is a function of that salt's relative molar or weight abundance in the simple-salt assemblage. Because the more diagnostic salts commonly have low abundance we have adopted the convention of equating segment radius to the cube root of the salt's fraction in the assemblage (Fig. 2B), recognizing that small-to-moderate differences in abundance above 25 percent will not be readily apparent.

Fig. 3 contains the simple-salt rose diagrams illustrating the variations of the salt norms for the array of waters in Table 3. Most full salt norm features that characterize these waters are preserved in the simple-salt assemblage.

THE WIPP SITE

The Waste Isolation Pilot Plant (WIPP) site is located 40 kilometers (25 miles) east of Carlsbad, New Mexico in an area of Eddy County referred to as Los Medanos (Fig. 4). On this and all ensuing maps the site is identified by the distinctive Zone IV boundary that formerly defined the exclusion area controlled by the Department of Energy (POWERS *et al.*, 1978). The site is in the northern part of the Delaware Basin about 10 kilometers (6 miles) south of the buried Capitan reef front. The site area has little relief and, in general, slopes gently westward. To the west of the site is the escarpment of Livingstone Ridge, which marks the eastern margin of Nash Draw, a pronounced, but broad valley trending south-southwest. The area is drained by the Pecos River, a perennial southerly flowing stream 16 kilometers (10 miles) west-southwest of the WIPP site boundary at its closest point. The land surface is partially blanketed with sand dunes and is sparsely vegetated with a northern Chihuahuan desert flora.

Geologic setting, Delaware Basin

The geology of the Delaware Basin has been extensively studied over the past half century. In addition to the recent geologic investigations of the WIPP-site area, the Delaware Basin has long been a focus of geologic interest because of its abundant fluid hydrocarbon resources, its thick and somewhat unusual marine evaporite succession containing the nation's major potash deposits, and its striking geologic features, particularly the complex reef systems culminating with the imposing Capitan reef that is so well exposed in the Guadalupe Mountains along the western margin of the basin.

In this report we rely heavily on data from POWERS *et al.* (1978), MERCER (1983), and DAVIES (1989) for our summary of WIPP-site geology and hydrology.

The Delaware Basin is a north–south elongated structural basin in western Texas and southeastern New Mexico that is 220–260 kilometers (135–160 miles) long and 120–160 kilometers (75–100 miles) wide. The stratigraphic relations are illustrated in Fig. 5. Tectonic activity other than downwarping and subsidence has been minor within the northern part of the basin giving it an intercratonic character. Subsidence of the basin began in early Pennsylvanian and continued to the end of the Permian resulting in maximum structural relief of about 6,000 meters (20,000 feet). Normal marine sediments were deposited throughout much of its depositional history, but in the latest Permian (Ochoan) Series the basin was restricted, and a thick pile of evaporite salts and associated clastics accumulated. At the WIPP site about 4,500 meters (15,000 feet) of Pennsylvanian and Permian sediments were deposited, of which the upper 1,200 meters (4,000 feet) are the Ochoan evaporite units.

The Delaware Basin has been emergent since the

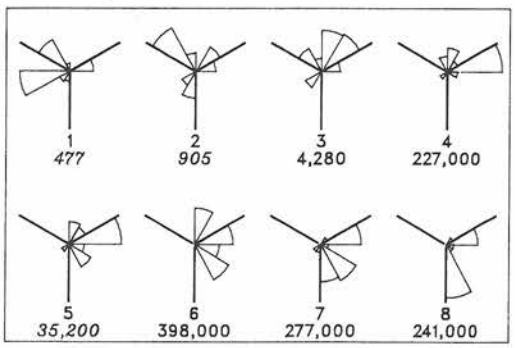

FIG. 3. Simple-salt rose diagrams of representative waters in Table 3. Identity of the segments is from Fig. 2A, segment radius proportional to the cube root of the salt's weight fraction is from Fig. 2B, and labels under each rose are the sample identification and total dissolved solids in the sample as mg/L or, if in italics, mg/kg; these specifications apply to all subsequent rose diagrams.

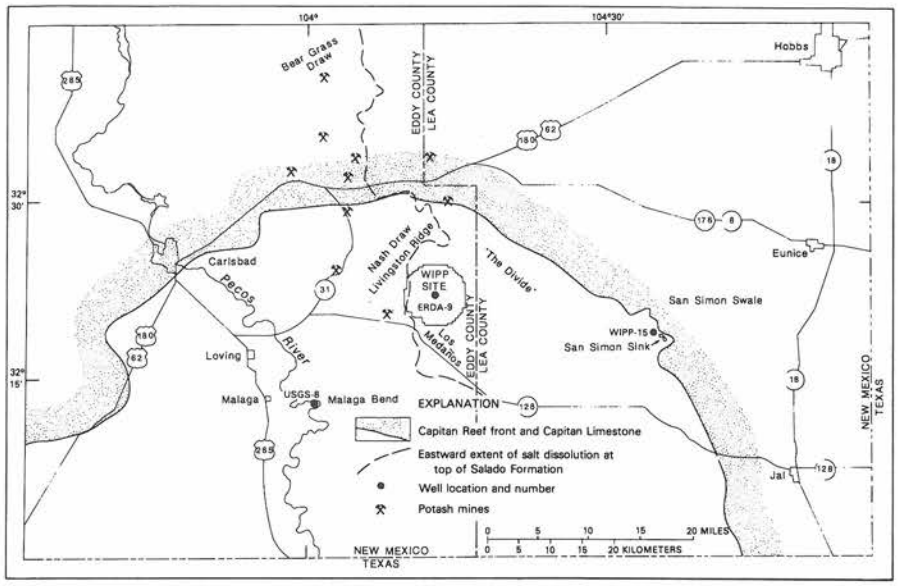

FIG. 4. Location map of the WIPP site and relevant geographic features in the northern part of the Delaware Basin, southeastern New Mexico, showing the Capitan reef front, locations of nearby potash mines, and the eastward boundary of any apparent salt dissolution in the uppermost Salado Formation from POWERS *et al.*, 1978.

Permian with only two relatively short Pre-Pleistocene depositional episodes. These sediments, Late Triassic and Miocene-Pliocene in age, are exclusively terrestrial with a total (present day) thickness of less than 150 meters (500 feet) in the WIPP-site vicinity. A discontinuous veneer of Pleistocene bolson-type deposits in channels and depressions, a Pleistocene calcrete, and nearly omnipresent recent

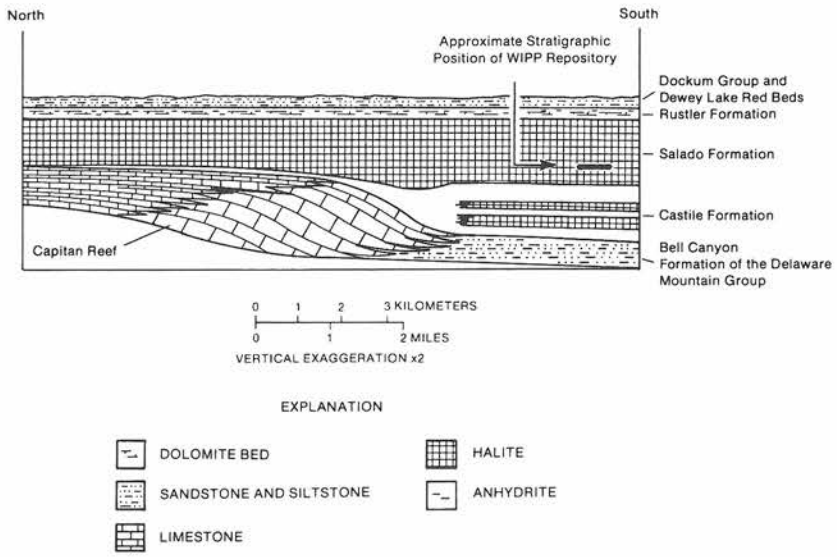

FIG. 5. Generalized stratigraphic section (from DAVIES, 1989) showing the relationships among the Guadalupian Series reef complex, the fore-reef Bell Canyon Formation of the Delaware Mountain Group (stippled), and the later Ochoan Series evaporite rocks in the Delaware Basin; along the northern and eastern segments of the Capitan reef, the Salado Formation and younger Ochoan Series rocks overlap the reef.

dune sands with minor alluvium and small playa deposits complete the depositional history of the basin.

The basin was gently tilted one or more times after the Late Triassic, resulting in a net regional dip of about 2 degrees to the east. Thus, the Capitan reef front on the western margin of the basin is well exposed and there is a west-to-east sequence of Pre-Pleistocene north–south trending outcrop belts of successively younger strata extending across the basin. Along the eastern rim of the reef the Permian Capitan Limestone is overlain by nearly a kilometer of Pre-Pleistocene strata.

Salt flowage in the Ochoan strata has resulted in the development of salt anticlines with extension and fracturing of the overlying more brittle strata at various localities throughout the basin. Dissolution and removal of salt is common throughout the basin. This process has resulted in sagging and collapse of overlying beds with concomitant fracturing and brecciation of the more brittle lithologies. Near-surface dissolution sink holes, discontinuous drainage patterns, and other geomorphic features of karst processes have developed (BACHMAN, 1985). The most conspicuous result of such processes is the formation of Nash Draw, the distinct valley to the west of the WIPP site.

Stratigraphic-geohydrologic framework of Permian units

The stratigraphic interval that is related to the WIPP facility extends from the upper Guadalupian Series water-bearing rocks immediately below the basal evaporites upward through the Ochoan Series and younger rocks. A stratigraphic summary based on core from the ERDA-9 drill hole (Fig. 4) is given in Table 4.

Inasmuch as the focus of the effort was on fluids in the Rustler Formation, only the strata above and immediately below this unit will be considered here. The description emphasizes hydrologic properties discussed in the reports of MERCER (1983) and DAVIES (1989).

Salado Formation

This formation, consisting chiefly of halite (Table 4), contains no evidence of regionally circulating water. Most drill-stem tests in the Salado yield permeability values below the sensitivity of the procedures. Some slightly higher permeabilities can be associated with anhydrite and polyhalite beds and with clay seams. Small isolated pockets of brine have been encountered during mining and drilling, as well as nonflammable pressurized gas pockets ("blowouts"). In addition, inclusion fluids are abundant in the salts throughout the formation, and in underground workings slowly accumulating brine "seeps" on the floors and "drips" from the backs are common. The only recognized groundwater circulation associated with the Salado Formation occurs at the contact with the overlying Rustler Formation.

West of WIPP site the Salado Formation is close to the land surface, and most of the soluble salts have been removed by dissolution (Fig. 4). Solution features such as sinks and karst mounds are common in the west, and within Nash Draw the uppermost Salado salts have been dissolved.

Rustler Formation

At least three well-defined aquifers occur in the Rustler Formation: the Rustler-Salado contact zone (see above), the Culebra Dolomite member, and the Magenta Dolomite member (Table 4). These are separated by varying proportions of halite, anhydrite or gypsum, and clastic beds. Halite can account for as much as 50 meters (160 feet) or more of the formation's total thickness and occurs above and below both the Culebra and Magenta aquifers. Halite dissolution in the Rustler Formation (Fig. 6) affects progressively deeper stratigraphic horizons from west to east. Only at the eastern boundary of the WIPP site is halite present throughout the formation. In the center of the site halite is present only below the Culebra aquifer. No halite is in the Rustler Formation at the western site boundary. Except in areas of obvious dissolution, such as associated with the Pecos River Valley or Nash Draw, or zones affected by secondary fracturing, there appears to be little hydrologic connection among the three aquifers.

DAVIES (1989) references several authors providing geologic evidence for halite dissolution in the Rustler and underlying Salado Formations in the vicinity of the WIPP site, and to the west. This evidence is primarily the spatial distribution of halite beds (Fig. 6) and the stratigraphic correlation of halite strata at depth in the east with mudstone beds near the land surface in the west. Further, the spatial correlation between halite dissolution and permeability in the Rustler led MERCER (1983) and others to underline the apparent causative link of the deformation accompanying dissolution with generation of secondary permeability in the Rustler Formation.

HOLT and POWERS (1988) have recently concluded that lateral variation in halite occurrence in

Table 4. Summary of the stratigraphy at the WIPP site (POWERS *et al.*, 1978)

Formation		Thickness meters (feet)
	RECENT	
Surficial sands	Blanket sands; chiefly dune sand, some alluvium and playa deposits.	0–30 (0–100)
	PLEISTOCENE	
Mescalero caliche Gatuña Formation	Hard, white crystalline caliche (limestone) crust. Pale reddish brown, fine grained, friable sandstone.	0–10 (0–35)
	UPPER TRIASSIC	
Santa Rosa Sandstone	Pale red to gray, crossbedded, arkosic nonmarine medium- to coarse-grained friable sandstone; preserved only in eastern half of site.	0–75 (0–250)
	PERMIAN-OCHOAN	
Dewey Lake Redbeds	Uniform dark red-brown marine mudstone and siltstone with interbedded very fine-grained sandstone; thins westward.	30–170 (100–550)
Rustler Formation[1]	Gray, gypsiferous anhydrite with siltstone interbeds in upper part; reddish-brown siltstone or very fine silty sandstone in lower part, halitic throughout. Contains two dolomite marker beds: Magenta in upper part and Culebra in lower part. Thickens eastward due to increasing content of undissolved rock salt.	85–130 (275–425)
Salado Formation[2]	Mainly rock salt (85–90%) with minor interbedded anhydrite, polyhalite, and clayey to silty clastics. Trace of potash minerals in the McNutt interval. Minor interbeds are thin and occur in complexly alternating sequences. Thickest nonhalite bed is the Cowden anhydrite. Multiple anhydrite beds are most common immediately below the Cowden and immediately above the base of the formation.	535–610 (1750–2000)
Castile Formation[3]	Thick massive units of finely laminated ("varved") anhydrite-calcite alternating with thick halite units containing thinly interbedded anhydrite. Top anhydrite unit lacks calcite interlaminations.	380± (1250±)
	PERMIAN-GUADALUPIAN	
Bell Canyon Formation[4]	Mostly light gray fine-grained sandstone with varying amount of silty and shaley interbeds and impurities. Contains considerable limestone interbeds and lime-rich intervals. Fore-reef facies of the Capitan reef system.	300± (1000±)

[1] In the ERDA-9 drill hole the Rustler Formation is 94.5 meters (310 feet) thick; the Magenta Dolomite, 7.3 meters (24 feet) thick, occurs 17.7 meters (58 feet) below the top of the formation, and the Culebra Dolomite, 7.9 meters (26 feet) thick, occurs 36.6 meters (120 feet) above the base of the formation.

[2] In the ERDA-9 drill hole the Salado Formation is 602 meters (1976 feet) thick; with 156 meters (512 feet) of upper member, 112.5 meters (369 feet) of McNutt potash interval, and 334 meters (1095 feet) of lower member. The Cowden anhydrite bed, 5.5 meters (18 feet) thick, occurs 84.7 meters (278 feet) above the base of the formation in the lower member.

[3] In the WIPP-site vicinity the following approximate thicknesses have been assigned to the major lithologic intervals from the base to the top of the Castile Formation: Anhydrite I—75 meters (250 feet); Halite I—100 meters (330 feet); Anhydrite II—30 meters (100 feet); Halite II—65 meters (210 feet); and the upper anhydrite interval, presumably Anhydrites III and IV (halite III is absent)—110 meters (360 feet).

[4] On approaching the margin of the basin the Bell Canyon Formation interfingers with and grades into the Capitan Limestone, the thick, up to 600 meters (2000 feet) reef lithology that virtually encircles the basin. The Capitan Limestone is a light colored, fossiliferous and vuggy limestone, dolomite, and carbonate breccia. The belt of Capitan Limestone reaches 16–23 kilometers (10–14 miles) in width along the Northwestern Shelf and is always at least 6 times as broad as thick.

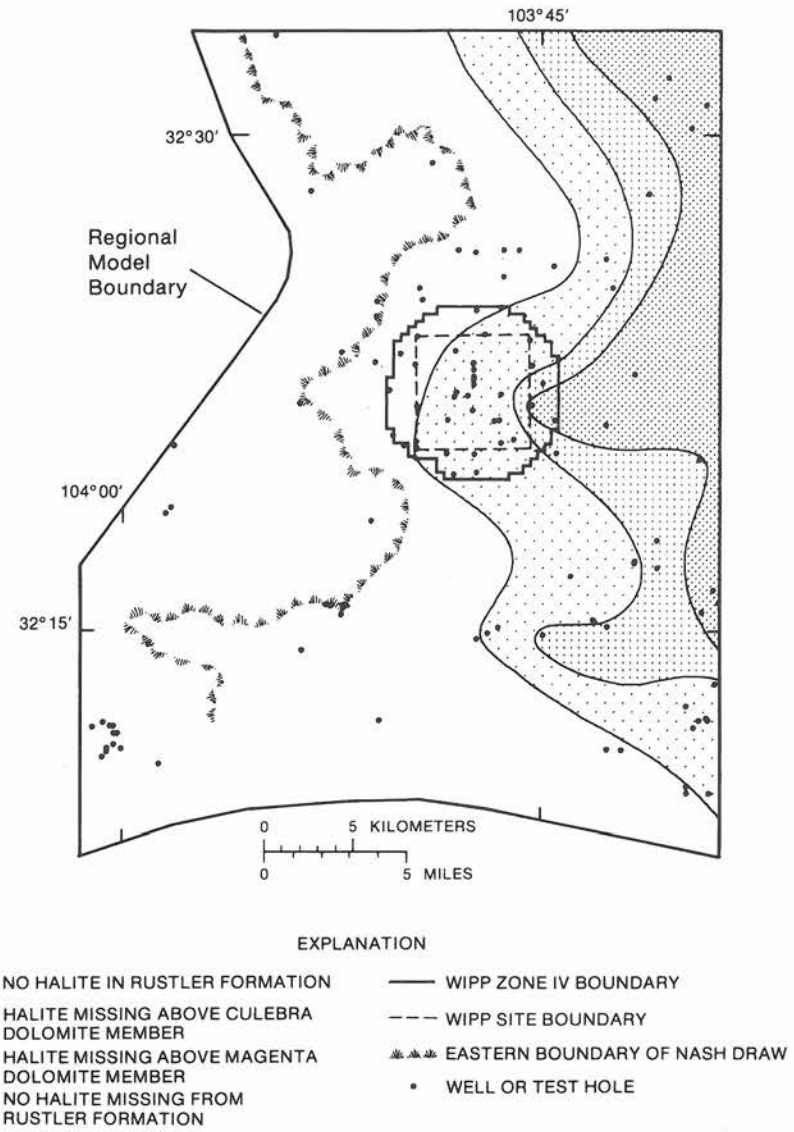

FIG. 6. Areal distribution of halite in the Rustler Formation of the WIPP site and vicinity, from MERCER (1983) and SNYDER (1985).

the Rustler formation is more the result of facies changes and syndepositional dissolution than later ground-water circulation. As DAVIES (1989) points out, if these were the only processes operative (particularly syndepositional dissolution versus later ground-water effects), other unknown mechanisms would have to be called on to produce several orders of magnitude of secondary permeability variation in the Culebra.

Certainly evaporite dissolution and related secondary processes have been active in Nash Draw, where subsidence has produced a marked valley. This feature trends north–south and has two important eastwardly trending reentrants, one to the north of the WIPP site and one to the south.

The *Rustler-Salado contact aquifer* at the WIPP site consists of a clayey dissolution residuum containing fragmental gypsum and some mudstone or siltstone. Salt associated magnesium clays of the Salado Formation have been described by BODINE (1978). The residuum thickens markedly to the west and in some exposures along the Pecos River in-

volves the entire Salado Formation. To the east of the site the residuum grades into and interfingers with its original clayey halite lithology.

Two flow regimes have been postulated for the Rustler-Salado Formation contact aquifer. To the west of the WIPP site (Fig. 7) is a region of relatively high transmissivity that was first described by ROBINSON and LANG (1938) and referred to as the "brine aquifer." They suggested it begins with a recharge area some 40 kilometers (25 miles) north-northwest of the northern WIPP-site boundary in the Bear Grass Draw area, flows southerly into the Nash Draw area, and turns southwest to discharge into the Pecos River at Malaga Bend (Fig. 7). The area of greatest permeability is associated with the residuum of the Nash Draw area, where flow is primarily through fractures and intergranular pore spaces. MERCER (1983) has confirmed the earlier reports of a well developed Rustler-Salado contact zone and brine under artesian conditions in the central and northern parts of Nash Draw. Drilling in support of the site investigations also has extended the eastern border of the "brine aquifer" across the western boundary of the WIPP site.

The second regime lies to the east of the "brine aquifer" in the WIPP-site area. Here transmissivities are low and flow rates are extremely slow if not stagnant. In this area the Rustler-Salado contact residuum is less well developed or absent, and halite in the lower part of the Rustler Formation suggests that little or no meteoric water has infiltrated directly into the Rustler-Salado Formation contact aquifer. What flow exists is primarily along bedding planes at the formational contact and in the lowermost part of the Rustler Formation. Transmissivities range from greater than 0.1 foot squared per day to the west in the "brine aquifer" to less than 0.001 foot squared per day in the east.

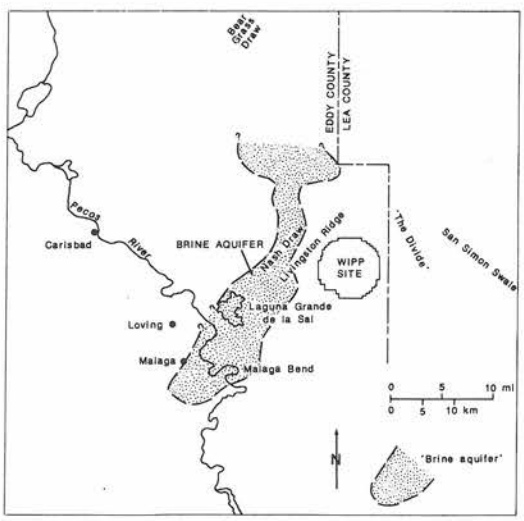

FIG. 7. Location of the "brine aquifer" from MERCER (1983).

The *Culebra Dolomite aquifer* (Table 4) is a vuggy finely crystalline dolomite that is the most persistent and productive aquifer in the WIPP-site area. Water flows through fractures in the dolomite and is confined by the overlying thick anhydrite or gypsum and the underlying clay and anhydrite. As with the Rustler-Salado contact aquifer, the principal recharge probably has come from the north, and principal discharge is at Malaga Bend. The flow path is generally southerly in the Nash Draw area.

The extent of structural deformation of the Culebra Dolomite, and thus its hydraulic properties, are related to the degree of dissolution of the enclosing evaporite strata, which varies considerably throughout the WIPP-site vicinity. Where the Rustler Formation has been subjected to considerable anhydrite/gypsum dissolution, as in Nash Draw and vicinity, the Culebra aquifer has been fractured and broken into large disconnected blocks with steep, erratic dips. In contrast, to the east where the Dewey Lake Redbeds overlie the Rustler formation, halite dissolution is negligible and fracturing within the Culebra aquifer is minimal. Within the WIPP-site, for example, the variable extent of salt dissolution in the Rustler Formation (Fig. 6) and resultant fracturing of the Culebra aquifer yield transmissivities that range from 0.001 to 140 feet squared per day (MERCER, 1983). Because of the directional differences in hydraulic conductivity imposed by the fracture flow (anisotropy), local flow paths are difficult to determine. An extensive program of multiscale flow modelling of the Culebra aquifer system, coupled with site-specific tracer and aquifer tests, has been carried out and is continuing (DAVIES, 1989; LAPPIN and HUNTER, 1989).

The *Magenta Dolomite aquifer* (Table 4), the uppermost aquifer in the Rustler Formation, is a clastic carbonate unit containing thin laminae of anhydrite. The Magenta is a confined aquifer except where the dolomite and its underlying strata are severely fractured. Flow in the aquifer characteristically occurs along thin silt or silty dolomite beds and, in places, along bedding planes. In the Nash Draw area, however, fracture flow is dominant. Recharge of the Magenta is most likely to the north, as with the underlying Rustler aquifers, but it is supplemented in other nearby areas where the aquifer is near the surface. Based on potentiome-

tric-surface data, MERCER (1983) suggested that another recharge area occurs east of the WIPP site.

The development of Nash Draw had a profound effect upon the geohydrology of the Magenta Dolomite. Within the central part of the draw and continuing southwestward to the Malaga Bend, the Magenta has been removed by erosion. The dolomite is exposed along the western rim of the draw, but it is weathered and not saturated; the Magenta, along with its underlying anhydrite beds, are highly fractured. Furthermore, immediately east of the draw and west of the WIPP site the aquifer is also unsaturated. Because of the fracturing in the underlying anhydrite, the absence of water in several wells immediately east of Nash Draw, and the trend of the potentiometric surface, it is likely that Magenta waters drain into the underlying fractured anhydrites and clastics. They may also enter the Culebra aquifer in the Nash Draw area for eventual discharge into the Malaga Bend.

Dewey Lake Redbeds

The Dewey Lake Redbeds (Table 4) overlie the Rustler Formation throughout the WIPP site but are absent in Nash Draw to the west, except for occasional erratic blocks preserved in collapse structures. The unit consists of alternating thin-bedded siltstones and mudstones with occasional lenticular bodies of fine-grained sandstone; the siltstones and mudstones in the subsurface contain pervasive veins of selenite gypsum.

Because of their generally low permeability the Dewey Lake Redbeds contain little water, although during drilling in the WIPP-site area minor zones of saturation (moist well cuttings), mostly in the lenticular sands, were encountered. Groundwater movement in the Dewey Lake is highly restricted because of the lenticular geometry of the sand "aquifers." There is little indication of hydrologic connection between the Dewey Lake Redbeds and the underlying Rustler Formation.

Stratigraphic-geohydrologic framework of younger rocks

The Santa Rosa Sandstone and Chinle Formations (Triassic) unconformably overly the Ochoan strata. MCGOWEN *et al.* (1979) suggested that the Triassic rocks in western Texas and eastern New Mexico cannot be correlated with the Santa Rosa and Chinle Formations and should be collectively referred to as the Dockum Group in the Delaware Basin (Fig. 5). However, we have here retained the formational designations that conform with previous hydrogeologic reports for the WIPP site (see, for example, POWERS *et al.*, 1978; BACHMAN, 1980; MERCER, 1983). The Miocene-Pliocene Ogallala Formation unconformably overlies the Triassic strata. This fluvial sand and gravel unit is absent at the WIPP site but is exposed at, and east of, the Divide (Fig. 4). Above the Ogallala is the Pleistocene Gatuna Formation which occurs throughout the region as discontinuous bolson-type deposits, and the dense Mescalero caliche. Recent surficial sands, chiefly dunes, blanket the entire WIPP-site area.

Santa Rosa Sandstone

The Santa Rosa Sandstone (Table 4) is preserved in the eastern half of the WIPP site. West of ERDA-9 (Fig. 4) the unit has been completely removed by erosion. Its large-scale trough-type cross bedding, lack of sorting, arkosic composition, and grain angularity suggest rapid deposition in a fluvial system draining a predominantly crystalline terrain.

Although the Santa Rosa is an important aquifer in southwestern Lea County, only a small quantity of water has been found in the unit at the WIPP site. This occurs in a single drill hole in the lowermost sandstone interval immediately overlying the Dewey Lake Redbeds. The water was under water-table conditions but an attempt to test the zone failed other than collecting a sample for chemical analysis. The Santa Rosa is presumably recharged by precipitation in areas where the unit is directly overlain by permeable Cenozoic sediments. The water moves downward through the formation to the contact with the Dewey Lake aquitard, and then most likely moves down dip toward the east.

Chinle Formation

The Chinle Formation is a reddish-brown mudstone intercalated with greenish-gray mudstone and small, uncommon lenses of sandstone and conglomerate. The Chinle conformably overlies the Santa Rosa Sandstone. It has been completely eroded from the WIPP site with its nearest occurrence being 8 kilometers (5 miles) to the east near the Lea County line (Fig. 4) where it reaches a maximum thickness of 30 meters (100 feet). About 18 kilometers (11 miles) northeast of the site up to 250 meters (800 feet) of the unit has been observed.

The Chinle Formation's overwhelming dominant mudstone lithology precludes more than negligible groundwater. For this reason, and because of its distance from the site, Chinle waters are not included in this report.

Cenozoic deposits

The Miocene-Pliocene Ogallala sands and gravels, although forming one of the major regional aquifers to the east, occur only as isolated erosional remnants in the northern Delaware Basin. The closest of these to the WIPP site are along the Divide to the east (Fig. 4) and are not water bearing. The veneer of Pleistocene sediments that forms the surface of the WIPP-site area only rarely contains groundwater and no water has been found in these sediments at the site. Only some distance away from the site, such as along the Pecos River, are more than sporadic occurrences and minor quantities of groundwater present. Although the surficial sands and underlying Gatuna Formation in the WIPP-site area are characteristically permeable, they act principally as conduits for downward percolating waters rather than as reservoirs. In contrast, the dense Mescalero Caliche generally acts as a barrier. Except for a single water sample from the thick Pleistocene fill in the San Simon sink (Fig. 4, site WIPP-15) no information is available on water compositions from these units. Stream gravels of the Gatuna Formation found north of the WIPP site boundary indicate that Nash Draw was the location of a major stream during middle Pleistocene (BACHMAN, 1985). Groundwater circulation associated with the stream apparently caused considerable dissolution and subsidence in both the Rustler and upper part of the Salado Formation, and provided a major mechanism responsible for the formation of Nash Draw.

Gypsiferous spring deposits on the eastern margin of Nash Draw indicate that by the late Pleistocene Nash Draw was a well developed valley, and that dissolution was still active at that time (BACHMAN, 1985). These deposits at an elevation well above the present water table illustrate that the late Pleistocene ground water system contained more water than the present day flow system, reflecting wetter climatic conditions.

Regional hydrology

With particular attention to the Culebra Dolomite member of the Rustler Formation, DAVIES (1989) has presented a comprehensive series of analyses of groundwater flow in the vicinity of the WIPP site including variable-density flow simulations (Fig. 8). This work has developed the regional flow field from simulation both with and without consideration of vertical flux. It indicates that flow velocities are relatively fast west of the WIPP site and east and northeast of the site. In the transition zone between the two extremes, velocities are highly variable. The simulations also indicate that up to 25 percent of total inflow to the Culebra could enter vertically, but most of the influx must be in the western part of the transition zone adjacent to Nash Draw.

DAVIES (1989) has also presented a simple cross-sectional model for flow system drainage across the WIPP site to Nash Draw following recharge during a past pluvial period. This model suggests that the system could sustain flow from purely transient drainage since the last glacial maximum. The model also indicates that the observed underpressuring of the Culebra in the vicinity of the WIPP site is most likely the hydrodynamic result of the Culebra having a relatively high hydraulic conductivity, and being well connected to its discharge area, but poorly connected to sources of recharge.

Water samples

We have selected 128 chemical analyses of water from 42 sites (Table 5) representing 77 horizon-site sampling points. Multiple analyses from the same site and horizon are either replicate data from different investigators for the water sample, or data for samples collected at different times.

Site locations

Almost all sites that provided data for our study are located on Fig. 9, using base map coordinates from RICHEY (1989). Many of the wells were drilled in support of the WIPP-site geologic and hydrologic characterization studies (the DOE, H, P, and WIPP groups of wells in Table 5). A few were drilled in support of the GNOME project (an underground nuclear test) and one (USGS-8; Fig. 4) was drilled as part of the Malaga Bend Salinity Alleviation project. The remainder were drilled for a variety of other purposes ranging from petroleum and potash exploration to domestic water supply. A few samples came from sites without exact coordinates (Table 6).

Chemical analyses

Analytical data for these waters are from a wide variety of sources. Most have been published, principally in reports concerned with site characterization studies for the WIPP project. Unpublished analyses include those compiled for us by Karen Robinson and Steven Lambert of Sandia Laboratories for this study. Others are from the U.S. Geological Survey's Water Resources Division either in older Technical Files or more recent data from the

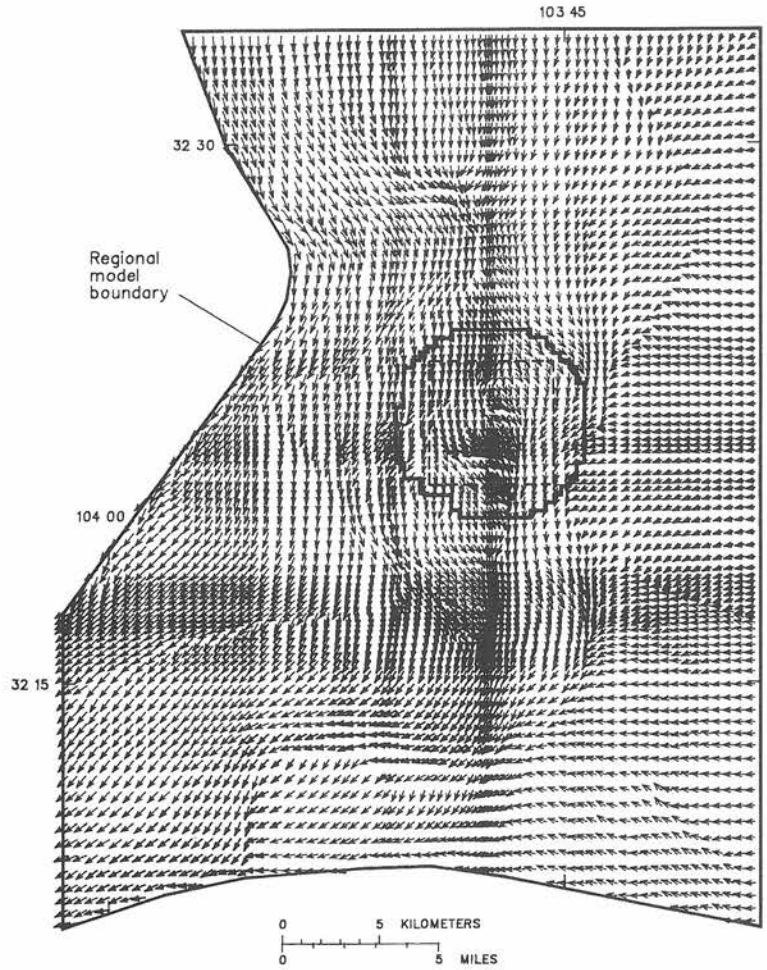

FIG. 8. Direction and magnitude of ground water flow produced by the baseline simulation model of DAVIES (1989).

Denver Central Laboratory. In addition, 34 new analyses by S. L. Rettig (U.S. Geological Survey, Reston), heretofore unpublished, are included. Most of these are replicate samples previously analyzed by the Denver Central Laboratory and reported in MERCER (1983); these new analyses generally yield improved ionic balances and include analytical data for bromide.

RESULTS

Tables 7 through 11 report our SNORM-calculated salt norm and simple-salt assemblages as well as the original analytical data for each of the 128 chemical analyses. The tables are arranged stratigraphically from the Rustler-Salado contact waters (Table 7), discharge waters from the Rustler Formation in the Pecos River area (Table 8), waters from the Culebra Dolomite (Table 9) and Magenta Dolomite (Table 10) aquifers in the Rustler Formation, and four waters from younger strata (Table 11).

Each table identifies the site of sample collection, and if known, reports sample collection date, sample density, and sample pH. The chemical analysis, excluding solutes not forming normative salts, is reported with its source cited in the footnote. Those analyses used for plotting on maps and diagrams with simple-salt rose are marked with an asterisk. The total dissolved solids (TDS), rounded to three significant figures, is the sum from SNORM of the solutes reported, and is neither the residue weight

Table 5. Sample site abbreviations, site names, location data, and stratigraphic horizons sampled, with number of analyses

		Location data	Stratigraphic horizon					
			1	2	3	4	5	6
ANDER-1	Anderson Lake (surface)	Table 6	1					
ANDER-2	Anderson Lake (10 ft. d)	Table 6	1					
D-1	DOE-1 well	Fig. 9		1				
D-2	DOE-2 well	Fig. 9		1				
ENGEL	Engel well	Fig. 9		1				
GNOME	GNOME shaft	Fig. 9		1				
GNOME-1	GNOME USGS-1 well	Fig. 9		1				
GNOME-4	GNOME USGS-4 well	Fig. 9		1				
GNOME-5	GNOME USGS-5 well	Fig. 9	1		1			
GNOME-8	GNOME USGS-8 well	Fig. 9		1				
GRANDE	Laguna Grande de la Sal	Table 6	1					
H-1	H-1 (Hydrology hole)	Fig. 9	1	1	1			
H-2	H-2 (Hydrology hole)	Fig. 9	1	2	1			
H-3	H-3 (Hydrology hole)	Fig. 9	1	3	1			
H-4	H-4 (Hydrology hole)	Fig. 9	2	4	1			
H-5	H-5 (Hydrology hole)	Fig. 9	2	4	1		1	
H-6	H-6 (Hydrology hole)	Fig. 9	1	3	1			
H-7	H-7 (Hydrology hole)	Fig. 9	2	3				
H-8	H-8 (Hydrology hole)	Fig. 9	2	3	2			
H-9	H-9 (Hydrology hole)	Fig. 9	2	2	2			
H-10	H-10 (Hydrology hole)	Fig. 9	2	1	1			
H-11	H-11 Hydrology hole)	Fig. 9		1				
H-12	H-12 (Hydrology hole)	Fig. 9		1				
INDIAN	Indian well	Fig. 9		1				
P-14	P-14 (Potash hole)	Fig. 9	2	2				
P-15	P-15 (Potash hole)	Fig. 9	1	1				
P-17	P-17 (Potash hole)	Fig. 9	1	2				
P-18	P-18 (Potash hole)	Fig. 9	1	1				
SOUTH	South well	Fig. 9		1				
SURPRISE	Surprise spring	Table 6	2					
TWIN	Twin Pasture well	Table 6					1	
TWO-MILE	Two-mile mill well	Fig. 9		1				
USGS-8	USGS-8 well	Fig. 4	3					
W-15	WIPP-15 well	Fig. 4						1
W-25	WIPP-25 well	Fig. 9	2	4	3			
W-26	WIPP-26 well	Fig. 9	3	3				
W-27	WIPP-27 well	Fig. 9	2	2	2			
W-28	WIPP-28 well	Fig. 9	2	2				
W-29	WIPP-29 well	Fig. 9	2	3				
W-30	WIPP-30 well	Fig. 9	2	2	1			
WALKER	Walker well	Fig. 9				1		
WINDMILL	Little windmill well	Fig. 9		2				

1. Rustler Formation: Rustler-Salado contact.
2. Rustler Formation: Culebra aquifer.
3. Rustler Formation: Magenta aquifer.
4. Dewey Lake Redbeds.
5. Santa Rosa Sandstone.
6. Pleistocene collapse fill.

after drying, nor necessarily the value reported in the cited reference. The Cl/Br ratio is reported as the weight ratio.

The cation–anion charge balance for each analysis, recorded as "balance (+/−)", is calculated by SNORM and is the ratio of the sum of cation equivalencies to the sum of anion equivalencies with elemental boron calculated as the borate anion. In general, the greater the balance departs from unity, the less reliable the analytical data and the ensuing SNORM results. Except for the possibility of offsetting analytical errors, we are confident of the salt

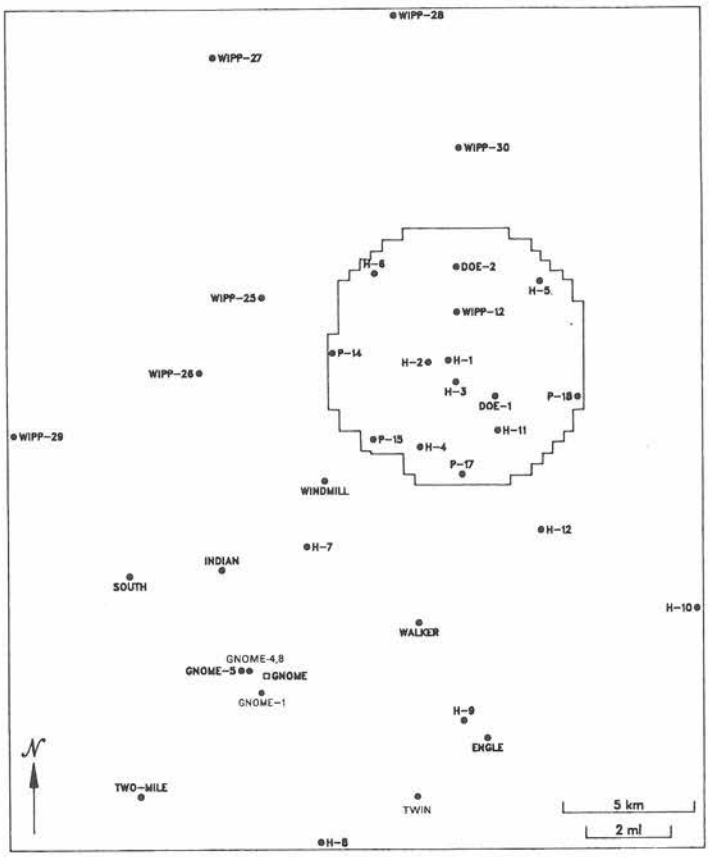

FIG. 9. Water sample locations within and near the WIPP site; solid circles are well sites and open squares are mine shafts. Locations are from RICHEY, 1989, DAVIES, 1989, and LAPPIN and HUNTER, 1989.

norm if the balance is within 1.00 ± 0.02, but feel that balances greater than 1.05 or less than 0.95 may give misleading results, particularly for speciation and abundance of salts with quantities of less than 5 percent in the normative assemblages.

The salt norm for each analysis is reported in full. The major salt abundances, that is, those salts composed solely of major solutes (Table 1), are listed in the body of the table, whereas those for salts containing one or more minor solutes are reported in the table's footnotes. The simple-salt assemblage for each analysis, often plotted on maps or illustrations as simple-salt rose diagrams, is also listed. Normative salt abundance is reported in anhydrous weight percentage and simple salt abundance in weight percentage of their respective assemblages.

We have not reported all replicate analyses. For example, we have excluded many of the analyses reported by MERCER (1983). They are either nearly identical to S. L. Rettig's data reported here or yield charge balances that deviate markedly from unity. Furthermore, none of the analyses in MERCER (1983) report bromide concentrations. We have also excluded the analyses, chiefly of waters from the Culebra aquifer, that were reported by UHLAND and RANDALL (1986) and UHLAND *et al.* (1987). These data yield charge balances that frequently deviate appreciably from unity and are replicated by other data.

DISCUSSION

Fluids from the three aquifers in the Rustler Formation (Tables 7, 9, and 10) and from surface and near-surface sites in the discharge area of Rustler waters (Table 8) exhibit a wide range of salinities and salt norms. The variation is attributed to multiple origins of the waters and their solutes. Retention of connate or primitive brines, diagenetic pro-

Table 6. Approximate locations of water-sample sites lacking map coordinates

ANDERSON	Waters from Anderson Lake in the vicinity of Malaga Bend on the Pecos River and USGS-8 (Fig. 4).
GRANDE	Water samples from Laguna Grande de la Sal approximately 18 kilometers (12 miles) west-southwest of the WIPP site (Fig. 7).
SURPRISE	Water from Surprise spring immediately north of Laguna Grande de la Sal (Fig. 7).
TWIN	Twin Pastures Well (also called Twin well) located (Fig. 9) approximately 19 kilometers (12 miles) south of the WIPP site (UHLAND and RANDALL, 1986).

cesses within the Rustler Formation, influx of younger meteoric weathering waters, and dissolution of evaporite minerals within the formation all played a role in the evolution of these fluids. We also include data for 4 waters in units that overlie the Rustler Formation (Table 11) as potential examples of downward percolating waters that may have recharged the Rustler Formation.

Seawater evaporation salt norms

For discussion of norms for waters from the Rustler Formation we will refer to salt norms calculated for progressively evaporating sea water brines (Table 12). The first group, Group (A) with waters A–1 through A–7, are brine compositions determined from 25°C experimental salt solubility studies, chiefly in the Na-K-Mg-Cl-SO_4-H_2O system, that are compiled and summarized in BRAITSCH (1971). These experiments exclude the precipitation of polyhalite or other Ca-bearing sulfate salts other than gypsum/anhydrite through initial halite formation. Beyond initial halite saturation calcium in the brine is arbitrarily omitted. The second group, Group (B) with waters B-1 through B-7, are the Ca-Mg-Na-K-Cl-SO_4-H_2O computer-simulated brine compositions for 25°C from EUGSTER *et al.* (1980), beginning with sea water composition. The data show equilibrium precipitation throughout the succession; thus, for example, primary polyhalite, rarely, if ever, observed in natural primary assemblages, begins to crystallize in the model during precipitation of the halite facies. The program of EUGSTER *et al.* (1980) continuously re-equilibrates the brine composition with salts already crystallized with the result that no transitory salts, such as gypsum, polyhalite, or epsomite, remain in the assemblage after the brine composition leaves the stability fields for these phases.

The differences between the two sets of data in Table 12 reflect the inclusion of polyhalite in the calculations by EUGSTER *et al.* (1980). Reaching the polyhalite stability field within the halite facies results not only in direct precipitation of polyhalite on continued evaporation, but also in replacing most of the previously precipitated anhydrite with polyhalite. This sufficiently reduces sulfate, potassium, and magnesium concentrations in the brine so that neither bloedite nor kainite saturation is attained. Thus, when the epsomite field is reached in Group (B), carnallite in the salt norm of the coexisting brine (B-5) is only 6.86 percent of the assemblage, rather than the 23.6 percent (A-4) coexisting with initial epsomite in Group (A). Carnallite is at a maximum (25.6 percent) in the norm for the brine at initial kainite precipitation (A-5) in Group (A), whereas in Group (B) maximum carnallite (15.0 percent) in the norm is reached well before initial bitter salt deposition at initial stability of polyhalite (B-4).

In Table 13 we summarize the salt norms and Cl/Br weight ratios from two successions of marine brine ponds constructed for the commercial retrieval of halite. The first of these, a succession of pans at the Secovljo salt works near Portoroz, Yugoslavia, was sampled and analyzed (HERRMANN *et al.*, 1973) only through the early third of the halite facies of the marine succession. The second, the Morton Bahama salt works on Great Inagua Island in the Bahamas, was sampled and analyzed (MCCAFFREY *et al.*, 1987) through more than half of the halite facies. Furthermore, three samples of the most concentrated Bahamian brines were further evaporated in the laboratory through the remaining interval of the halite facies, the magnesium sulfate facies, and into the potash salt facies. Unfortunately, the mineralogy of the bitter salts was not determined. It also appears that some addition of water, possibly from water vapor sorption by the experimental brines with very low water activity, diluted some solutions between their separation from the precipitated salts and their analysis; the decrease in salinity from no. 36-4 to no. 39-6 and, in particular, from no. 39-6 to no. 39-4 (Table 13) can only be attributed to dilution.

In each set of analyses, the Cl/Br ratio between seawater and at initial halite saturation (Seawater through Pan 13d and W-64 through W-46 in Table 13) remains at about 300. The ratio begins decreasing markedly with increasing halite precipitation to about 50 at the initial precipitation of bitter salts

Table 7. Chemical analysis, salt norm (anhydrous weight percent),

	1*	2*	3*	4	5*
Site	H-1	H-2	H-3	H-4	H-4
Date collected	2/23/77	2/23/77	2/23/77	3/16/79	3/16/79
Density (g/cc)	—	—	—	—	1.212
pH	7.2	5.9	7.6	—	3.00
Chemical analysis	mg/L	mg/L	mg/L	mg/L	mg/kg
Mg	30,000.	25,000.	25,000.	27,000.	20,600.
Ca	13,000.	9,200.	18,000.	8,300.	7,140.
Sr	—	—	—	—	229.
Li	—	—	—	—	16.
Na	56,000.	66,000.	59,000.	66,000.	56,400.
K	17,000.	9,100.	14,000.	8,600.	6,850.
F	—	—	—	1.7	—
Cl	210,000.	200,000.	210,000.	210,000.	167,000.
Br	—	—	—	—	1,355.
NO_3	1.3	4.9	3.4	1.2	—
HCO_3	675.	199.	467.	1.0	—
SO_4	520.	1,300.	370.	1,400.	594.
B	110.	150.	1.9	360.	167.
TDS	327,000.	311,000.	327,000.	322,000.	260,000.
Balance (+/−)	1.006	0.989	0.990	0.959	0.995
Cl/Br	—	—	—	—	123.
Salt norm					
Dolomite	0.2	<0.1	0.1	<0.1	—
Magnesite	—	—	—	—	—
Anhydrite	0.2	0.6	0.2	0.6	0.3
Kieserite	—	—	—	—	—
Epsomite	—	—	—	—	—
Polyhalite	—	—	—	—	—
Leonite	—	—	—	—	—
Bloedite	—	—	—	—	—
Kainite	—	—	—	—	—
Halite	43.3	54.3	46.2	53.5	55.6
Sylvite	—	—	—	—	—
Carnallite	22.5	12.8	18.7	11.9	11.5
Bischofite	5.0	11.5	—	16.0	12.5
Tachyhydrite	28.7	20.5	31.1	17.5	19.5
Antarcticite	—	—	3.7	—	—
Simple salts					
$CaCO_3$	0.1	<0.1	0.1	<0.1	—
$MgCO_3$	0.1	<0.1	0.1	<0.1	—
$CaSO_4$	0.2	0.6	0.2	0.6	0.3
$MgSO_4$	—	—	—	—	—
K_2SO_4	—	—	—	—	—
Na_2SO_4	—	—	—	—	—
Na_2Cl_2	43.4	54.4	46.2	53.8	55.9
K_2Cl_2	9.9	5.6	8.2	5.3	5.1
$MgCl_2$	35.7	31.7	30.1	33.9	31.5
$CaCl_2$	10.6	7.6	15.2	6.5	7.2

* Simple-salt rose plotted on subsequent maps and diagrams.

Source of analysis; minor normative salts (anhydrous weight percent):

1. MERCER (1983). Inyoite—0.2, nitrocalcite—0.0005.
2. MERCER (1983). Inyoite—0.2, nitrocalcite—0.002.
3. MERCER (1983). Inyoite—0.003, nitrocalcite—0.001.
4. MERCER (1983). Inyoite—0.5, fluorite—0.001, nitrocalcite—0.0005.
5. Rettig (this report). Inyoite—0.3, $SrCl_2 \cdot 2H_2O$—0.2, $LiCl \cdot H_2O$—0.04.

and simple salts (weight percent) of Rustler-Solado contact waters

6	7*	8*	9	10*	11	12*
H-5	H-5	H-6	H-7	H-7	H-8	H-8
5/16/79	5/16/79	4/9/79	3/20/80	3/20/80	9/6/80	9/6/80
—	1.263	1.209	1.048	1.047	—	1.085
—	4.34	2.91	6.80	7.13	7.60	7.22
mg/L	mg/kg	mg/kg	mg/L	mg/kg	mg/L	mg/kg
82,000.	63,300.	16,500.	910.	788.	430.	392.
2,100.	1,580.	3,470.	2,600.	2,340.	1,200.	1,110.
—	26.	83.	—	42.	—	18.
—	18.	1.7	—	0.3	—	—
14,000.	12,400.	68,800.	22,000.	21,500.	46,000.	43,700.
21,000.	14,100.	6,450.	210.	164.	660.	350.
—	—	—	0.8	—	0.4	—
290,000.	207,000.	166,000.	41,000.	37,800.	70,000.	66,400.
—	3,060.	907.	—	12.	—	8.3
—	—	—	0.1	—	—	—
300.	—	—	—	47.	—	—
2,000.	1,090.	1,220.	2,900.	2,710.	5,300.	4,700.
67.	194.	117.	3.1	25.	1.3	3.4
412,000.	303,000.	264,000.	69,600.	65,400.	124,000.	117,000.
0.972	1.052	0.993	0.959	0.998	1.014	1.015
—	68.	183.	—	3,150.	—	8,000.
0.1	—	—	—	0.1	—	—
—	—	—	—	—	—	—
0.7	0.5	0.7	5.8	5.9	1.4	2.2
—	—	—	—	—	0.9	—
—	—	—	—	—	—	1.1
—	—	—	—	—	3.8	2.2
—	—	—	—	—	—	—
—	—	—	—	—	—	0.3
—	—	—	—	—	—	—
8.8	10.1	66.4	82.5	83.6	93.8	94.3
—	—	—	—	—	—	—
22.6	19.6	10.7	1.3	1.1	<0.1	—
65.6	67.3	13.6	—	—	—	—
2.2	2.1	8.1	7.1	6.5	—	—
—	—	—	3.2	2.6	—	—
<0.1	—	—	—	<0.1	—	—
<0.1	—	—	—	<0.1	—	—
0.7	0.5	0.7	5.8	5.9	3.3	3.2
—	—	—	—	—	1.7	1.6
—	—	—	—	—	1.2	0.7
—	—	—	—	—	—	0.2
8.8	10.1	66.9	82.5	83.9	93.8	94.3
9.9	8.7	4.7	0.6	0.5	<0.1	—
79.7	79.9	24.7	5.3	4.7	<0.1	—
0.8	0.8	3.0	5.9	5.0	—	—

* Simple-salt rose plotted on subsequent maps and diagrams.

Source of analysis; minor normative salts (anhydrous weight percent):

6. MERCER (1983). Inyoite—0.08.
7. Rettig (this report). Inyoite—0.3, $LiCl \cdot H_2O$—0.04, $SrCl_2 \cdot 2H_2O$—0.02.
8. Rettig (this report). Inyoite—0.2, $SrCl_2 \cdot 2H_2O$—0.06, $LiCl \cdot H_2O$—0.004.
9. MERCER (1983). Inyoite—0.02, fluorite—0.002, nitrocalcite—0.0002.
10. Rettig (this report). Inyoite—0.2, $SrCl_2 \cdot 2H_2O$—0.1, $LiCl \cdot H_2O$—0.003.
11. MERCER (1983). Indirite—0.005, sellaite—0.0005.
12. Rettig (this report). Celestite—0.03, indirite—0.01.

Table 7. (Continued)

	13	14*	15	16*	17
Site	H-9	H-9	H-10	H-10	P-14
Date collected	5/20/80	5/20/80	5/19/80	5/19/80	2/24/77
Density (g/cc)	1.202	1.203	1.198	1.202	—
pH	7.0	6.21	6.3	5.74	7.2
Chemical analysis	mg/L	mg/kg	mg/L	mg/kg	mg/L
Mg	870.	707.	11,000.	8,400.	1,200.
Ca	1,300.	1,120.	1,500.	1,120.	570.
Sr	—	15.	—	42.	—
Li	—	3.3	—	3.7	—
Na	130,000.	102,000.	100,000.	86,500.	120,000.
K	1,200.	790.	4,000.	2,950.	1,300.
F	0.1	—	0.7	—	—
Cl	190,000.	155,000.	190,000.	155,000.	180,000.
Br	—	79.	—	832.	—
NO_3	4.9	—	3.7	—	1.5
HCO_3	—	—	—	—	222.
SO_4	2,600.	3,990.	3,300.	3,830.	10,000.
B	19.	20.	120.	97.	1.7
TDS	326,000.	264,000.	310,000.	259,000.	313,000.
Balance (+/−)	1.075	1.027	0.999	1.027	1.017
Cl/Br	—	1,960.	—	186.	—
Salt norm					
Dolomite	—	—	—	—	—
Magnesite	—	—	—	—	<0.1
Anhydrite	1.2	1.2	1.5	1.4	—
Kieserite	—	0.5	—	0.6	—
Epsomite	—	—	—	—	0.1
Polyhalite	—	0.4	—	—	1.3
Leonite	—	—	—	—	0.9
Bloedite	—	—	—	—	2.3
Kainite	—	—	—	—	—
Halite	97.0	96.8	82.0	83.7	95.4
Sylvite	—	—	—	—	—
Carnallite	1.5	1.0	5.6	4.9	—
Bischofite	—	—	10.7	9.2	—
Tachyhydrite	0.2	—	—	—	—
Antarcticite	<0.1	—	—	—	—
Simple salts					
$CaCO_3$	—	—	—	—	—
$MgCO_3$	—	—	—	—	<0.1
$CaSO_4$	1.2	1.4	1.5	1.5	0.6
$MgSO_4$	—	0.6	—	0.6	1.8
K_2SO_4	—	0.1	—	—	0.9
Na_2SO_4	—	—	—	—	1.2
Na_2Cl_2	97.1	96.9	82.1	83.9	95.4
K_2Cl_2	0.7	0.5	2.5	2.1	—
$MgCl_2$	1.0	0.6	13.9	12.0	—
$CaCl_2$	0.1	—	—	—	—

* Simple-salt rose plotted on subsequent maps and diagrams.

Source of analysis; minor normative salts (anhydrous weight percent):

13. MERCER (1983). Inyoite—0.03, nitrocalcite—0.002, fluorite—0.00006.
14. Rettig (this report). Indirite—0.03, celestite—0.01, $Li_2SO_4 \cdot H_2O$—0.01.
15. MERCER (1983). Inyoite—0.2, indirite—0.03, nitrocalcite—0.002, fluorite—0.0005.
16. Rettig (this report). Indirite—0.2, celestite—0.03, $Li_2SO_4 \cdot H_2O$—0.01.
17. MERCER (1983). Indirite—0.002, niter—0.0008.

Table 7 (Continued)

18*	19	20*	21*	22*	23	24
P-14	P-15	P-17	P-18	WIPP-25	WIPP-25	WIPP-26
2/4/80	4/3/79	5/11/79	5/20/80	3/19/80	7/17/80	3/18/80
1.126	1.042	1.193	1.266	1.171	—	1.078
3.55	7.98	6.36	5.35	7.14	7.4	8.5
mg/kg	mg/kg	mg/kg	mg/kg	mg/kg	mg/L	mg/L
941.	240.	29,300.	41,100.	2,390.	3,260.	1,300.
1,190.	864.	14,400.	22,400.	572.	560.	2,700.
20.	30.	380.	55.	9.4	11.3	—
—	—	1.0	8.5	0.8	1.58	—
70,200.	21,900.	20,100.	15,200.	78,600.	122,800.	52,000.
1,380.	1,250.	9,640.	11,800.	2,050.	3,330.	1,000.
—	—	—	—	—	—	—
111,000.	34,400.	152,000.	199,000.	127,000.	192,000.	88,000.
—	28.	2,725.	3,120.	41.	51.	—
—	—	—	—	—	—	0.2
—	152.	—	—	105.	130.	—
7,640.	3,220.	478.	197.	9,380.	12,400.	7,600.
42.	3.4	184.	161.	40.	40.9	30.
192,000.	62,100.	229,000.	293,000.	220,000.	335,000.	153,000.
0.980	1.007	0.981	0.974	0.980	1.009	0.957
—	1,230.	56.	64.	3,100.	3,760.	—
—	—	—	—	—	—	—
—	0.2	—	—	<0.1	<0.1	—
<0.1	2.1	0.3	0.1	—	—	6.2
1.1	—	—	—	2.8	1.9	0.7
—	—	—	—	—	—	—
4.2	5.4	—	—	1.9	1.2	—
—	—	—	—	—	—	—
—	—	—	—	—	—	—
0.1	—	—	—	1.4	2.8	—
93.9	89.4	22.7	13.6	92.0	92.9	88.9
—	2.1	—	—	—	—	—
0.4	0.7	18.6	18.0	1.7	1.2	2.9
—	—	11.1	9.5	—	—	1.2
—	—	46.7	58.5	—	—	—
—	—	—	—	—	—	—
—	—	—	—	—	—	—
—	0.2	—	—	<0.1	<0.1	—
2.1	4.7	0.3	0.1	0.9	0.6	6.2
2.1	1.2	—	—	4.1	3.9	0.7
1.4	1.7	—	—	0.6	0.4	—
—	—	—	—	—	—	—
94.0	89.5	22.8	13.6	92.1	92.9	89.0
0.2	2.4	8.2	7.9	1.3	1.6	1.3
0.2	0.4	51.4	56.8	1.0	0.6	2.8
—	—	17.3	21.6	—	—	—

* Simple-salt rose plotted on subsequent maps and diagrams.

Source of analysis; minor normative salts (anhydrous weight percent):

18. Rettig (this report). Indirite—0.1, celestite—0.02.
19. Rettig (this report). Celestite—0.1, indirite—0.03.
20. Rettig (this report). Inyoite—0.4, $SrCl_2 \cdot 2H_2O$—0.3, $LiCl \cdot H_2O$—0.03.
21. Rettig (this report). Inyoite—0.3, $SrCl_2 \cdot 2H_2O$—0.04, $LiCl \cdot H_2O$—0.02.
22. Rettig (this report). Indirite—0.08, celestite—0.009, $Li_2SO_4 \cdot H_2O$—0.003.
23. Bendix (unpub.). Indirite—0.06, celestite—0.007, $Li_2SO_4 \cdot H_2O$—0.004.
24. MERCER (1983). Indirite—0.09, nitromagnesite—0.0002.

Table 7 (Continued)

	25	26*	27	28	29*
Site	WIPP-26	WIPP-26	WIPP-27	WIPP-27	WIPP-28
Date collected	3/18/80	7/23/80	5/21/80	7/24/80	3/20/80
Density (g/cc)	1.107	—	1.204	1.073	1.138
pH	8.03	7.7	7.43	7.31	6.72
Chemical analysis	mg/kg	mg/L	mg/kg	mg/kg	mg/kg
Mg	1,170.	1,660.	1,040.	1,680.	2,070.
Ca	1,310.	1,410.	1,160.	1,070.	615.
Sr	20.	27.	10.	21.	11.
Li	1.0	1.15	1.2	2.0	0.9
Na	50,100.	68,600.	102,000.	32,100.	65,000.
K	814.	1,200.	2,570.	1,580.	2,070.
F					—
Cl	82,400.	108,000.	154,000.	52,400.	102,000.
Br	24.	19.3	51.	16.	36.
NO_3	—	—	—	—	—
HCO_3	123.	270.	—	—	260.
SO_4	6,730.	7,480.	5,190.	8,670.	11,000.
B	43.	31.8	13.	16.	54.
TDS	143,000.	189,000.	266,000.	97,600.	183,000.
Balance (+/−)	0.957	1.004	1.043	0.982	0.990
Cl/Br	3,430.	5,600.	3,020.	3,280.	2,830.
Salt norm					
Dolomite	—	—	—	—	—
Magnesite	<0.1	0.1	—	—	0.1
Anhydrite	2.6	2.1	0.1	0.6	—
Kieserite	2.4	2.4	—	4.9	—
Epsomite	—	—	—	—	3.0
Polyhalite	1.2	0.8	2.8	6.5	2.4
Leonite	—	—	—	—	1.4
Bloedite	—	—	—	—	—
Kainite	—	—	—	—	2.2
Halite	91.7	92.2	95.0	84.6	90.8
Sylvite	—	—	0.3	—	—
Carnallite	1.8	2.3	1.8	3.2	—
Bischofite	—	—	—	—	—
Tachyhydrite	—	—	—	—	—
Antarcticite	—	—	—	—	—
Simple salts					
$CaCO_3$	—	—	—	—	—
$MgCO_3$	<0.1	0.1	—	—	0.1
$CaSO_4$	3.2	2.5	1.4	3.8	1.2
$MgSO_4$	2.7	2.5	0.6	6.3	5.4
K_2SO_4	0.4	0.3	0.9	2.0	1.6
Na_2SO_4	—	—	—	—	—
Na_2Cl_2	91.8	92.3	95.0	84.7	91.0
K_2Cl_2	0.8	1.0	1.1	1.4	0.8
$MgCl_2$	1.0	1.3	1.0	1.8	—
$CaCl_2$	—	—	—	—	—

* Simple-salt rose plotted on subsequent maps and diagrams.

Source of analysis; minor normative salts (anhydrous weight percent):

25. Rettig (this report). Indirite—0.1, celestite—0.03, $Li_2SO_4 \cdot H_2O$—0.006.
26. Bendix (unpub.). Indirite—0.08, celestite—0.03, $Li_2SO_4 \cdot H_2O$—0.005.
27. Rettig (this report). Indirite—0.02, celestite—0.008, $Li_2SO_4 \cdot H_2O$—0.004.
28. Rettig (this report)—"recollect" (shallower in aquifer). Indirite—0.07, celestite—0.05, $Li_2SO_4 \cdot H_2O$—0.02.
29. Rettig (this report). Indirite—0.1, celestite—0.01, $Li_2SO_4 \cdot H_2O$—0.004.

Table 7 (Continued)

30 WIPP-28 7/31/80 1.180 7.00	31* WIPP-29 3/18/80 1.067 6.86	32 WIPP-29 7/24/80 — 7.20	33 WIPP-30 3/19/80 1.200 6.23	34* WIPP-30 7/17/80 — 7.50	35* GNOME-5 11/27/61 1.200 7.0
mg/L	mg/kg	mg/L	mg/kg	mg/L	mg/kg
3,400.	1,930.	2,320.	1,830.	2,770.	2,710.
605.	872.	1,080.	758.	955.	424.
11.6	17.	21.	12.	18.4	33.
1.82	0.9	1.34	—	0.72	2.82
97,100.	29,500.	36,100.	92,500.	120,600.	94,700.
4,300.	842.	1,480.	1,330.	2,180.	2,090.
—	—	—	—	—	4.2
155,000.	45,200.	58,000.	150,000.	192,000.	156,000.
29.	12.	12.5	72.	78.	5.5
—	—	—	—	—	0.4
170.	154.	200.	—	620.	18.
16,700.	11,300.	12,000.	6,300.	7,390.	540.
46.2	45.	19.9	79.	81.6	—
277,000.	89,900.	111,000.	253,000.	327,000.	257,000.
0.983	0.995	0.981	0.972	0.999	1.001
5,340.	3,770.	4,640.	2,080.	2,460.	28,400.
—	—	—	—	—	<0.1
<0.1	0.1	0.1	—	0.1	—
—	<0.1	<0.1	0.8	0.9	0.3
—	—	7.5	2.0	1.9	—
2.0	7.9	—	—	—	—
1.6	6.8	6.9	0.4	0.1	—
1.2	—	—	—	—	—
—	2.2	—	—	—	—
5.2	—	—	—	—	—
90.0	82.7	83.6	94.6	94.0	93.8
—	—	—	—	—	—
—	—	1.8	2.1	2.8	3.5
—	—	—	—	—	1.8
—	—	—	—	—	0.6
—	—	—	—	—	—
—	—	—	—	—	<0.1
<0.1	0.1	0.1	—	0.1	<0.1
0.7	3.3	3.3	1.0	1.0	0.3
6.0	10.3	9.0	2.1	1.9	—
1.2	2.1	2.1	0.1	<0.1	—
—	1.2	—	—	—	—
90.0	82.9	83.7	94.7	94.1	93.8
2.0	—	0.8	0.9	1.2	1.6
—	—	1.0	1.2	1.6	4.1
—	—	—	—	—	0.2

* Simple-salt rose plotted on subsequent maps and diagrams.

Source of analysis; minor normative salts (anhydrous weight percent):

30. Bendix (unpub.). Indirite—0.07, celestite—0.009, $Li_2SO_4 \cdot H_2O$—0.005.
31. Rettig (this report). Indirite—0.2, celestite—0.04, $Li_2SO_4 \cdot H_2O$—0.008.
32. Bendix (unpub.). Indirite—0.08, celestite—0.04, $Li_2SO_4 \cdot H_2O$—0.01.
33. Rettig (this report). Indirite—0.1, celestite—0.01.
34. Bendix (unpub.). Indirite—0.1, celestite—0.01, $Li_2SO_4 \cdot H_2O$—0.002.
35. U.S.G.S. (unpub. Tech files). $SrCl_2 \cdot 2H_2O$—0.02, $LiCl \cdot H_2O$—0.007, fluorite—0.003, $Sr(NO_3)_2$—0.0003.

Table 8. Chemical analysis, salt norm (anhydrous weight percent), and simple salts (weight percent) of

	1	2*	3
Site	USGS-8	USGS-8	USGS-8
Date collected	2/25/54	1/17/64	5/1/64
Density (g/cc)	1.207	1.209	1.214
pH	—	—	—
Chemical analysis	mg/L	mg/L	mg/L
Mg	2,020.	2,750.	3,540.
Ca	411.	550.	436.
Sr	—	—	—
Li	—	—	—
Na	101,000.	120,000.	119,000.
K	3,310.	4,500.	6,300.
Cl	158,000.	187,000.	187,000.
Br	—	—	—
HCO_3	78.	102.	146.
SO_4	10,200.	13,100.	15,300.
B	—	15.	19.
TDS	275,000.	328,000.	332,000.
Balance (+/−)	0.999	1.007	1.010
Cl/Br	—	—	—
Salt norm			
Dolomite	—	—	—
Magnesite	<0.1	<0.1	<0.1
Anhydrite	—	—	—
Epsomite	0.5	0.3	—
Leonite	0.9	0.5	0.1
Kieserite	—	—	—
Polyhalite	1.1	1.2	0.9
Kainite	4.1	5.4	8.1
Halite	93.4	92.6	90.7
Sylvite	—	—	0.3
Carnallite	—	—	—
Bischofite	—	—	—
Tachyhydrite	—	—	—
Simple salts			
$CaCO_3$	—	—	—
$MgCO_3$	<0.1	<0.1	<0.1
$CaSO_4$	0.5	0.6	0.4
$MgSO_4$	3.6	4.1	5.2
K_2SO_4	0.8	0.6	0.3
Na_2Cl_2	93.4	92.6	90.7
K_2Cl_2	1.6	2.1	3.3
$MgCl_2$	—	—	—
$CaCl_2$	—	—	—

* Simple-salt rose plotted on subsequent maps and diagrams.
Source of analysis; minor normative salts (anhydrous weight percent):
1. KUNKLER (1980).
2. KUNKLER (1980). Indirite—0.02.
3. KUNKLER (1980). Indirite—0.03.

(between no. 40-4 and no. 36-4) and further drops to 34 in their most fractionated brine (no. 39-4) precipitating potash salts. Salt norms for the two successions (Table 13) and their corresponding salt precipitates are similar to the succession calculated from experimental data (A-1 through A-7 in Table 12) indicating that polyhalite was not forming in either succession of pans.

Validity of rustler water samples

LAMBERT and HARVEY (1987), as part of their stable isotope study, have designated certain water samples from drill sites of questionable validity based on drilling records and properties of the sampled fluids. Coupled with our own evaluation of fluid properties and site locations, samples from one

waters discharged in the Malaga Bend area (1–5), Laguna Grande de Sal (6), and Surprise Spring (7–8)

4	5	6	7	8
ANDERSON	ANDERSON	GRANDE	SURPRISE	SURPRISE
4/20/66	4/20/66	9/81	1938	1975
1.214	1.215	1.213	—	—
—	—	7.40	—	—
mg/L	mg/L	mg/kg	mg/L	mg/L
3,790.	3,820.	5,610.	304.	2,200.
480.	428.	376.	76.6	2,000.
—	—	24.	1.0	6.0
—	—	7.5	—	4.0
118,000.	118,000.	87,400.	1,175.	14,400.
6,920.	6,930.	15,700.	128.	580.
187,000.	187,000.	157,000.	3,080.	30,000.
—	—	73.2	—	16.
158.	164.	—	150.	170.
17,100.	16,900.	12,900.	2,610.	3,470.
29.	28.	29.	—	—
334,000.	333,000.	279,000.	8,210.	52,900.
1.002	1.003	0.997	0.819	1.003
—	—	2,144.	—	1,875.
—	—	—	—	0.2
<0.1	<0.1	—	1.2	—
—	—	—	36.7	9.3
—	—	—	—	—
0.6	0.5	—	—	—
—	—	—	5.3	—
1.0	0.9	1.0	—	—
8.2	8.4	8.0	—	—
89.8	89.9	79.7	42.1	69.2
0.2	0.3	4.5	—	—
—	—	6.8	7.8	4.8
—	—	—	6.9	8.8
—	—	—	—	7.4
—	—	—	—	0.1
<0.1	<0.1	—	1.2	0.1
0.5	0.4	0.5	36.7	9.3
5.5	5.6	5.1	5.3	—
0.7	0.6	0.3	—	—
89.9	89.9	79.8	42.1	69.4
3.4	3.5	10.5	3.4	2.1
—	—	3.8	11.2	16.2
—	—	—	—	2.7

* Simple-salt rose plotted on subsequent maps and diagrams.
Source of analysis; minor normative salts (anhydrous weight percent):
4. Lake surface water. KUNKLER (1980). Indirite—0.04.
5. Water at 10 foot depth. KUNKLER (1980). Indirite—0.04.
6. Rettig (this report). Indirite—0.05, $Li_2SO_4 \cdot H_2O$—0.02, celestite—0.02.
7. U.S.G.S. (unpublished). Celestite—0.03.
8. U.S.G.S. (unpublished). $SrCl_2 \cdot 2H_2O$—0.2, $LiCl \cdot H_2O$—0.05.

or more of the Rustler horizons at three sites were eliminated from further consideration in this discussion (Table 14).

Five samples in Table 14 questioned by LAMBERT and HARVEY (1987) were retained for our discussion, as their salt norms and Cl/Br ratios (when available) suggest only negligible contamination. Furthermore, we have added to the list three samples from two sites where recent anthropogenic activity, chiefly the release of waters from nearby potash mining, have locally influenced water composition.

Table 9. Chemical analysis, salt norm (anhydrous weight

	1*	2	3*	4	5*	6
Site	H-1	H-2	H-2	H-3	H-3	H-3
Date collected	6/2/76	2/22/77	4/21/86	3/17/77	6/11/84	2/4/85
Density (g/cc)	—	—	1.009	—	1.035	—
pH	7.6	8.4	8.0	7.4	7.4	7.4
Chemical analysis	mg/L	mg/L	mg/L	mg/L	mg/L	mg/L
Mg	280.	160.	167.	670.	829.	783.
Ca	780.	690.	743.	1,500.	1,550.	1,470.
Sr	—	—	9.54	—	22.6	30.5
Li	—	—	0.225	—	0.53	0.4
Na	9,400.	2,100.	3,570.	19,000.	17,400.	18,000.
K	190.	91.	93.5	630.	495.	425.
F	5.1	2.0	2.24	0.5	2.09	1.94
Cl	12,000.	2,800.	5,310.	29,600.	29,500.	30,300.
Br	—	—	5.6	—	28.8	25.8
I	—	—	0.081	—	0.133	0.138
NO_3	—	0.04	—	0.3	—	—
HCO_3	105.	59.	60.	115.	52.0	52.0
CO_3	—	5.0	—	—	—	—
SO_4	7,400.	3,000.	2,980.	5,700.	5,130.	4,820.
B	2.4	9.5	10.4	20.	30.	26.3
TDS	30,200.	8,920.	13,000.	57,200.	55,000.	55,900.
Balance (+/−)	0.962	0.987	0.977	1.017	0.973	0.974
Cl/Br	—	—	948.	—	1,020.	1,170.
Salt norm						
Dolomite	—	—	—	—	—	—
Magnesite	0.2	0.5	0.3	0.10	0.1	0.1
Anhydrite	—	19.9	17.2	6.8	9.7	9.1
Kieserite	—	—	—	3.0	2.9	2.6
Epsomite	—	—	0.4	—	—	—
Polyhalite	—	7.5	5.3	4.3	—	—
Bloedite	9.4	14.3	9.1	—	—	—
Glauberite	18.4	5.7	—	—	—	—
Aphthitalite	1.8	—	—	—	—	—
Thenardite	5.2	—	—	—	—	—
Syngenite	—	—	—	—	—	—
Kainite	—	—	—	—	—	—
Halite	64.8	51.6	67.1	83.5	81.8	83.2
Sylvite	—	—	—	—	—	—
Carnallite	—	—	—	2.2	4.0	3.4
Bischofite	—	—	—	—	1.3	1.4
Tachyhydrite	—	—	—	—	—	—
Antarcticite	—	—	—	—	—	—
Simple salts						
$CaCO_3$	—	—	—	—	—	—
$MgCO_3$	0.2	0.5	0.3	0.11	0.1	0.6
$CaSO_4$	9.0	26.4	19.9	8.8	9.8	9.1
$MgSO_4$	4.3	8.2	5.7	3.9	2.9	2.6
K_2SO_4	1.4	2.3	1.6	1.3	—	—
Na_2SO_4	20.2	10.7	5.0	—	—	—
Na_2Cl_2	64.8	51.8	67.5	83.7	82.0	83.4
K_2Cl_2	—	—	—	1.0	1.8	1.5
$MgCl_2$	—	—	—	1.2	3.5	3.3
$CaCl_2$	—	—	—	—	—	—

* Simple-salt rose plotted on subsequent maps and diagrams.

Source of analysis; minor normative salts (anhydrous weight percent):

1. MERCER (1983). Borax—0.04, sellaite—0.03.
2. MERCER (1983). Ulexite—0.5, sellaite—0.04, niter—0.0007.
3. Bendix (unpub.). Indirite—0.4, celestite—0.2, sellaite—0.03, $Li_2SO_4 \cdot H_2O$—0.01.
4. MERCER (1983). Indirite—0.2, sellaite—0.001, niter—0.0009.
5. Bendix (unpub.). Indirite—0.2, celestite—0.09, $Li_2SO_4 \cdot H_2O$—0.008, sellaite—0.006.
6. Bendix (unpub.). Indirite—0.2, celestite—0.1, $Li_2SO_4 \cdot H_2O$—0.006, sellaite—0.006.

percent), and simple salts (weight percent) of Culebra waters

7	8	9	10*	11	12	13
H-4	H-4	H-4	H-4	H-5	H-5	H-5
12/14/78	5/29/81	8/10/84	7/20/85	12/19/78	6/1/81	10/15/81
—	1.010	1.010	1.015	—	1.100	1.100
7.6	8.0	7.8	7.7	6.8	7.9	7.9
mg/L	mg/L	mg/L	mg/L	mg/L	mg/L	mg/L
430.	455.	505.	427.	1,900.	2,140.	2,150.
180.	700.	698.	691.	360.	1,710.	1,720.
—	14.	17.8	14.3	—	31.6	31.3
—	0.39	0.49	0.40	—	0.77	0.77
5,800.	6,080.	6,150.	5,850.	53,000.	52,400.	52,300.
180.	215.	222.	210.	1,400.	1,290.	1,300.
1.9	—	2.13	—	1.4	—	—
7,500.	7,980.	7,950.	7,480.	86,000.	89,500.	89,500.
—	41.5	47.7	42.6	—	62.5	64.
—	—	0.226	—	—	—	—
0.09	—	—	—	0.04	—	—
59.	71.	75.	70.	41.	80.	86.
—	—	—	—	—	—	—
4,000.	6,230.	5,700.	5,520.	810.	7,360.	7,570.
19.	17.9	19.8	14.1	36.	33.2	35.2
18,200.	21,800.	21,400.	20,300.	144,000.	155,000.	155,000.
1.015	0.959	1.014	1.007	1.029	0.963	0.958
—	192.	167.	176.	—	1,430.	1,400.
—	—	—	—	<0.1	—	—
0.2	0.2	0.2	0.2	—	<0.1	<0.1
—	2.0	5.5	3.3	0.8	3.0	3.9
—	—	—	—	—	2.5	2.6
—	—	—	—	—	—	—
0.5	7.3	7.5	7.5	—	—	—
24.3	19.0	21.0	18.4	—	—	—
2.5	11.2	3.5	9.1	—	—	—
—	—	—	—	—	—	—
—	—	—	—	—	—	—
3.6	—	—	—	—	—	—
—	—	—	—	—	—	—
68.3	59.6	61.7	61.0	92.2	88.4	88.3
—	—	—	—	—	—	—
—	—	—	—	4.2	3.7	3.8
—	—	—	—	2.7	1.4	1.4
—	—	—	—	—	—	—
—	—	—	—	—	—	—
—	—	—	—	<0.1	—	—
0.2	0.2	0.2	0.2	<0.1	<0.1	<0.1
3.1	11.1	10.8	11.4	0.8	3.9	3.9
11.3	10.4	11.3	10.1	—	2.5	2.6
2.2	2.3	2.3	2.3	—	—	—
14.5	16.1	13.2	14.7	—	—	—
68.7	60.0	62.1	61.3	92.3	88.5	88.4
—	—	—	—	1.8	1.6	1.7
—	—	—	—	5.0	3.5	3.5
—	—	—	—	—	—	—

* Simple-salt rose plotted on subsequent maps and diagrams.

Source of analysis; minor normative salts (anhydrous weight percent):

7. MERCER (1983). Ulexite—0.5, sellaite—0.02, niter—0.0008.
8. Bendix (unpub.). Ulexite—0.4, celestite—0.1, $Li_2SO_4 \cdot H_2O$—0.02.
9. Bendix (unpub.). Ulexite—0.5, celestite—0.2, $Li_2SO_4 \cdot H_2O$—0.02, sellaite—0.02.
10. Bendix (unpub.). Ulexite—0.3, celestite—0.1, $Li_2SO_4 \cdot H_2O$—0.02.
11. MERCER (1983). Indirite—0.1, inyoite—0.01, fluorite—0.002, nitrocalcite—0.00004.
12. Bendix (unpub.). Indirite—0.1, celestite—0.04, $Li_2SO_4 \cdot H_2O$—0.004.
13. Bendix (unpub.). Indirite 0.1, celestite—0.04, $Li_2SO_4 \cdot H_2O$—0.004.

Table 9 (Continued)

	14*	15	16	17*	18	19
Site	H-5	H-6	H-6	H-6	H-7	H-7
Date collected	8/27/85	12/20/78	5/2/81	9/15/85	3/20/80	3/20/87
Density (g/cc)	1.104	—	1.040	1.042	1.001	1.000
pH	7.4	7.3	7.0	6.9	7.0	7.65
Chemical analysis	mg/L	mg/L	mg/L	mg/L	mg/L	mg/kg
Mg	2,170.	970.	1,080.	1,040.	130.	130.
Ca	1,700.	1,200.	2,150.	2,040.	590.	530.
Sr	29.3	—	32.0	30.4	—	12.
Li	0.81	—	0.44	0.45	—	0.1
Na	54,100.	18,000.	18,600.	18,000.	210.	238.
K	1,350.	500.	450.	375.	1.4	11.
F	1.95	1.5	—	1.9	1.4	—
Cl	85,400.	28,000.	33,000.	32,330.	350.	337.
Br	48.6	—	34.3	34.0	—	0.76
I	0.191	—	—	0.096	—	—
NO_3	—	0.09	—	—	1.8	—
HCO_3	49.	—	96.	94.	—	130.
CO_3	—	—	—	—	—	—
SO_4	7,840.	3,800.	3,980.	3,570.	1,900.	1,960.
B	33.7	9.5	10.9	10.4	0.78	1.9
TDS	153,000.	52,500.	59,400.	58,000.	3,190.	3,350.
Balance (+/−)	1.030	1.076	1.001	0.992	0.995	0.915
Cl/Br	1,760.	—	962.	951.	—	443.
Salt norm						
Dolomite	—	—	0.1	0.1	—	—
Magnesite	<0.1	—	—	—	—	2.7
Anhydrite	3.7	7.4	9.5	8.8	63.1	57.1
Kieserite	3.2	2.8	—	—	18.8	—
Epsomite	—	—	—	—	—	13.0
Polyhalite	—	—	—	—	—	2.6
nBloedite	—	—	—	—	—	7.1
Glauberite	—	—	—	—	—	—
Aphthitalite	—	—	—	—	—	—
Thenardite	—	—	—	—	—	—
Syngenite	—	—	—	—	—	—
Kainite	—	—	—	—	—	—
Halite	88.4	83.3	79.6	80.0	16.8	16.4
Sylvite	—	—	—	—	—	—
Carnallite	3.8	4.0	3.3	2.9	0.2	—
Bischofite	0.7	2.5	1.6	1.0	0.9	—
Tachyhydrite	—	—	5.8	7.0	—	—
Antarcticite	—	—	—	—	—	—
Simple salts						
$CaCO_3$	—	—	0.1	0.1	—	—
$MgCO_3$	<0.1	—	0.1	0.1	—	2.7
$CaSO_4$	3.7	7.4	9.5	8.8	63.3	59.0
$MgSO_4$	3.2	2.8	—	—	18.8	17.0
K_2SO_4	—	—	—	—	—	0.8
Na_2SO_4	—	—	—	—	—	3.9
Na_2Cl_2	88.6	83.4	79.7	80.2	16.9	16.6
K_2Cl_2	1.7	1.7	1.5	1.3	0.1	—
$MgCl_2$	2.9	4.7	7.1	7.1	1.0	—
$CaCl_2$	—	—	2.1	2.6	—	—

* Simple-salt rose plotted on subsequent maps and diagrams.

Source of analysis; minor normative salts (anhydrous weight percent):

14. Bendix (unpub.). Indirite—0.1, celestite—0.04, $Li_2SO_4 \cdot H_2O$—0.004, sellaite—0.002.
15. MERCER (1983). Indirite—0.08, sellaite—0.005, nitromagnesite—0.0002.
16. Bendix (unpub.). Inyoite—0.09, $SrCl_2 \cdot 2H_2O$—0.1, $LiCl \cdot H_2O$—0.005.
17. Bendix (unpub.). Inyoite—0.09, $SrCl_2 \cdot 2H_2O$—0.1, $LiCl \cdot H_2O$—0.005, fluorite—0.007.
18. MERCER (1983). Indirite—0.1, nitromagnesite—0.07, sellaite—0.07.
19. Rettig (this report). Celestite—0.8, indirite—0.3, $Li_2SO_4 \cdot H_2O$—0.03.

Table 9 (Continued)

20*	21	22	23*	24	25*	26*
H-7	H-8	H-8	H-8	H-9	H-9	H-10
3/26/86	2/11/80	2/11/80	1/22/86	2/5/80	11/14/85	3/21/80
1.001	1.000	1.000	1.002	1.000	1.002	1.044
7.2	7.3	7.61	7.6	7.57	7.4	8.01
mg/L	mg/L	mg/kg	mg/L	mg/kg	mg/L	mg/kg
130.	170.	150.	157.	150.	137.	785.
587.	570.	530.	548.	580.	590.	1,580.
8.51	—	7.0	6.92	11.	7.5	19.
0.1	—	0.1	0.115	0.2	0.175	0.6
207.	82.	81.	55.1	220.	146.	20,600.
7.0	4.7	4.3	3.83	8.	6.85	479.
1.51	2.4	—	2.45	—	3.31	—
320.	57.0	60.	30.5	327.	194.	33,600.
0.57	—	0.18	0.085	0.58	.24	12.
0.0525	—	—	0.145	—	0.11	—
—	4.2	—	—	110.	110.	50.
120.	—	76.	95.	—	—	—
—	—	—	—	—	—	—
1,850.	2,000.	2,050.	1,950.	2,070.	1,903.	4,950.
0.755	0.58	0.89	0.485	1.1	0.63	29.
3,230.	2,890.	2,960.	2,850.	3,480.	3,100.	62,100.
0.995	1.061	0.933	0.994	0.947	1.007	0.999
561.	—	333.	359.	564.	808.	2,800.
—	—	—	—	—	—	—
2.6	—	1.8	2.4	2.2	2.5	0.1
62.3	63.9	64.3	66.2	58.9	64.7	8.6
—	—	—	—	—	—	2.3
16.0	23.7	19.7	20.6	17.4	16.2	—
1.6	0.5	1.1	1.0	1.8	1.6	—
0.1	8.1	9.28	7.2	3.3	3.6	—
—	—	—	—	—	—	—
—	—	—	—	—	—	—
—	—	—	—	—	—	—
—	—	—	—	—	—	—
—	—	—	—	—	—	—
16.6	3.3	3.3	1.8	15.5	10.5	84.3
—	—	—	—	—	—	—
—	—	—	—	—	—	3.4
—	—	—	—	—	—	1.1
—	—	—	—	—	—	—
—	—	—	—	—	—	—
—	—	—	—	—	—	—
2.6	—	1.8	2.4	2.2	2.5	0.1
63.6	64.5	65.3	67.2	60.3	66.1	8.7
16.5	27.7	24.3	24.4	19.5	18.3	2.3
0.5	0.1	0.3	0.3	0.5	0.5	—
0.1	4.4	5.0	4.0	1.8	2.0	—
16.7	3.3	3.4	1.8	15.7	10.6	84.6
—	—	—	—	—	—	1.5
—	—	—	—	—	—	3.0
—	—	—	—	—	—	—

* Simple-salt rose plotted on subsequent maps and diagrams.

Source of analysis; minor normative salts (anhydrous weight percent):

20. Bendix (unpub.). Celestite—0.6, indirite—0.1, sellaite—0.078, $Li_2SO_4 \cdot H_2O$—0.03.
21. MERCER (1983). Niter—0.2, indirite—0.09, sellaite—0.1.
22. Rettig (this report). Celestite—0.5, indirite—0.1, $Li_2SO_4 \cdot H_2O$—0.03.
23. Bendix (unpub.). Celestite—0.5, indirite—0.08, sellaite—0.1, $Li_2SO_4 \cdot H_2O$—0.03.
24. Rettig (this report). Celestite—0.7, indirite—0.1, $Li_2SO_4 \cdot H_2O$—0.05.
25. Bendix (unpub.). Celestite—0.5, indirite—0.09, sellaite—0.2, $Li_2SO_4 \cdot H_2O$—0.05.
26. Rettig (this report). Indirite—0.2, celestite—0.6, $Li_2SO_4 \cdot H_2O$—0.008.

Table 9 (Continued)

	27*	28*	29	30	31*	32
Site	H-11	H-12	ENGEL	P-14	P-14	P-15
Date collected	6/3/85	8/8/85	3/5/85	3/14/77	2/26/86	5/10/77
Density (g/cc)	1.090	1.096	—	—	1.019	—
pH	7.2	7.2	7.4	6.0	6.8	—
Chemical analysis	mg/L	mg/L	mg/L	mg/L	mg/L	mg/L
Mg	1,320.	1,980.	152.	760.	840.	63.
Ca	1,700.	1,760.	588.	3,100.	3,510.	770.
Sr	24.7	30.6	8.36	—	50.8	—
Li	0.615	1.15	0.17	—	0.275	—
Na	40,400.	49,200.	200.	7,600.	4,360.	6,900.
K	943.	1,270.	5.6	600.	37.9	1,700.
F	—	—	2.8	0.9	1.69	1.2
Cl	65,900.	79,000.	231.	20,000.	14,470.	11,000.
Br	47.4	76.	0.27	—	72.	—
I	—	—	0.116	—	0.415	—
NO_3	55.	53.	110.	0.04	—	0.2
HCO_3	—	—	—	357.	110.	63.
CO_3	—	—	—	—	—	24.
SO_4	7,180.	7,210.	1,990.	1,400.	1,590.	3,200.
B	31.7	39.3	0.97	0.7	0.72	4.7
TDS	118,000.	141,000.	3,290.	33,800.	25,000.	23,700.
Balance (+/−)	0.983	1.018	1.019	0.940	0.983	1.022
Cl/Br	1,390.	1,040.	856.	—	201.	—
Salt norm						
Dolomite	—	—	—	0.8	0.3	—
Magnesite	<0.1	0.026	2.4	—	—	0.3
Anhydrite	4.8	4.20	60.3	5.8	9.0	2.4
Kieserite	3.1	2.71	—	—	—	—
Epsomite	—	—	15.1	—	—	—
Polyhalite	0.3	—	1.2	—	—	3.8
Bloedite	—	—	8.2	—	—	—
Glauberite	—	—	—	—	—	—
Aphthitalite	—	—	—	—	—	—
Thenardite	—	—	—	—	—	—
Syngenite	—	—	—	—	—	15.1
Kainite	—	—	—	—	—	—
Halite	88.3	88.0	11.8	59.7	45.0	73.0
Sylvite	—	—	—	—	—	5.3
Carnallite	3.3	3.88	—	8.1	0.7	—
Bischofite	—	1.02	—	—	—	—
Tachyhydrite	—	—	—	6.8	20.3	—
Antarcticite	—	—	—	18.9	24.4	—
Simple salts						
$CaCO_3$	—	—	—	0.4	0.2	—
$MgCO_3$	<0.1	0.26	2.4	0.4	0.2	0.3
$CaSO_4$	5.0	4.21	61.4	5.8	9.0	10.9
$MgSO_4$	3.1	2.72	19.4	—	—	0.8
K_2SO_4	0.1	—	0.4	—	—	9.7
Na_2SO_4	—	—	4.5	—	—	—
Na_2Cl_2	88.4	88.1	11.9	59.7	45.1	73.1
K_2Cl_2	1.5	1.71	—	3.5	0.3	5.3
$MgCl_2$	1.9	3.20	—	8.8	13.2	—
$CaCl_2$	—	—	—	21.4	32.0	—

* Simple-salt rose plotted on subsequent maps and diagrams.

Source of analysis; minor normative salts (anhydrous weight percent):

27. Bendix (unpub.). Indirite—0.1, celestite—0.04, $Li_2SO_4 \cdot H_2O$—0.004.
28. Bendix (unpub.). Indirite—0.1, celestite—0.05, $Li_2SO_4 \cdot H_2O$—0.006.
29. Bendix (unpub.). Celestite—0.5, indirite—0.1, sellaite—0.1, $Li_2SO_4 \cdot H_2O$—0.04.
30. MERCER (1983). Inyoite—0.01, fluorite—0.005, nitrocalcite—0.0002.
31. Bendix (unpub.). $SrCl_2 \cdot 2H_2O$—0.3, inyoite—0.01, fluorite—0.01, $LiCl \cdot H_2O$—0.007.
32. MERCER (1983). Ulexite—0.1, sellaite—0.008, niter—0.001.

Table 9 (Continued)

33	34*	35*	36	37	38*	39
P-17	P-17	P-18	WIPP-25	WIPP-25	WIPP-25	WIPP-25
5/10/77	3/17/86	5/10/77	8/14/80	8/14/80	8/20/80	2/12/86
—	1.065	—	1.014	1.011	1.010	1.010
7.4	7.5	7.2	7.3	7.11	6.9	7.2
mg/L	mg/L	mg/L	mg/L	mg/kg	mg/L	mg/L
1,600.	1,460.	16,000.	250.	247.	260.	315.
1,700.	1,620.	5,600.	920.	890.	905.	1,140.
—	29.1	—	—	12.	12.	16.6
—	0.87	—	—	0.2	0.2	0.22
30,000.	28,300.	9,200.	5,100.	5,300.	3,160.	3,180.
120.	782.	6,200.	0.9	69.	73.5	102.
1.5	1.87	1.2	1.4	—	—	1.68
54,000.	48,220.	80,000.	8,300.	8,020.	5,250.	6,320.
—	71.5	—	—	2.4	2.6	3.35
—	0.175	—	—	—	—	0.042
0.3	—	3.6	3.0	—	—	—
77.	61.	310.	—	—	210.	130.
—	—	—	—	—	—	—
5,000.	6,020.	980.	2,400.	2,570.	2,500.	2,380.
1.7	37.5	100.	1.9	1.8	1.52	1.67
92,500.	86,600.	118,000.	17,000.	17,100.	12,400.	13,600.
0.936	0.978	0.942	1.014	1.063	1.013	0.974
—	674.	—	—	3,340.	2,020.	1,890.
—	—	0.2	—	—	—	0.7
0.1	<0.1	—	—	—	1.2	—
6.5	6.5	1.2	18.2	17.0	24.9	24.7
0.9	2.9	—	1.7	4.1	3.5	—
—	—	—	—	—	—	—
—	—	—	—	—	—	—
—	—	—	—	—	—	—
—	—	—	—	—	—	—
—	—	—	—	—	—	—
—	—	—	—	—	—	—
—	—	—	—	—	—	—
—	—	—	—	—	—	—
86.0	84.4	20.6	75.7	75.8	65.0	60.8
—	—	—	—	—	—	—
0.6	4.0	23.7	<0.1	1.7	2.6	3.3
6.0	2.0	20.6	4.3	1.2	2.6	1.7
—	—	33.4	—	—	—	8.4
—	—	—	—	—	—	—
—	—	0.1	—	—	—	0.4
0.1	<0.1	0.1	—	—	1.2	0.3
6.5	6.5	1.2	18.3	17.0	24.9	24.8
0.9	2.9	—	1.7	4.1	3.5	—
—	—	—	—	—	—	—
—	—	—	—	—	—	—
86.0	84.6	20.6	75.7	75.9	65.1	61.0
0.3	1.8	10.4	<0.1	0.7	1.1	1.5
6.3	4.3	55.2	4.3	2.2	4.1	8.9
—	—	12.3	—	—	—	3.1

* Simple-salt rose plotted on subsequent maps and diagrams.

Source of analysis; minor normative salts (anhydrous weight percent):

33. MERCER (1983). Indirite—0.008, sellaite—0.003, nitromagnesite—0.0004.
34. Bendix (unpub.). Indirite—0.2, celestite—0.07, $Li_2SO_4 \cdot H_2O$—0.008, sellaite—0.004.
35. MERCER (1983). Inyoite—0.4, nitrocalcite—0.004, fluorite—0.002.
36. MERCER (1983). Indirite—0.05, nitromagnesite—0.02, sellaite—0.01.
37. Rettig (this report). Celestite—0.1, indirite—0.05, $Li_2SO_4 \cdot H_2O$—0.009.
38. Bendix (unpub.). Celestite—0.2, indirite—0.06, $Li_2SO_4 \cdot H_2O$—0.01.
39. Bendix (unpub.). $SrCl_2 \cdot 2H_2O$—0.2, inyoite—0.06, fluorite—0.03, $LiCl \cdot H_2O$—0.01.

Table 9 (Continued)

	40*	41	42	43	44	45
Site	WIPP-26	WIPP-26	WIPP-26	WIPP-27	WIPP-27	WIPP-28
Date collected	8/18/80	8/24/80	11/25/85	8/22/80	9/3/80	8/21/80
Density (g/cc)	1.009	1.005	1.012	1.092	1.090	1.041
pH	7.34	6.9	7.1	6.63	6.3	6.80
Chemical analysis	mg/kg	mg/L	mg/L	mg/kg	mg/L	mg/kg
Mg	362.	355.	380.	1,740.	1,900.	624.
Ca	1,190.	1,240.	1,340.	2,700.	3,210.	1,130.
Sr	19.	16.8	19.5	44.	50.9	17.
Li	0.2	0.24	0.23	—	0.33	—
Na	3,770.	3,620.	4,220.	38,500.	39,200.	19,900.
K	149.	170.	343.	7,140.	8,060.	346.
F	—	—	1.73	—	—	—
Cl	7,260.	7,200.	8,770.	73,300.	78,500.	32,400.
Br	3.0	3.2	3.9	27.	28.3	1.0
I	—	—	0.0695	—	—	—
NO_3	—	—	—	—	—	—
HCO_3	—	140.	120.	—	120.	—
CO_3	—	—	—	—	—	—
SO_4	2,380.	2,480.	2,420.	3,300.	3,830.	3,360.
B	1.8	1.45	1.65	2.1	2.3	2.9
TDS	15,100.	15,200.	17,600.	127,000.	135,000.	57,800.
Balance (+/−)	1.012	0.985	0.970	1.000	0.971	0.999
Cl/Br	2,420.	2,250.	2,250.	2,710.	2,770.	32,400.
Salt norm						
Dolomite	—	0.7	0.5	—	0.1	—
Magnesite	—	—	—	—	—	—
Anhydrite	22.4	23.1	19.3	3.7	4.0	6.6
Kieserite	—	—	—	—	—	1.4
Epsomite	—	—	—	—	—	—
Polyhalite	—	—	—	—	—	—
Bloedite	—	—	—	—	—	—
Glauberite	—	—	—	—	—	—
Aphthitalite	—	—	—	—	—	—
Thenardite	—	—	—	—	—	—
Syngenite	—	—	—	—	—	—
Kainite	—	—	—	—	—	—
Halite	62.8	61.3	62.3	77.2	75.3	87.6
Sylvite	—	—	—	6.5	7.2	—
Carnallite	4.2	4.9	8.7	9.6	10.0	2.6
Bischofite	—	—	—	—	—	1.7
Tachyhydrite	9.0	9.7	5.6	—	—	—
Antarcticite	1.2	<0.1	3.4	2.9	3.4	—
Simple salts						
$CaCO_3$	—	0.4	0.3	—	0.1	—
$MgCO_3$	—	0.3	0.2	—	—	—
$CaSO_4$	22.4	23.1	19.4	3.7	4.0	6.7
$MgSO_4$	—	—	—	—	—	1.4
K_2SO_4	—	—	—	—	—	—
Na_2SO_4	—	—	—	—	—	—
Na_2Cl_2	63.0	61.5	62.5	77.3	75.3	87.7
K_2Cl_2	1.9	2.2	3.8	10.8	11.6	1.1
$MgCl_2$	9.3	8.9	8.40	5.4	5.6	3.1
$CaCl_2$	3.3	3.6	5.4	2.9	3.4	—

* Simple-salt rose plotted on subsequent maps and diagrams.

Source of analysis; minor normative salts (anhydrous weight percent):

40. Rettig (this report). $SrCl_2 \cdot 2H_2O$—0.2, inyoite—0.06, $LiCl \cdot H_2O$—0.008.
41. Bendix (unpub.). $SrCl_2 \cdot 2H_2O$—0.2, inyoite—0.05, $LiCl \cdot H_2O$—0.01.
42. Bendix (unpub.). $SrCl_2 \cdot 2H_2O$—0.2, inyoite—0.05, fluorite—0.002, $LiCl \cdot H_2O$—0.008.
43. Rettig (this report). $SrCl_2 \cdot 2H_2O$—0.06, inyoite—0.008.
44. Bendix (unpub.). $SrCl_2 \cdot 2H_2O$—0.07, inyoite—0.008, $LiCl \cdot H_2O$—0.002.
45. Rettig (this report). Celestite—0.06, indirite—0.02.

Table 9 (Continued)

46*	47	48	49	50*	51
WIPP-28	WIPP-29	WIPP-29	WIPP-29	WIPP-30	WIPP-30
9/11/80	8/20/80	8/28/80	12/14/85	8/13/80	9/6/80
1.030	1.174	1.160	1.216	1.070	1.020
6.5	6.88	6.1	5.9	6.36	8.8
mg/L	mg/kg	mg/L	mg/L	mg/kg	mg/L
555.	3,750.	5,480.	6,500.	804.	460.
1,180.	6,980.	950.	413.	1,010.	1,140.
15.5	20.	28.8	12.8	15.	17.9
0.3	1.0	0.78	0.7	—	0.27
15,200.	67,600.	71,400.	94,900.	35,500.	8,570.
485.	1,270.	15,600.	23,300.	888.	255.
—	—	—	4.59	—	—
24,800.	123,000.	138,000.	178,800.	56,500.	14,600.
7.2	44.	45.	61.	30.	10.5
—	—	—	0.385	—	—
—	—	—	—	—	40.
—	—	210.	160.	—	17.
—	—	—	—	5,050.	4,120.
4,380.	1,120.	14,000.	20,000.	—	—
5.83	—	4.4	5.17	18.	6.09
46,600.	219,000.	246,000.	324,000.	99,800.	29,200.
0.984	0.975	0.956	0.967	0.991	0.950
3,440.	2,800.	3,070.	2,930.	1,880.	1,390.
—	—	—	—	—	—
—	—	0.1	<0.1	—	0.2
7.7	—	—	—	1.9	13.5
3.1	—	—	—	1.9	5.0
—	—	—	—	—	—
2.0	2.3	2.8	0.9	3.2	0.3
—	—	—	—	—	—
—	—	—	—	—	—
—	—	—	—	—	—
—	—	—	—	—	—
—	—	—	—	—	—
—	7.1	7.8	11.1	—	—
83.7	79.7	76.0	76.0	90.9	77.0
—	5.6	5.1	7.6	—	—
3.3	5.3	8.6	4.3	2.0	3.7
—	—	—	—	—	—
—	—	—	—	—	—
—	—	—	—	—	—
—	—	—	—	—	—
—	—	0.1	<0.1	—	0.2
8.7	1.1	1.4	0.4	3.5	13.7
3.5	4.9	5.2	7.0	2.6	5.1
0.6	0.7	0.9	0.3	1.0	0.1
—	—	—	—	—	—
83.8	79.7	76.0	76.0	91.0	77.2
1.5	10.6	11.7	13.8	0.9	1.6
1.9	3.0	4.8	2.4	1.1	2.1
—	—	—	—	—	—

* Simple-salt rose plotted on subsequent maps and diagrams.

Source of analysis; minor normative salts (anhydrous weight percent):

46. Bendix (unpub.). Indirite—0.06, celestite—0.07, $Li_2SO_4 \cdot H_2O$—0.005.
47. Rettig (this report). Celestite—0.02, $Li_2SO_4 \cdot H_2O$—0.004.
48. Bendix (unpub.). Celestite—0.03, indirite—0.008, $Li_2SO_4 \cdot H_2O$—0.003.
49. Bendix (unpub.). Indirite—0.007, celestite—0.009, sellaite—0.002, $Li_2SO_4 \cdot H_2O$—0.002.
50. Rettig (this report). Indirite—0.08, celestite—0.03.
51. Bendix (unpub.). Indirite—0.09, celestite—0.1, $Li_2SO_4 \cdot H_2O$—0.008.

Table 9 (Continued)

Site	52 GNOME SHAFT	53* GNOME-1	54 GNOME-4	55 GNOME-8	56* INDIAN
Date collected	12/10/60	8/18/60	12/5/61	1/27/63	1/22/63
Density (g/cc)	—	—	—	—	—
pH	7.7	7.6	7.5	7.1	7.6
Chemical analysis	mg/kg	mg/kg	mg/kg	mg/kg	mg/kg
Mg	153.	146.	134.	155.	169.
Ca	597.	608.	644.	624.	624.
Sr	—	—	8.8	1.0	1.1
Li	—	—	0.1	0.25	0.27
Na	555.	520.	640.	630.	315.
K	17.	11.	16.	27.	8.6
F	1.9	0.3	1.0	2.4	2.1
Cl	828.	770.	948.	1,190.	533.
Br	—	—	—	—	—
I	—	—	—	—	—
NO_3	11.	7.8	10.	7.6	4.2
HCO_3	106.	114.	114.	108.	193.
CO_3	—	—	—	—	—
SO_4	2,040.	1,960.	1,950.	2,050.	1,950.
B	12.	—	0.8	—	—
TDS	4,320.	4,140.	4,470.	4,800.	3,810.
Balance (+/−)	0.981	1.011	1.031	0.923	1.005
Cl/Br	—	—	—	—	—
Salt norm					
Dolomite	—	—	—	—	—
Magnesite	1.7	1.9	1.8	1.53	3.6
Anhydrite	47.3	49.7	47.9	47.1	56.9
Kieserite	—	—	—	10.7	15.1
Epsomite	12.7	13.6	11.4	—	—
Polyhalite	1.8	1.1	1.5	—	—
Bloedite	3.8	2.1	0.8	—	—
Glauberite	—	—	—	—	—
Aphthitalite	—	—	—	—	—
Thenardite	—	—	—	—	—
Syngenite	—	—	—	—	—
Kainite	—	—	—	—	—
Halite	31.8	31.2	35.8	35.6	21.5
Sylvite	—	—	—	—	—
Carnallite	—	—	—	2.61	1.0
Bischofite	—	—	—	1.60	0.9
Tachyhydrite	—	—	—	—	—
Antarcticite	—	—	—	—	—
Simple salts					
$CaCO_3$	—	—	—	—	—
$MgCO_3$	1.7	2.0	1.8	1.55	3.6
$CaSO_4$	48.6	50.4	49.0	47.5	57.4
$MgSO_4$	15.0	14.8	12.2	10.8	15.3
K_2SO_4	0.5	0.3	0.5	—	—
Na_2SO_4	2.1	1.2	0.4	—	—
Na_2Cl_2	32.1	31.3	36.1	35.9	21.7
K_2Cl_2	—	—	—	1.15	0.4
$MgCl_2$	—	—	—	3.08	1.5
$CaCl_2$	—	—	—	—	—

* Simple-salt rose plotted on subsequent maps and diagrams.

Source of analysis; minor normative salts (anhydrous weight percent):

52. U.S.G.S. (unpub. tech file). Niter—0.4, wagnerite—0.4, $Mg_3(PO_4)_2$—0.08.
53. U.S.G.S. (unpub. tech file). Niter—0.3, sellaite—0.01.
54. U.S.G.S. (unpub. tech file). Celestite—0.4, niter—0.4, sellaite—0.03, wagnerite—0.03, $Li_2SO_4 \cdot H_2O$—0.02.
55. U.S.G.S. (unpub. tech file). Celestite—0.5, nitromagnesite—0.2, sellaite—0.08, $Li_2SO_4 \cdot H_2O$—0.04.
56. U.S.G.S. (unpub. tech file). Celestite—0.6, nitromagnesite—0.1, sellaite—0.09, $Li_2SO_4 \cdot H_2O$—0.06.

Table 9 (Continued)

57* DOE-1 4/24/85 1.090 7.1	58* DOE-2 3/11/85 1.040 7.0	59* TWO-MILE 8/8/62 — 6.7	60* WINDMILL 9/14/61 — 8.0	61 WINDMILL 8/8/62 — 6.8	62* SOUTH 8/8/62 — 7.4
mg/L	mg/L	mg/kg	mg/kg	mg/kg	mg/kg
1,610.	1,060.	177.	139.	138.	90.
1,730.	1,960.	630.	564.	580.	589.
26.2	37.7	14.	—	10.	10.
0.635	0.47	0.32	—	0.32	0.2
45,800.	18,400.	1,410.	525.	500.	24.
1,100.	410.	25.	23.	28.	4.8
—	1.69	2.0	—	3.0	1.4
73,600.	34,600.	2,200.	515.	588.	18.
56.	33.5	—	—	—	—
—	0.225	—	—	—	—
—	—	2.5	—	2.6	9.0
45.	67.	66.	108.	113.	196.
—	—	—	—	—	—
7,350.	3,950.	2,200.	2,290.	2,080.	1,660.
36.6	15.6	—	—	—	—
131,000.	60,500.	6,730.	4,160.	4,040.	2,600.
1.004	0.940	0.993	0.985	1.018	0.993
1,310.	1,030.	—	—	—	—
—	0.1	—	—	—	—
<0.1	—	0.7	1.8	2.0	5.4
4.5	9.0	31.1	45.2	46.6	80.4
3.0	—	11.5	—	—	—
—	—	—	0.8	5.6	8.8
—	—	2.1	4.1	4.7	—
—	—	—	27.5	15.8	2.7
—	—	—	—	—	—
—	—	—	—	—	—
—	—	—	—	—	—
—	—	—	—	—	—
—	—	—	—	—	—
88.4	80.4	53.8	20.6	24.5	1.2
—	—	—	—	—	—
3.6	3.1	0.3	—	—	—
0.2	2.3	—	—	—	—
—	4.9	—	—	—	—
—	—	—	—	—	—
—	<0.1	—	—	—	—
<0.1	<0.1	0.7	1.8	2.0	5.5
4.5	9.1	32.3	47.1	49.2	81.6
3.1	—	12.0	14.3	14.0	10.2
—	—	0.7	1.3	1.5	—
—	—	—	14.9	8.7	1.5
88.6	80.6	54.1	20.6	24.7	1.2
1.6	1.4	0.1	—	—	—
2.3	7.1	0.1	—	—	—
—	1.8	—	—	—	—

* Simple-salt rose plotted on subsequent maps and diagrams.

Source of analysis; minor normative salts (anhydrous weight percent):

57. Bendix (unpub.). Indirite—0.1, celestite—0.04, $Li_2SO_4 \cdot H_2O$—0.004.
58. Bendix (unpub.). Inyoite—0.1, $SrCl_2 \cdot 2H_2O$—0.1, $LiCl \cdot H_2O$—0.005, fluorite—0.006.
59. U.S.G.S. (unpub. tech file). Celestite—0.4, niter—0.06, sellaite—0.049, $Li_2SO_4 \cdot H_2O$—0.03.
60. U.S.G.S. (unpub. tech file).
61. U.S.G.S. (unpub. tech file). Celestite—0.5, sellaite—0.1, niter—0.1, $Li_2SO_4 \cdot H_2O$—0.06.
62. U.S.G.S. (unpub. tech file). Celestite—0.8, niter—0.5, sellaite—0.09, $Li_2SO_4 \cdot H_2O$—0.064, soda niter—0.07.

Table 10. Chemical analysis, salt norm (anhydrous weight

	1*	2*	3	4*
Site	H-1	H-2	H-3	H-3
Date collected	6/4/76	2/22/77	5/10/77	7/1/85
Density (g/cc)	—	—	—	1.006
pH	7.4	8.6	8.0	8.0
Chemical analysis	mg/L	mg/ml	mg/L	mg/L
Mg	270.	170.	480.	292.
Ca	890.	820.	1,200.	1,000.
Sr	—	—	—	17.3
Li	—	—	—	0.32
Na	5,700.	2,700.	9,300.	1,520.
K	70.	81.	250.	34.5
F	2.8	—	1.8	2.43
Cl	8,000.	4,100.	15,000.	3,360.
Br	—	—	—	5.85
I	—	—	—	1.2
NO_3	—	0.2	0.4	—
HCO_3	92.	74.	51.	46.
SO_4	3,900.	2,400.	3,400.	2,310.
B	2.2	0.22	13.	2.05
TDS	18,900.	10,400.	29,700.	8,590.
Balance (+/−)	1.025	1.045	1.030	0.982
Cl/Br	—	—	—	574.
Salt norm				
Dolomite	—	—	—	0.4
Magnesite	0.3	0.5	0.1	—
Anhydrite	14.5	25.1	13.5	38.0
Kieserite	—	5.4	2.6	—
Epsomite	0.6	—	—	—
Polyhalite	2.7	2.5	—	—
Bloedite	11.4	—	—	—
Glauberite	—	—	—	—
Aphthitalite	—	—	—	—
Thenardite	—	—	—	—
Syngenite	—	—	—	—
Halite	70.5	64.7	78.1	45.6
Sylvite	—	—	—	—
Carnallite	—	1.8	3.6	1.8
Bischofite	—	—	1.9	10.0
Tachyhydrite	—	—	—	3.6
Antarcticite	—	—	—	—
Simple salts				
$CaCO_3$	—	—	—	0.2
$MgCO_3$	0.3	0.5	0.1	0.2
$CaSO_4$	15.8	26.3	13.5	38.2
$MgSO_4$	6.4	5.9	2.6	—
K_2SO_4	0.8	0.8	—	—
Na_2SO_4	6.2	—	—	—
Na_2Cl_2	70.5	64.7	78.3	45.9
K_2Cl_2	—	0.8	1.6	0.8
$MgCl_2$	—	1.0	3.9	13.4
$CaCl_2$	—	—	—	1.4

* Simple-salt rose plotted on subsequent maps and diagrams.

Source of analysis; minor normative salts (anhydrous weight percent):

1. MERCER (1983). Indirite—0.5, sellaite—0.03.
2. MERCER (1983). Indirite—0.01, niter—0.003.
3. MERCER (1983). Indirite—0.2, sellaite—0.01, nitromagnesite—0.002.
4. Bendix (unpub.). $SrCl_2 \cdot 2H_2O$—0.4, inyoite—0.1, fluorite—0.06, $LiCl \cdot H_2O$—0.02.

percent), and simple salts (weight percent) of Magenta waters

5*	6*	7*	8	9*
H-4	H-5	H-6	H-8	H-8
12/14/78	12/14/78	12/20/78	2/12/80	2/12/80
—	—	—	1.006	1.004
8.0	7.8	7.3	9.3	7.8
mg/L	mg/L	mg/L	mg/L	mg/kg
410.	170.	160.	17.	15.
210.	240.	520.	870.	845.
—	—	—	—	20.
—	—	—	—	0.2
7,000.	1,500.	1,100.	2,400.	2,300.
130.	53.	46.	84.	75.
2.5	2.8	1.4	0.7	—
7,500.	880.	1,200.	3,500.	3,520.
—	—	—	—	0.82
—	—	—	—	—
0.04	0.04	0.1	0.3	34.
63.	50.	51.	—	2,490.
7,000.	3,200.	2,700.	2,100.	6.9
13.	11.	2.5	3.1	
22,300.	6,110.	5,780.	8,980.	9,310.
0.980	0.996	0.967	1.061	0.959
—	—	—	—	4,290.
—	—	—	—	—
0.2	0.6	0.6	—	0.3
—	—	23.6	29.3	26.0
—	—	—	—	—
—	—	—	—	—
—	—	5.9	4.1	2.2
19.4	28.0	25.9	—	—
6.6	27.3	9.8	—	7.2
1.7	2.5	—	—	—
16.9	17.0	—	—	—
—	—	—	0.6	2.1
55.0	23.7	34.0	65.4	61.4
—	—	—	0.3	—
—	—	—	—	—
—	—	—	—	—
—	—	—	—	—
—	—	—	—	—
—	—	—	—	—
0.2	0.6	0.6	—	0.3
3.3	13.5	31.3	31.7	31.8
8.9	13.0	13.2	0.9	0.5
1.3	2.0	1.8	1.6	1.9
31.2	47.1	19.0	—	3.7
55.1	23.9	34.1	65.5	61.9
—	—	—	0.3	—
—	—	—	—	—
—	—	—	—	—

* Simple-salt rose plotted on subsequent maps and diagrams.

Source of analysis; minor normative salts (anhydrous weight percent):

5. MERCER (1983). Borax—0.3, sellaite—0.02, niter—0.0003.
6. MERCER (1983). Borax—0.8, sellaite—0.08, niter—0.001.
7. MERCER (1983). Ulexite—0.2, sellaite—0.04, niter—0.003.
8. MERCER (1983). Ulexite—0.2, sellaite—0.01, niter—0.006.
9. Rettig (this report). Ulexite—0.4, celestite—0.5, $Li_2SO_4 \cdot H_2O$—0.02.

Table 10 (Continued)

	10*	11	12*	13
Site	H-9	H-9	H-10	WIPP-25
Date collected	2/5/82	2/5/82	3/21/80	9/4/80
Density (g/cc)	1.003	1.000	1.171	1.010
pH	8.5	7.2	4.70	7.5
Chemical analysis	mg/L	mg/kg	mg/kg	mg/L
Mg				
Ca	170.	170.	2,130.	240.
Sr	550.	535.	2,310.	910.
Li	—	15.	38.	—
Na	—	0.3	5.	—
K	800.	800.	78,600.	3,100.
F	28.	26.	307.	0.8
Cl	1.8	—	—	1.5
Br	750.	750.	136,000.	5,600.
I	—	2.5	158.	—
NO_3	0.09	—	—	2.8
HCO_3	—	42.	—	—
SO_4	2,700.	2,760.	2,680.	1,900.
B	2.6	2.5	22.	1.9
TDS	5,000.	5,100.	222,000.	11,800.
Balance (+/−)	0.992	0.963	0.955	1.012
Cl/Br	—	300.	861.	—
Salt norm				
Dolomite	—	—	—	—
Magnesite	—	0.565	—	—
Anhydrite	34.6	32.4	1.7	23.0
Kieserite	—	—	—	—
Epsomite	—	—	—	—
Polyhalite	4.1	3.80	—	—
Bloedite	34.7	33.5	—	—
Glauberite	1.7	4.75	—	—
Aphthitalite	—	—	—	—
Thenardite	—	—	—	—
Syngenite	—	—	—	—
Halite	24.6	24.1	92.5	66.5
Sylvite	—	—	—	—
Carnallite	—	—	0.6	<0.1
Bischofite	—	—	0.8	3.8
Tachyhydrite	—	—	4.2	6.6
Antarcticite	—	—	—	—
Simple salts				
$CaCO_3$	—	—	—	—
$MgCO_3$	—	0.570	—	—
$CaSO_4$	37.6	36.9	1.7	23.0
$MgSO_4$	16.8	16.3	—	—
K_2SO_4	1.3	1.18	—	—
Na_2SO_4	19.7	20.8	—	—
Na_2Cl_2	24.7	24.3	92.6	66.6
K_2Cl_2	—	—	0.3	<0.1
$MgCl_2$	—	—	3.9	8.0
$CaCl_2$	—	—	1.6	2.4

* Simple-salt rose plotted on subsequent maps and diagrams.

Source of analysis; minor normative salts (anhydrous weight percent):

10. MERCER (1983). Ulexite—0.3, sellaite—0.06, niter—0.003.
11. Rettig (this report). Celestite—0.6, ulexite—0.2, $Li_2SO_4 \cdot H_2O$—0.05.
12. Rettig (this report). Inyoite—0.05, $SrCl_2 \cdot 2H_2O$—0.03, $LiCl \cdot H_2O$—0.01.
13. MERCER (1983). Inyoite—0.08, nitrocalcite—0.03, fluorite—0.03.

Table 10 (Continued)

14* WIPP-25 9/4/80 1.007 7.41	15 WIPP-25 9/17/80 1.004 6.9	16 WIPP-27 7/24/80 1.095 6.66	17 WIPP-27 9/25/80 1.090 6.3	18* WIPP-30 9/24/80 1.012 8.2	19* GNOME-5 11/15/61 — 7.6
mg/kg	mg/L	mg/kg	mg/L	mg/kg	mg/kg
248.	260.	1,690.	2,100.	203.	122.
893.	905.	3,290.	3,660.	731.	648.
12.	12.	50.	58.6	15.	—
0.2	0.2	—	0.34	0.2	—
3,340.	2,910.	38,900.	43,200.	5,930.	150.
65.	71.5	7,030.	8,090.	119.	8.3
—	—	—	—	—	1.5
5,460.	5,250.	75,500.	85,200.	7,980.	250.
2.1	2.5	26.	28.3	2.1	—
—	—	—	—	—	13.
—	180.	—	210.	—	103.
2,480.	2,490.	2,830.	3,410.	3,660.	1,940.
1.4	1.54	4.9	2.32	10.	0.72
12,500.	12,100.	129,000.	146,000.	18,700.	3,240.
1.032	0.963	0.994	0.986	1.042	0.993
2,600.	2,100.	2,900.	3,010.	3,800.	—
—	—	—	0.1	—	—
—	1.0	—	—	—	2.2
23.8	26.3	3.1	3.3	7.3	69.4
4.0	2.3	—	—	—	14.7
—	—	—	—	—	—
—	—	—	—	4.5	—
—	—	—	—	9.4	—
—	—	—	—	6.9	—
—	—	—	—	—	—
—	—	—	—	—	—
—	—	—	—	—	—
66.6	63.3	76.7	76.0	71.5	11.7
—	—	6.4	6.2	—	—
2.2	2.7	9.2	10.1	—	1.1
3.2	4.2	—	—	—	—
—	—	—	—	—	—
—	—	4.5	4.2	—	—
—	—	—	0.1	—	—
—	1.0	—	—	—	2.3
23.8	26.4	3.1	3.3	12.9	69.9
4.0	2.3	—	—	5.3	14.8
—	—	—	—	1.4	—
—	—	—	—	8.6	—
66.7	63.4	76.8	76.0	71.8	11.8
1.0	1.2	10.4	10.7	—	0.5
4.5	5.7	5.1	5.7	—	0.6
—	—	4.5	4.2	—	—

* Simple-salt rose plotted on subsequent maps and diagrams.

Source of analysis; minor normative salts (anhydrous weight percent):

14. Rettig (this report). Celestite—0.2, indirite—0.05, $Li_2SO_4 \cdot H_2O$—0.01.
15. Bendix (unpub.). Celestite—0.2, indirite—0.06, $Li_2SO_4 \cdot H_2O$—0.01.
16. Rettig (this report). $SrCl_2 \cdot 2H_2O$—0.07, inyoite—0.02.
17. Bendix (unpub.). $SrCl_2 \cdot 2H_2O$—0.07, inyoite—0.008, $LiCl \cdot H_2O$—0.001.
18. Rettig (this report). Ulexite—0.3, celestite—0.2, $Li_2SO_4 \cdot H_2O$—0.008.
19. U.S.G.S. (unpub. tech file). Soda niter—0.4, nitromagnesite—0.1, indirite—0.1, sellaite—0.08.

Table 11. Chemical analysis, salt norm (anhydrous weight percent), and simple salts (weight percent) of Dewey Lake (1, 2), Santa Rosa (3), and Quaternary sediment (4) waters

	1	2	3	4
Site	WALKER WELL	TWIN PASTURE	H-5	WIPP-15
Date collected	7/31/62	1/30/86	5/24/78	3/12/79
Density (g/cc)	—	0.998	—	—
pH	7.1	7.7	—	—
Chemical analysis	mg/kg	mg/L	mg/L	mg/L
Mg	145.	22.5	51.	81.
Ca	613.	80.4	56.	35.
Sr	8.4	1.06	—	—
Ba	—	—	—	0.2
Li	0.19	—	—	—
Na	140.	25.4	280.	300.
K	3.6	3.85	25.	19.
F	2.0	0.58	1.2	2.0
Cl	325.	44.1	120.	93.
Br	—	0.17	—	—
NO_3	8.0	—	1.6	—
HCO_3	134.	230.	240.	988.
SO_4	1,790.	75.1	530.	170.
B	—	0.13	0.89	1.0
TDS	3,170.	483.	1,310.	1,690.
Balance (+/−)	1.001	1.070	1.072	0.975
Cl/Br	—	259.	—	—
Salt norm				
Calcite	—	7.2	—	—
Dolomite	—	42.0	0.1	13.1
Magnesite	3.0	—	14.2	16.8
Trona	—	—	—	30.7
Burkeite	—	—	—	22.2
Anhydrite	67.1	29.7	—	—
Kieserite	12.6	—	—	—
Glauberite	—	—	30.3	—
Aphthitalite	—	—	5.5	4.4
Thenardite	—	—	32.0	—
Halite	11.5	16.9	17.1	12.1
Sylvite	—	0.9	—	—
Carnallite	0.5	2.3	—	—
Bischofite	4.3	—	—	—
Simple salts				
$CaCO_3$	—	30.3	0.1	7.5
$MgCO_3$	3.0	19.4	14.4	24.2
Na_2CO_3	—	—	—	33.7
$CaSO_4$	67.8	30.0	15.0	—
$MgSO_4$	12.7	—	—	—
K_2SO_4	—	—	4.3	3.6
Na_2SO_4	—	—	49.1	18.1
Na_2Cl_2	11.6	17.0	17.2	12.9
K_2Cl_2	0.2	1.9	—	—
$MgCl_2$	4.6	1.3	—	—

Source of analysis; minor normative salts (anhydrous weight percent):
1. U.S.G.S. (unpub. tech file). Celestite—0.6, nitromagnesite—0.3, sellaite—0.1, $Li_2SO_4 \cdot H_2O$—0.05.
2. Bendix (unpub.). $SrCl_2 \cdot 2H_2O$—0.5, fluorite—0.3, inyoite—0.2.
3. MERCER (1983). Borax—0.4, niter—0.2, fluorite—0.2.
4. GONZOLES (1981). Borax—0.4, villiaumite—0.4, barite—0.03.

Characterization of Rustler Formation waters

The salt norms for the Rustler Formation fluids readily fit four water types: (1) highly concentrated primitive or primary brines, most of which have been involved in diagenetic exchange of magnesium for calcium, and thus termed *primitive-diagenetic* waters; (2) dilute *alkali-bearing carbonate recharge*

Table 12. Salt norms of synthetic isothermal (25°C) evaporating sea water: (A) Experimental data compiled and summarized in BRAITSCH (1971); and (B) Computer-simulated Ca-Mg-Na-K-Cl-SO_4 brines (EUGSTER *et al.*, 1980)

(A)	A-1	A-2	A-3	A-4	A-5	A-6	A-7
TDS (mg/kg)	106,200	273,800	346,600	321,700	328,000	331,900	359,900
Percent water remaining	29.8	9.12	1.66	1.53	1.37	0.82	0.61
Normative salts							
Anhydrite	3.53	0.56	—	—	—	—	—
Kieserite	6.56	6.75	26.5	27.4	24.3	8.41	1.11
Halite	78.4	80.9	27.2	14.5	12.5	3.18	1.08
Carnallite	4.82	4.95	19.4	23.6	25.6	6.60	0.78
Bischofite	6.66	6.88	26.9	34.6	37.6	81.8	97.0

(B)	B-1	B-2	B-3	B-4	B-5	B-6	B-7
TDS (mg/kg)	35,400	181,600	275,200	295,300	308,400	331,700	357,000
Percent water remaining	100.0	15.58	9.16	2.45	1.34	0.84	0.41
Normative salts							
Anhydrite	3.50	1.50	0.328	0.071	0.024	0.013	0.017
Kieserite	6.59	6.85	8.88	21.6	22.1	8.94	1.36
Halite	78.5	80.0	80.7	39.1	13.1	3.40	0.980
Carnallite	4.79	4.93	4.90	15.0	6.86	6.62	0.657
Bischofite	6.64	6.69	5.24	24.3	57.9	81.0	97.0

A-1. At initial gypsum.
A-2. At initial halite.
A-3. At initial bloedite.
A-4. At initial epsomite.
A-5. At initial kainite.
A-6. At initial carnallite.
A-7. At bischofite saturation.

B-1. Sea water.
B-2. During gypsum precipitation.
B-3. Shortly after initial halite.
B-4. Shortly after initial polyhalite.
B-5. Shortly after initial epsomite.
B-6. Shortly after initial carnallite.
B-7. At bischofite saturation.

Table 13. Chloride-bromide ratio (weight) and salt norm (anhydrous weight percent) of marine brines from commercial seawater evaporation pan successions from analyses of Yugoslavian brines (HERRMAN *et al.*, 1973) and Bahamian brines (MCCAFFREY *et al.*, 1987)

Evaporating pans at the Sečovljo salt works, Portorož, Yugoslavia

Sample†	Seawater	Pan 11	Pan 13a	Pan 13d	Pan 13e	Pan 13i
Cl/Br	295	309	326	305	180	140
TDS (mg/kg)	34,500	124,000	170,000	256,000	274,000	274,000
Normative salts						
Anhydrite	4.0	3.8	2.0	0.5	0.2	0.2
Kieserite	6.3	6.5	8.1	7.4	13.4	15.1
Halite	76.4	76.5	78.2	78.7	61.3	51.5
Carnallite	5.2	5.0	4.9	5.1	7.7	10.2
Bischofite	8.1	8.2	6.8	8.3	17.4	23.0

Evaporating pans at the Morton Bahamas salt works, Great Inagua Island, Bahamas

Sample†	W-64	W-56	W-46	W-43	W-39	40-4	36-4*	39-6*	39-4*
Cl/Br	283	295	286	214	80	53	48	43	34
TDS (mg/L)	36,900	125,000	318,000	331,000	374,000	422,000	449,000	414,000	309,000
Normative salts									
Anhydrite	3.6	4.2	0.2	0.1	**	**	**	**	**
Kieserite	6.5	6.4	6.8	9.0	22.3	30.2	32.5	17.7	13.0
Halite	78.8	77.8	80.8	76.9	39.2	14.1	8.1	5.2	2.8
Carnallite	5.1	5.2	5.3	6.7	16.2	22.6	25.0	20.5	6.1
Bischofite	6.0	6.4	6.9	7.2	22.2	33.0	34.3	56.6	78.0

* Evaporated in laboratory with starting brine from halite precipitating pans.
** Calcium not determined.
† Sample description and salt precipitating: Seawater; Pans 11 and 13a, carbonate; Pan 13d, gypsum; Pans 13e and 13i, halite; W-64 (seawater); W-56 (pan R2A); W-46 (pan R9), gypsum; W-43 (pan Y3-Middle), W-39 (pan D3-Middle), and 40-4 (pan F4), halite; 36-4 (pan C4-Middle), magnesium sulfate; and 39-6 (pan D3-Middle) and 39-4 (pan D3-Middle), potash salt(s).

Table 14. Samples from sites in the Rustler Formation of questionable validity

Site/horizon	LAMBERT and HARVEY (1987)	This report
H-1 Culebra	Very low yield, and possible mixing with Rustler-Salado contact fluids.	Salt norm (Table 9, #1) suggests no or little mixing with Rustler-Salado fluid (Table 7, #1); norm even more alkali sulfate-rich than neighboring (H-2 and H-3) Culebra norms (Table 9, #2–6). Retained for this discussion.
P-15 R-S contact	Unit not productive; likely contaminated with Culebra fluids; unexpectedly low salinity.	Normative potassium sulfate (Table 9, #19) and low salinity abnormal. Omitted from this discussion.
P-15 Culebra	Similarities to Rustler-Salado water suggests contamination.	Concur. Omitted from this discussion.
P-17 Culebra	Packer leak suspected.	Salinities, norms, and Cl/Br different (Table 9, #32 and Table 7, #19); little mixing indicated. Retained for this discussion.
P-18 R-S contact and Culebra	Neither very productive; each possibly contaminated with well bore fluids.	Substantial salinity difference (Table 7, #21 and Table 9, #35); location for preserving primitive norms appropriate. Retained for this discussion.
WIPP-27 R-S contact, Culebra, and Magenta	Dropping water level and pump rate, and high iron content suggest prolonged contact with pipe (R-S). Culebra and Magenta not questioned.	Concur (R-S); very high potassium (Culebra and Magenta fluids (Table 9, #44 and Table 10, #16 and 17) suggests Mississippi mine outfall. Omitted from this discussion.
WIPP-29 Culebra	Not questioned.	Abnormally high salinity and high abundance of normative potassium salts (Table 9, #47–49) suggest IMC mine outfall. Omitted from this discussion.
WIPP-30 Magenta	No stability of field measurements.	May be due to continued dissolution along flow path. Retained for this discussion.

waters that obtained their solutes chiefly through carbonic acid hydrolysis of detrital silicate minerals in the weathering environment, such as the feldspars of the Gatuna Formation (Table 4); (3) dilute *sulfate-rich recharge* waters in which meteoric weathering waters were modified by interaction with Rustler anhydrite along a relatively halite-free flow path; and (4) variably concentrated *halite-rich resolution* brines in which meteoric waters were modified by interaction not only with Rustler anhydrite but also with Rustler and uppermost Salado halite.

Primitive-diagenetic waters

The primitive endmember brine is chloride-rich with appreciable quantities of normative carnallite and bischofite coexisting with halite and anhydrite-kieserite. The presence of anhydrite and halite intervals throughout the Rustler Formation, indicative of penesaline to hypersaline depositional conditions, requires connate water compositions that vary from normal seawater to that approaching bitter salt saturation, that is, brine compositions from A-1 to A-3 and B-1 to B-5 from the Yugoslavian salt pans in Table 12, and from samples W-64 to 40-4 from the Bahamian salt pans in Table 13. For these marine-evaporite-brine sequences halite abundance in the salt norm never exceeds 81 percent and is as low as 15–25 percent after halite precipitation. At the same time, kieserite abundance is always appreciably greater than that of anhydrite, and bischofite is always greater in abundance than carnallite (Tables 12 and 13). Primitive brines are also characterized by low Cl/Br ratios; seawater (~300) is about the maximum value, and values as low as 50 accompany halite precipitation (Table 13).

None of the fluids in the three Rustler Formation aquifers illustrate a truly pure, primary, primitive hypersaline brine. To be sure, some of the Rustler-Salado contact waters are hypersaline, contain normative halite abundance equal to or less than that in the seawater norm, exhibit the characteristic normative carnallite-bischofite association, and have a Cl/Br ratio of ~300 or less. However, their norms contain no kieserite and always tachyhydrite, indicating that these brines have been modified to a varying degree by diagenetic fluid-rock reaction.

According to LAMBERT (pers. com., 1987), less productive horizons of wells that have been extensively treated with process fluids during development may derive solute $CaCl_2$ from the leaching of concrete behind the casing; $CaCl_2$ is a commonly used additive to cement mixes in the well service industry. This might be the case with P-18 Rustler/Salado (Table 7, no. 21) and Culebra samples (Table 9, no. 35).

The extent of diagenetic exchange through dolomitization can be reflected in the norm by loss of kieserite and appearance of tachyhydrite, with concomitant decrease in normative bischofite. The loss of normative kieserite ($MgSO_4$) can be expressed by

$$\underset{\text{brine}}{Mg^{2+} + SO_4^{2-}} + \underset{\text{calcite}}{2CaCO_3} = \underset{\text{dolomite}}{CaMg(CO_3)_2} + \underset{\text{anhydrite (or gypsum)}}{CaSO_4} \quad (1)$$

wherein calcium released by dolomitization is precipitated as calcium sulfate. After sulfate concentration is reduced and normative kieserite is eliminated the further exchange of calcium for magnesium through the reaction

$$Mg^{2+} + 2CaCO_3 = Ca^{2+} + CaMg(CO_3)_2 \quad (2)$$

results in normative tachyhydrite (Mg_2CaCl_6), or eventually antarcticite ($CaCl_2$) at the expense of bischofite. With increased calcium concentration, additional loss of sulfate is required to maintain saturation with gypsum or anhydrite.

An example of a primitive hypersaline Rustler-Salado contact brine showing limited diagenesis is H-5 (Table 7, nos. 6 and 7); only enough Ca-Mg exchange has occurred to eliminate kieserite and produce minor tachyhydrite in the norm. In contrast, there has been sufficient Ca-Mg exchange in the Rustler-Salado contact brine from P-17 (Table 7, no. 20) for tachyhydrite to dominate the norm with only minor bischofite remaining. For both of these brines, anhydrite in the norm is low (0.1–0.5 percent), carnallite abundance is moderate (18.0–22.6 percent), and alkaline-earth chloride salts (68.0–69.4 percent) dominate the assemblages. When compared to the norms in Tables 12 and 13, these Rustler-Salado contact brines suggest a primary seawater evaporite brine that had progressed to the end of halite facies or possibly into the early stages of bitter salt deposition (though the P-17 fluid appears somewhat diluted).

Among Culebra fluids only the brine from P-18 (Table 9, no. 35) appears to be sufficiently concentrated to be classed primitive-diagenetic; its norm is tachyhydrite-rich with coexisting carnallite-halite-bishofite-anhydrite. Unfortunately no bromide determination was made. Except for salinity, the brine is very similar to that from the Rustler-Salado contact below (Table 7, no. 21), and thus might reflect contamination due to minimal purging of low productivity units (MERCER, 1983).

Alkali-bearing carbonate recharge

The other water types, the recharge waters, have a meteoric origin and entered the Rustler Formation by lateral migration and/or downward percolation from overlying strata. The solutes in these waters can be expected to reflect the extent and character of weathering reactions with framework minerals in the host rock and other mineral-rock interaction in the aquifer. Their isotopic compositions are consistent with a purely meteoric origin for their water molecules (LAMBERT and HARVEY, 1987).

The alkali-bearing water type gains solutes through dissolution of carbonate minerals and carbonic acid hydrolysis of framework silicates. A representative silicate hydrolysis reaction involving the albite component of plagioclase feldspar, for example, can be written as follows:

$$\underset{\text{albite}}{2NaAlSi_3O_8} + H_2O + 2H_2CO_3 = \underset{\text{kaolinite}}{Al_2Si_2O_5(OH)_4} + \underset{\text{quartz}}{4SiO_2} + 2Na^+ + 2HCO_3^- \quad (3)$$

in which a kaolin-type mineral and quartz (or hydrous silica) are formed and sodium and bicarbonate are added to the solution. Similar reactions can be written for the hydrolysis of potash feldspar or mafic silicate minerals yielding dissolved potassium or magnesium with the bicarbonate in solution. Such reactions generate salt norms with alkali-bearing carbonate/bicarbonate salts, as exemplified by the norm for a water from Pleistocene sediment, the Gatuna Formation, deposited in a collapse structure at WIPP-15 (Table 11, no. 4) east of the site (Fig. 4). The presence of burkeite (Table 2) in the norm suggests either some sulfuric acid hydrolysis of silicates accompanying the oxidation of sulfide minerals or, more likely, dissolution of small quantities of calcium sulfate, most likely secondary gypsum, with subsequent precipitation of calcite. As might be expected the WIPP-15 fluid contains only a minor quantity of chloride, all as normative halite. The chloride most likely came from dissolution of atmospheric aerosol particles.

Sulfate-rich recharge water

Interaction of the alkali-bearing carbonate-type recharge water with Rustler Formation rocks that contained anhydrite, but from which halite had been dissolved would produce the *sulfate-rich recharge* type. With a carbonate-rich, sulfate-poor water, such as the WIPP-15 water (Table 11, no. 4), the principal interaction would be dissolution of anhydrite and precipitation of calcite through the reaction

$$2HCO_3^- + CaSO_4 = CaCO_3 + CO_2 + H_2O + SO_4^{2-} \quad (4)$$

that decreases carbonate salts in the norm and replaces them with sulfate salts. Because anhydrite/gypsum is considerably more soluble than calcite, calcium concentration in the fluid will be enhanced as dissolved carbonate is depressed.

Where only minor silicate hydrolysis has occurred in the weathering environment, anhydrite dissolution will give rise to salt norms with strikingly high abundances of anhydrite. Examples of this include the H-7, H-8, H-9, INDIAN, and SOUTH waters from the Culebra aquifer (Table 9, nos. 18–20, 21–23, 24–25, 56, and 62, respectively) and the GNOME-5 water from the Magenta aquifer (Table 10, no. 19). All contain more than 55 percent normative anhydrite, with the norm for Culebra water from SOUTH (Table 9, no. 62) containing a maximum observed normative anhydrite of 80 percent. These waters contain only small quantities of alkali-bearing sulfate salts in the norm.

Alternatively, if silicate hydrolysis in the weathering zone has been appreciable, such as for the WIPP-15 water (Table 11, no. 4), the dissolution of anhydrite in the Rustler Formation results in the replacement of carbonate in the water by sulfate and, rather than producing norms with abundant anhydrite, yields a normative sulfate salt assemblage with a large proportion of alkali sulfate. Extreme examples of this are the norms for the H-1 Culebra water (Table 9, no. 1) and the H-4 and H-5 Magenta water (Table 10, nos. 5 and 6) that contain normative aphthitalite and thenardite coexisting with glauberite and bloedite.

Halite-rich recharge water

The *halite-rich recharge* type of water is characterized by normative halite that substantially exceeds the 78 percent of the seawater norm (Table 3, no. 5, Table 13, Seawater and no. W-64). Examples of Rustler Formation recharge waters in which halite dissolution apparently played a dominant role include H-8, H-9, P-14, WIPP-25, WIPP-27, and GNOME-5 Rustler-Salado contact brines (Table 7, nos. 12, 13–14, 18, 23, 27–28, and 35, respectively), H-5, H-11, H-12, WIPP-30, and DOE-1 Culebra fluids (Table 9, nos. 11–14, 27, 28, 50, and 57), and the H-10 Magenta brine (Table 10, no. 12). The norms contain more than 85 percent halite (several more than 90 percent) and, as expected, these waters have Cl/Br ratios that range from 810 to 8,000, where measured. Cl/Br ratios far greater than 300, the approximate seawater value, reflect resolution of the characteristically low-bromine halites initially precipitated from marine evaporate brines.

Hypersaline halite-rich mixed recharge-primitive waters

Halite dissolution alone cannot destroy a meteoric signature. In other words, the absence of alkaline-earth chlorides and the presence of normative alkali-bearing sulfate salts in the norm may be preserved even though extensive halite dissolution occurs. This latter feature of the norm should only be diluted, not destroyed, during halite dissolution by recharge waters. Yet the above cited norms nearly always contain alkaline-earth-bearing chloride salts. Furthermore, sodium-bearing sulfate normative salts, except in one analysis of H-8 (Table 7, nos. 11–12), are absent from these assemblages and the only commonly occurring, alkali sulfate-bearing, normative salt is polyhalite. The presence of these characteristics is attributed to mixing of solutes picked up during halite dissolution into the recharge waters. Such dissolution releases intergranular and intragranular (fluid inclusion) solutes, which are added to the recharge water. Thus, brines from the Rustler Formation that are rich in halite all contain solutes characteristic of primitive fluids to a variable degree.

Mixing a sulfate-rich recharge water containing normative alkali-bearing sulfates with a primitive water containing normative bischofite and carnallite or a primitive-diagenetic fluid containing normative tachyhydrite and carnallite (with or without bischofite or antarcticite) produces considerable variation in the mixed-water norm. These brines are all highly saline; nearly all contain greater than 100,000 mg/l dissolved solids and many, particularly those from the Rustler-Salado contact zone, contain more than 200,000 mg/l.

Significant changes in the composition and salt norm of mixed hypersaline fluids can be produced by effective titration. For example, the alkali sulfate in the recharge waters mixing with the calcium

chloride component of a primitive-diagenetic brine can result in precipitation of secondary calcium sulfate. This can be the origin of gypsum veins and pods in post-Salado strata. Similarly, effective titration of a normative alkali sulfate in the recharge water by normative magnesium and potassium chloride of a primitive brine can result in either direct precipitation of polyhalite or the replacement of primary anhydrite by polyhalite. The formation of polyhalite by fluid mixing may explain the origin of the polyhalite that SNYDER (1985) describes in some cores of the Tamarisk Member between the Magenta and Culebra aquifers. If the mixed fluid is taken to undersaturation, the components generated by the titration, halite and/or alkaline-earth sulfate, will appear in the salt norm. Only if all the other normative chloride salts of the primitive water are converted to halite can a sodium-bearing sulfate remain in the norm. The single example of this in the Rustler waters is one of two analyses of H-8 from the Rustler-Salado contact (Table 7, no. 12) in which the norm contains a very small fraction (0.3 percent) of bloedite with halite (94 percent) and the sulfates anhydrite-epsomite-polyhalite (5.5 percent). It is suggested that only a small increment of primitive brine mixed with the halite-dissolving recharge water; the extremely high Cl/Br ratio (8,000) in H-8 supports this interpretation.

Besides eliminating all normative sodium-bearing sulfate salts, a larger proportion of primitive brine in the mixed fluid will exchange potassium with calcium or magnesium to produce alkaline-earth sulfate and potassium chloride until all antarcticite, tachyhydrite, or bischofite are removed from the norm. However, carnallite-polyhalite is a stable salt-pair, and is the only instance in which the simple salts K_2SO_4-$MgCl_2$ coexist. Carnallite-polyhalite in the salt norm, or the K_2SO_4-$MgCl_2$ salt pair in the simple-salt assemblage, thus appears diagnostic of mixing marine-derived and meteoric waters. Many of the Rustler halite-dissolution fluids have this association in the norm. For example, four of the six Rustler-Salado contact brines and two of the five Culebra brines cited above contain the carnallite-polyhalite association in their norms.

Even larger proportions of primitive or primitive-diagenetic brines in the mixed fluid can result in retention of alkaline-earth chloride salts in the norm. The only indications of these fluids' mixed origins are the increased abundance of halite in the norm and a Cl/Br ratio in excess of 300. Halite-enriched, alkaline-earth chloride norms can also be attributed to a primitive-diagenetic fluid in which halite-resolution brines from gypsum dewatering have mixed with the primitive brine. Examples of such waters include H-7 and GNOME-5 from the Rustler-Salado contact zone (Table 7, nos. 9–10 and 35), H-3, H-5, H-6, H-10, H-12, WIPP-28, DOE-1, and DOE-2 from the Culebra aquifer (Table 9, nos. 4–5, 11–14, 15–17, 26, 28, 45–46, 57, and 58), and H-10 from the Magenta aquifer (Table 10, no. 12).

Less saline mixed recharge-primitive waters

A number of samples from the Culebra and Magenta aquifers that suggest mixing of sulfate-rich recharge with primitive or primitive-diagenetic waters are relatively dilute (generally less than 25,000 mg/l total dissolved solids). These waters have dissolved negligible to moderate amounts of halite, and are confined to the Culebra and Magenta aquifers because of omnipresent salt underlying the Rustler-Salado contact. Many of these waters yield norms that are difficult to interpret unequivocally, particularly those with relatively low normative chloride salt content.

For example, H-4 from the Culebra aquifer (Table 9, nos. 7–10), with approximately 20,000 mg/l total salinity, contains normative alkali-bearing sulfate salts and about 60 percent normative halite. The water appears to be essentially a recharge fluid. However, the Cl/Br ratio ranges from 167 to 192, which is too low to account for by halite resolution alone. Thus the normative halite concentration must result from mixing with primitive brine. This requires that the recharge water had sufficient normative alkali sulfate to eliminate the normative alkaline-earth chloride of the primitive brine and still not destroy the alkali-bearing sulfate signature of the recharge water's norm. In this way, the apparent conflict between the normative assemblage and the Cl/Br ratio can be reconciled.

With other examples, further contradictions develop. Samples from the Culebra in hole P-14 (Table 9, nos. 30–31) with total salinites of 34,000 mg/l (no. 30) and 25,000 mg/l (no. 31) yield salt norms with 60 and 45 percent halite (nos. 30 and 31, respectively). The available Cl/Br ratio is 201 (no. 31). Thus the primitive-diagenetic brine characteristics are preserved both in the salt norm and in the bromide data; dilution is apparently the result of either mixing with very dilute recharge water or with earlier diagenetic fluids from gypsum dewatering. Its water molecules, however, are isotopically meteoric (LAMBERT and HARVEY, 1987). In addition, WIPP-26 from the Culebra aquifer, with total salinity varying from 15,000 mg/l to nearly 18,000 mg/l in three analyses (Table 9, nos. 40–42), contains abundant tachyhydrite and antarcticite (9.7

to 10.2 percent) in the salt norm. This fluid, however, has a Cl/Br ratio that ranges from 2,250 to 2,420. Again, the water molecules are isotopically meteoric (LAMBERT and HARVEY, 1987).

These three similar moderately saline fluids from the same stratigraphic horizon show both internal and comparative inconsistencies: one (H-4) with a characteristic halite-dissolution recharge salt norm but a bromide content that suggests a primitive fluid; a second (P-14) with a strong primitive-diagenetic signature in both the salt norm and the bromide quantity; and a third (WIPP-26) with a salt norm that suggests a primitive-diagenetic fluid but a Cl/Br ratio and normative anhydrite that suggests extensive evaporite resolution by a recharge brine. We can only suggest that the apparent inconsistencies are related to the extent and character of silicate hydrolysis and evaporite resolution in the recharge water, which in turn, probably reflects permeability and flow path in strata overlying the Culebra. For the three sites discussed here, the post-Culebra detritus becomes thinner from H-4 westward, fractures are more likely close to the Nash Draw scarp (P-14), and extensive fracturing occurs in the Draw itself (WIPP-26); all of which are consistent with the nature of the mixtures proposed.

Areal distribution of salt norms from Rustler Formation fluids

The areal distribution of salt norms for waters from the three Rustler aquifers is shown by maps with simple-salt rose diagrams representing the salt norms of the water composition at each location (Figs. 10, 11, and 12). Because of the closely spaced boreholes within the WIPP-site boundary (Fig. 9), smaller scale diagrams are presented for a few samples which are located only approximately in order to avoid overlapping rose plots. We excluded from the maps samples that we regard of questionable validity or severely perturbed by anthropogenic activity (Table 14).

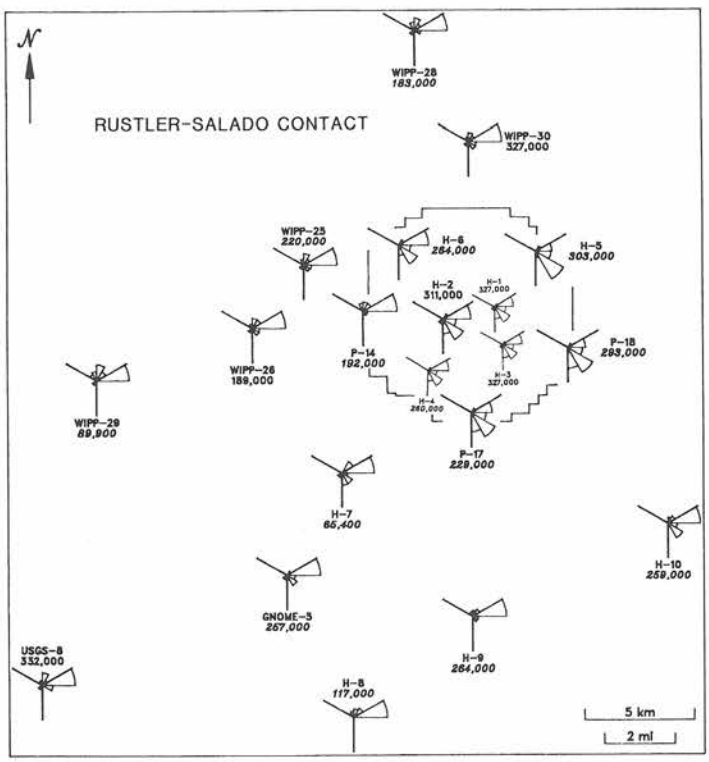

FIG. 10. Map of the WIPP-site area with simple-salt rose diagrams at sites (Fig. 9) of analyzed waters from the Rustler-Salado contact aquifer (the sample numbers plotted are identified in Tables 7 and 8 with an asterisk). For most of the rose diagrams, the intersection of axes is plotted exactly at the sample site. To avoid overlap, a few diagrams have been made smaller and plotted near the corresponding sample sites, given exactly in Fig. 9. The criteria for interpreting rose diagrams are presented in Figs. 2 and 3.

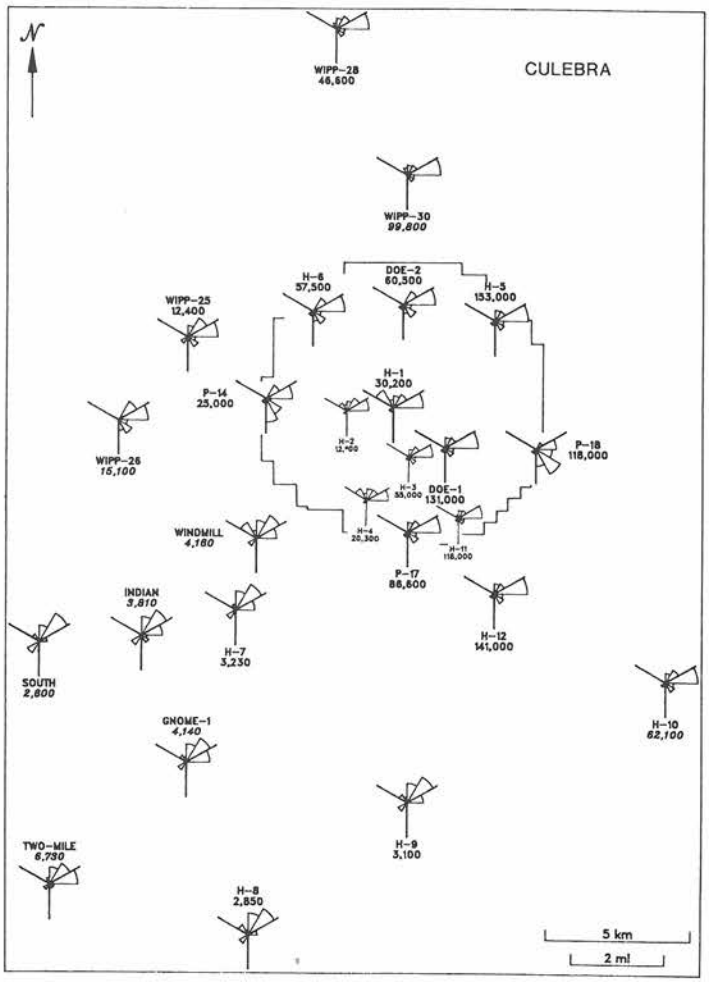

FIG. 11. Map of the WIPP-site area with simple-salt rose diagrams at sites (Fig. 9) of analyzed waters from the Culebra aquifer of the Rustler Formation (the sample numbers plotted are identified in Table 9 with an asterisk). For most of the rose diagrams, the intersection of axes is plotted exactly at the sample site. To avoid overlap, a few diagrams have been made smaller and plotted near the corresponding sample sites, given exactly in Fig. 9. The criteria for interpreting rose diagrams are presented in Figs. 2 and 3.

Rustler-Salado contact zone waters

The salt norms and total salinities of the Rustler-Salado contact fluids reflect zonation of chloride-rich brines east to west from a primitive-diagenetic type, through mixed primitive-recharge fluids, to waters dominated by halite resolution recharge.

Primitive-diagenetic normative assemblages characterize brine from the eastern central portion of the WIPP-site area, including H-5 and H-6 to the north and west, H-1, H-2, H-3, and P-18 in the central and eastern areas and P-17 and H-4 to the south (Fig. 10). Each Rustler-Salado contact brine within this area is hypersaline, contains less than 70 percent normative halite, and moderate to high quantities of normative tachyhydrite (2 to 31 percent) and bishofite (5 to 67 percent). The sum of normative bischofite and tachyhydrite always greatly exceeds carnallite, and the Cl/Br ratio ranges from 56 to 183. These fluids appear to be modified from brines that could have accompanied deposition of the halite or even of the initial bitter salts in the uppermost Salado Formation. The deuterium and oxygen-18 content for these brines also deviate significantly from the meteoric water relationship. The projection of a trend in isotope values and normative composition for these sample sites suggests an increasing primitive component eastward.

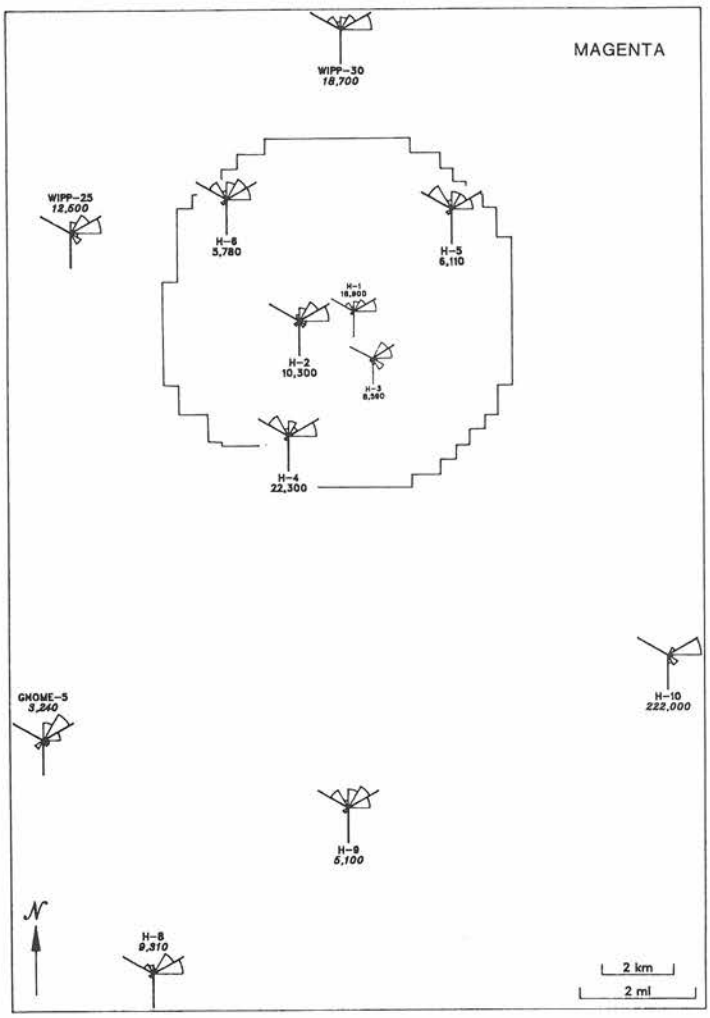

FIG. 12. Map of the WIPP-site area with simple-salt rose diagrams at sites (Fig. 9) of analyzed waters from the Magenta aquifer of the Rustler Formation (the sample numbers plotted are identified in Table 10 with an asterisk). For most of the rose diagrams, the intersection of axes is plotted exactly at the sample site. To avoid overlap, a few diagrams have been made smaller and plotted near the corresponding sample sites, given exactly in Fig. 9. The criteria for interpreting rose diagrams are presented in Figs. 2 and 3.

South and west of the WIPP site are Rustler-Salado contact brines characterized by moderate to high salinity, and a primitive-diagenetic, normative salt assemblage (anhydrite, carnallite, bischofite, generally tachyhydrite, and little or no kieserite), but with a pronounced excess of halite (84 to 94 percent) over the seawater norm. This strongly suggests mixing of recharge waters that dissolved substantial halite with a primitive-diagenetic fluid. This group is represented by H-7, GNOME-5, and H-10 (Fig. 10). The extent of apparent diagenesis among these waters is highly variable. Tachyhydrite in the norm ranges from none in H-10 and 0.6 percent in GNOME-5 to 6.5 percent (with 2.6 percent anarcticite) in H-7 (Table 7, nos. 15, 35, and 9, respectively). This range can develop through two disparate processes. One is a great variation in the exchange of solute calcium for magnesium accompanying dolomitization (note the Bardawil brines, LEVY, 1977, as cited by BODINE and JONES, 1986). The second is calcium precipitation as gypsum when a calcium-rich brine (primitive-diagenetic) mixes with an alkali sulfate-rich fluid (recharge). We suspect both processes played a role. Alternatively, one

or more of these fluids may have evolved solely as primitive-diagenetic brines in which gypsum dehydration provided fluid for halite resolution, and dolomitization eliminated kieserite and added tachyhydrite to the norm.

The brine of H-10 (Table 7, nos. 15 and 16) is an enigma. It has high normative halite that characterizes halite resolution, but has a Cl/Br ratio of only 186, suggestive of a primitive fluid. Our only suggestion is that a low chloride sodium-rich fluid, such as an alkaline evaporite water from an ephermeral surface playa, mixed with a calcium chloride-bearing, primitive-diagenetic brine with resultant precipitation of calcium and increase in normative halite.

To the north, west, and south of the WIPP site there is a progressive increase in the proportion of halite-resolution recharge water mixed with primitive-diagenetic waters. In the Rustler-Salado contact brines at WIPP-30, WIPP-25, P-14, WIPP-26, and H-9 (Fig. 10) normative halite (83–95 percent) coexists with normative polyhalite-carnallite (Table 7, nos. 33–34, 22–23, 17–18, 24–46, and 13–14, respectively). Such an assemblage is, as discussed above, good evidence for mixing of primitive-marine and recharge waters. All of these fluids have a high Cl/Br ratio (greater than 1,900) which along with the high normative halite abundance, indicates considerable halite resolution by the recharge water component. In the sample sites furthest north, west, and south of WIPP site at WIPP-28, WIPP-29, USGS-8, and H-8 (Table 7, nos. 29–30, nos. 31–32; Table 8, nos. 1–3; Table 7, nos. 11–12, respectively) all alkaline earth-bearing chlorides are absent from the norms and at WIPP-29 and H-8 small amounts of normative alkali-bearing sulfates present an added recharge signature. The normative halite abundance (84–94 percent) and high Cl/Br (greater than 2,800) indicate an extensive proportion of resolution halite in this group of waters.

It is not surprising that the Rustler-Salado contact fluids are highly saline; none contain less than 60,000 mg/kg total dissolved solids. This cannot be explained by halite dissolution in the overlying Rustler Formation for waters west of the halite dissolution front (Fig. 6). We envision recharge waters percolating downward or laterally through the Rustler Formation attaining their sulfate-rich character by interaction with Rustler anhydrite but, for the most part, not becoming chloride-rich until reaching the Rustler-Salado contact interval. Thereupon the recharge fluids dissolve Salado Formation halite that floors the Rustler-Salado contact interval and mix with any available uppermost Salado primitive-diagenetic brines and their solutes. Presumably uncontaminated primitive-diagenetic fluids are only preserved where tight masses of halite remain in the overlying Rustler Formation so as to inhibit downward percolation into the Rustler-Salado contact interval.

In Table 8 we have listed analyses and salt norms of Rustler and Salado waters from the "brine aquifer" that discharge along the Pecos River or have been retrieved by drilling. The geographic relationships between the "brine aquifer" (the best developed water-bearing zone associated with the Rustler-Salado contact), Nash Draw, Laguna Grande de la Sal (including Surprise Spring at its north end) and Malaga Bend, the discharge point for brines entering the Pecos River are shown in Fig. 7. These waters are highly saline and, except for greater concentrations of potassium, yield norms that are similar to the mixed halite-resolution recharge and primitive-diagenetic norms that are characteristic of the Rustler-Salado contact zone. We attribute the high potassium content, reflected in normative kainite and leonite (Table 8, nos. 1–5) in the Malaga Bend area, or in normative sylvite-carnallite-polyhalite in the Laguna Grande de Sal water (Table 8, no. 6), to contamination with outfall from the potash mining facilities to the north and east. The substantial increase in salinity of Surprise Spring water from 1938 to 1975 (Table 8, nos. 6 and 7) is most likely also the result of contamination from the potash operations. The deuterium and oxygen-18 values for the latest Surprise Spring sample is consistent with partial evaporation of waters imported for mine processing (LAMBERT and HARVEY, 1987).

Culebra waters

Salt norms and total salinites present an entirely different range of features for fluids from the Culebra aquifer. Salinities rarely exceed 100,000 mg/l and are frequently less than 10,000 mg/l. The salt norms are often dominated by sulfates and sodium-bearing sulfate salts are common. Furthermore, neither the salt norms nor the total salinities of these waters (Fig. 11) yield as distinct an areal pattern as do those for the Rustler-Salado contact brines.

In contrast to the results for Rustler-Salado contact fluids, only two Culebra norms can be readily interpreted as dominantly primitive-diagenetic. The sample from P-18 (Table 9, no. 35), comes from the eastern margin of the WIPP site (Fig. 11), and, based on the absence of extensive halite dissolution in the overlying strata of the Rustler Formation (Fig. 6), its normative character is not unexpected, despite

problems with small sample noted previously. Although no bromide data were obtained for this fluid, the abundances of tachyhydrite, bischofite, and carnallite (33, 21, and 24 percent respectively) are characteristic of a well-developed primitive-diagenetic assemblage. The norm of the other primitive-diagenetic Culebra fluid, P-14 (Table 9, no. 31) is somewhat different in that antarcticite, tachyhydrite, and carnallite (24, 20, and 1 percent, respectively; we doubt the validity of the low potassium concentration) constitute the alkaline earth-bearing chloride salts. The brine also has a Cl/Br ratio of 201, a primitive-diagenetic value. According to LAMBERT and HARVEY (1987), however, the isotopic composition of the water is clearly meteoric. Such a fluid in such a locality, characterized by high permeability, a meteoric isotope composition, and isolation from other primitive-diagenetic solute signatures, is decidely anomalous.

Two features of the chemistry of these Culebra waters are noteworthy. First, both brines are well undersaturated with halite or any other chloride salts; the sample from P-18 has a total salinity of 118,000 mg/l and that from P-14 has only 25,000 mg/l. Either these waters were severely diluted with recharge waters that underwent negligible reaction in the weathering regime, or the dilution occurred much earlier as a result of diagenetic dewatering of the primary bedded gypsum. The meteoric isotope signatures of both samples make the latter result very unlikely.

The second feature, restricted to the P-14 sample, is the markedly high Ca/Mg ratio when compared with the several primitive-diagenetic Rustler-Salado contact brines or the Culebra P-18 sample. In the P-14 sample, normative antarcticite is not only present, but its abundance is greater than that of tachyhydrite. Normative antarcticite does not occur in the associated Rustler-Salado contact brine or in the P-18 fluid from the Culebra. This may be the result of extensive dolomitization (or Mg-phyllosilicate authigenesis) in or near the Culebra aquifer by the P-14 fluid. This contrasts with the absence of bedded carbonate in the Rustler-Salado contact interval, and therefore, less opportunity for calcium-magnesium exchange between the fluid and the host rock, resulting in lower calcium concentrations in the fluid. The P-18 fluid from the Culebra contains no normative antarcticite and may not have been in contact with appropriate materials in or near the aquifer to effect such extensive exchange. The areal uniformity and carbon-13 content of both Culebra and Magenta dolomites suggest that they evolved not from alteration of limestone, but as evaporative dolomites. In contrast, evidence of dedolomitization in the presence of Rustler-like meteoric water has been found in the Magenta at WIPP-33, between the WIPP site and Nash Draw (LAMBERT and HARVEY, 1987).

Eight Culebra samples from H-3, H-5, H-6, H-10, H-12, P-17, DOE-1, and DOE-2 (Table 9, nos. 4–6, 11–14, 15–17, 26, 28, 33–34, 57, and 58) give salt norms qualitatively indicative of primitive-diagenetic origin. However, the normative halite abundances (80–88 percent) and Cl/Br ratios (674–2,800) significantly exceed the seawater values. Each is also quite saline (55,000–153,000 mg/l). Three alternative origins can be ascribed to these waters. The first is that a primitive-diagenetic fluid mixed with a halite-resolution recharge water. The second is that, like the origin proposed for P-18, early gypsum dehydration water diluted a primitive halite-precipitating brine, but in this case, effected considerable halite resolution. The third is that the original primitive water was undersaturated with halite, and dissolved halite after migrating to or into a neighboring bedded halite. The relatively high amount of normative carnallite, as contrasted with bischofite-tachyhydrite abundance, in most of these waters (all but H-6 and DOE-2) favors the first alternative, that is, mixing of the primitive-diagenetic brine with a halite-resolution recharge water. During the mixing process, alkali sulfate salts in the recharge water and abundant calcium in the primitive-diagenetic water interact to precipitate secondary gypsum and to decrease the normative alkaline-earth chlorides in the fluid. It appears plausible that all samples but H-6 and DOE-2 involved mixing with recharge waters, whereas the latter two brines evolved through an earlier diagenetic process of halite resolution accompanying diagenetic gypsum dewatering. However, the stable-isotope data indicate that all these waters are meteoric in origin (LAMBERT and HARVEY, 1987).

Two Culebra samples from WIPP-25 and WIPP-26 (Table 9, nos. 36–39 and 40–42) have normative halite quantities significantly less than seawater (63–65 percent), but have Cl/Br ratios well in excess (2,000–4,000) of the seawater value. Furthermore, they contain abundant normative alkaline-earth sulfate salts, chiefly anhydrite with minor kieserite in WIPP-25, and are unusually dilute (12,000–15,000 mg/l) for waters with carnallite-bischofite norms. These characteristics suggest substantial simple dissolution of calcium sulfate (and perhaps some dolomite) followed by dilution of primitive-diagenetic fluids. Isotopically, these waters are also of meteoric origin (LAMBERT and HARVEY, 1987).

The remaining Culebra waters with total salinity greater than 10,000 mg/l are H-1, H-4, H-11, WIPP-

28, and WIPP-30 (Table 9, nos. 1, 7–10, 27, 45–46, and 50–51). Three of these, H-11, WIPP-28, and WIPP-30, with 47,000 to 118,000 mg/l contain the diagnostic carnallite-polyhalite association indicating mixing of primitive-diagenetic fluids with sulfate-resolution recharge water. The high halite contents in the norms of these three waters (84–91 percent) and the high Cl/Br (1,400–3,400) point toward some halite resolution by the recharge waters. H-3, on the other hand, is less saline (30,000 mg/l) and contains normative thenardite and aphthitalite with 68 percent normative halite. This water is a typical anhydrite-resolution recharge water that has lost calcium to mixing with sodium carbonate derived from silicate hydrolysis, and has also dissolved minor amounts of halite. H-4, with 61 percent normative halite coexisting with the bloedite-glauberite association, also has an anhydrite-resolution recharge signature. The fluid's Cl/Br ratio is only 176, suggesting mixing of a primitive-diagenetic fluid with an anhydrite-resolution recharge water that contained negligible chloride. Again, the water molecules appear isotopically meteoric (LAMBERT and HARVEY, 1987).

Of the 13 Culebra sites with dilute waters, 10 (H-2, H-7, H-8, H-9, ENGEL, GNOME SHAFT, GNOME-1, GNOME-4, WINDMILL, and SOUTH in Table 9, nos. 2–3, 18–20, 23–23, 24–25, 29, 52, 53, 54, 60–61, and 62) yield norms containing sodium-bearing sulfates, either bloedite or the bloedite-glauberite pair, and halite abundances from 1.2 to 67 percent. The TWO-MILE (Table 9, no. 59) well, Culebra water, contains a polyhalite-carnallite association with 54 percent halite in the norm. Two wells (GNOME-8 and INDIAN in Table 9, nos. 55 and 56) yield Culebra waters with a normative carnallite-bischofite association and 36 and 22 percent halite, respectively. All 13 fluids must have been sodium carbonate-bearing recharge waters that have interacted with Rustler anhydrite, deposited secondary calcite, and, for those with greater than 15–25 percent chloride salts in the norm, redissolved minor remnants of Rustler halite.

Two of these 13 sites (H-8 and SOUTH) yielded waters with exceptionally low chloride content, less than 4 percent halite in otherwise chloride salt-free norms, suggesting recharge waters did not encounter any primitive-diagenetic fluid, nor participate in halite resolution accompanying migration into the Culebra aquifer. The very high abundance of anhydrite in each norm strongly suggests extensive dissolution of Rustler anhydrite.

The conclusions from the area distribution of the norms of the Culebra waters (Fig. 11) are (1) that the distribution of salt norms is compatible with the flow field presented by DAVIES (1989), and (2) that the Culebra Dolomite aquifer has extremely variable hydrologic properties. The basis for the first conclusion is that the one primitive-diagenetic, but somewhat diluted brine with a dominantly tachyhydrite-bischofite-carnallite norm and a very low Cl/Br ratio (P-18) occurs where the Rustler Formation is the least permeable; bedded halite is preserved above both the Culebra and Magenta members. P-18 is surrounded by sampling sites where the Culebra waters are moderately saline with norms yielding abundant halite (greater than 80 percent) coexisting with the carnallite-bischofite assemblage, with (H-6 and DOE-2), or without tachyhydrite (H-3, H-5, H-10, H-12, P-17, and DOE-1). These associations suggest mixing with anhydrite-halite-resolution recharge waters, while preserving the alkaline-earth chloride salt(s) in the normative assemblage. Two Culebra brines in Nash Draw north of the WIPP site (WIPP-28 and WIPP-30) contain normative polyhalite-carnallite, indicating a larger fraction of anhydrite-halite-resolution recharge water mixing with primitive-diagenetic fluids. Finally, the large area of dilute Culebra water with alkali sulfate-bearing norms south and west of the WIPP site clearly reflects (1) the paucity of halite above the Culebra, (2) significant infiltration of recharge waters, and (3) relatively rapid flow to the southwest. The normative and solute concentration patterns in Fig. 11 actually fit well with DAVIES (1989) flow-field simulation without vertical influx.

The variability of the Culebra aquifer's hydrologic properties (conclusion 2, above) is illustrated by the great diversity of normative characteristics for its fluids, such as the unusual preservation of a severely diluted primitive-diagenetic brine at P-14 and its apparent mixing to the west with anhydrite-halite-resolution recharge or halite-resolution gypsum-dehydration waters at WIPP-25 and WIPP-26. It is not at all clear what hydrologic conditions have preserved such normative compositions in an area where all Rustler halite is missing (Fig. 6), and where the primitive-diagenetic brine (P-14) is clearly separated by unequivocal resolution waters at H-1, H-2, and H-3 from the nearest primitive-diagenetic brine (P-18). It is also not clear what hydrologic features allow a closely spaced group of sites (H-1, H-2, and H-3) to yield waters of such vastly different salinities (8,920 to 55,000 mg/l) and normative character (thenardite-aphthitalite association *vs.* carnallite-bischofite association). Certainly hydrologic connections must be minimal. Evidence for significant vertical infiltration is given in the norms of dilute waters in the southwest quadrant of Fig.

11. These norms are relatively sulfate-rich and chloride-poor, but range in normative mineralogy from carnallite-bischofite (INDIAN) to abundant bloedite (WINDMILL). This strongly suggests recharge of the aquifer by infiltration of weathering waters. Local variations in the extent of silicate hydrolysis, interaction with Rustler anhydrite, and dissolution of isolated remnants of Rustler halite, rather than evolution along a well-defined flow path, best explain the random variations of the salt norms in this area.

Magenta waters

Waters from the Magenta member of the Rustler Formation were obtained at far fewer sites than either the Rustler-Salado contact-zone brines or the Culebra fluids because the Magenta horizon is along the eastern margin of Nash Draw, or removed by erosion within Nash Draw and throughout much of the area southwest of the WIPP and GNOME sites (Fig. 9).

No Magenta waters have solutes indicating a predominantly primitive origin. The only highly saline water (222,000 mg/kg) is H-10 (Table 10, no. 12) where the norm has tachyhydrite, bischofite, and carnallite, but also 93 percent halite. The Cl/Br ratio is 860. This is a typical mixture of a halite-rich recharge fluid and a primitive-diagenetic brine. Two other much more dilute waters from H-3 and WIPP-25 (Table 10, nos. 4 and 14) with 8,600 and 12,500 mg/l total dissolved solids, have qualitatively primitive norms characterized by bischofite, carnallite, anhydrite, and either tachyhydrite (H-3) or kieserite (WIPP-25), but in both the Cl/Br ratio is high (574 and 2,600, respectively). The low halite abundance is due to high anhydrite content, rather than abundant alkaline earth-bearing chloride. Thus, each appears to be a mixture of an anhydrite-halite resolution recharge water with a primitive-diagenetic fluid.

Two other wells (H-2 and GNOME-5; Table 10, nos. 2 and 19) have Magenta waters with slight primitive or primitive-diagenetic normative characteristics. The sample from H-2 with a total salinity of 10,000 mg/l contains small quantities of carnallite and polyhalite and 65 percent halite in the norm. The GNOME-5 fluid with 3,200 mg/l total dissolved solids contains 1.1 percent carnallite, 15 percent kieserite, only 12 percent halite, but 69 percent anhydrite in the norm. Bromide content was not determined in either water. Both waters are very dilute so that it is difficult to be certain of any primitive-diagenetic contribution.

The remaining 7 Magenta waters show substantial quantities of sodium-bearing alkali salts in the norm and are clearly dominated by anhydrite-resolution recharge waters with some halite resolution. In two samples, H-4 and H-5 (Table 10, nos. 5 and 6) silicate hydrolysis was sufficient to yield considerable thenardite (17 percent in both) and some aphthitalite (1.7 and 2.5 percent, respectively) in their norms. The moderate amounts of normative halite (55 and 24 percent, respectively) and low salinities (22,000 and 6,100 mg/l) indicate moderate to minor halite resolution; unfortunately bromide data for both H-4 and H-5 are lacking. The water from 4 of the remaining 5 sites (H-1, H-6, H-9, and WIPP-30 in Table 10, nos. 1, 7, 10–11 and 18) contains abundant normative bloedite (9–35 percent), glauberite and anhydrite. H-8 (Table 10, no. 9), on the other hand, contains the glauberite-syngenite-polyhalite assemblage of alkali-bearing sulfate salts. Salinities in these waters range from 5,000 to 19,000 mg/l with normative halite varying from 25 to 72 percent. Bromide determinations are reported for three of the waters (H-8, H-9, and WIPP-30) with Cl/Br ratios of 4,300, 300 and 3,800, respectively. While the value for H-9 appears anomalous, the low normative halite abundance (25 percent) and the low salinity (5,000 mg/l) suggest that the Cl/Br ratio probably reflects generation in the weathering environment. As expected, all Magenta waters analyzed for deuterium and ^{18}O gave meteoric values (LAMBERT and HARVEY, 1987).

The areal distribution of normative data for fluids from the Magenta aquifer (Fig. 12) locates the only highly saline water (H-10) to southeast of the WIPP site in an area in which bedded halite presumably remains in the strata overlying the Magenta dolomite (Fig. 7). This water is a mixed halite-resolution recharge and primitive-diagenetic fluid. No dominantly primitive-diagenetic Magenta fluid has been observed within the WIPP-site area.

The remaining Magenta waters are relatively dilute (less than 23,000 mg/l) and represent variable but lesser proportions of primitive-diagenetic solutes as compared to anhydrite-dissolution recharge solutes. Halite resolution is negligible or minor. As with the Culebra fluids, no definitive areal pattern occurs in the norms of these dilute Magenta waters, and much recharge is probably from vertical infiltration into the aquifer. For example, the norms for the closely spaced cluster of wells, H-1, H-2, and H-3 within the WIPP site, show considerable variation (Table 10, nos. 1, 2, and 3–4, and Fig. 12). H-3 has a strong primitive-diagenetic signature (normative tachyhydrite-bischofite), with a lesser

fraction of anhydrite-resolution recharge. H-2 shows a greater fraction of anhydrite-resolution recharge fluid (a polyhalite-carnallite association), whereas H-1, with normative bloedite-anhydrite, is characteristic of a water that dissolved minor amounts of halite and is dominated by anhydrite-resolution recharge solutes.

Other variations in the norms of Magenta fluids within the WIPP-site area, particularly the isolated occurrence of the WIPP-25 water with its $MgCl_2$-$CaSO_4$ character and evidence of halite resolution (Table 10, nos. 13–15 and Fig. 12) further document the variability of the aquifer. Note that this norm and individual solute values are very similar to those of the underlying Culebra sample (Table 9, no. 38). Taken with very similar isotopic composition (LAMBERT and HARVEY, 1987) and hydraulic properties (MERCER, 1983), this indicates that the Magenta and Culebra aquifers are interconnected at WIPP-25. This is one of the few places where there is such an interconnection. Here DAVIES (1989) has demonstrated the dissipation of a large pressure differential between the Magenta and the Culebra, which results from dissolution and fracture-induced hydraulic conductivity related to, but east of, Nash Draw.

Salt norm variations among Rustler Formation aquifers

Because the distribution of Rustler Formation salt norms in the WIPP-site area, particularly the Culebra and Magenta norms, indicate highly variable aquifer properties and hydrologic connections with overlying strata, variations in salt norms were examined among the three aquifers at each site where more than one Rustler Formation horizon was sampled. These comparisons are shown on Fig. 13 for eighteen sampling localities.

The general features are well illustrated. Most sites show a progressive drop in fluid salinities upward from the Rustler-Salado contact zone through the Culebra aquifer and into the Magenta Dolomite. Secondly, a progression upward in the norms at most sites represents the succession from primitive-diagenetic to anhydrite-resolution recharge with minor halite resolution characteristics. Waters from H-5 (Fig. 13), for example, illustrate both trends over broad ranges. The Rustler-Salado contact sample from this well is hypersaline (303,000 mg/l) and is dominated by primitive-diagenetic solutes yielding a bischofite-tachyhydrite salt norm with minor halite. The overlying Culebra water is substantially less saline, (153,000 mg/l), with a bischofite-carnallite association and 88 percent halite in a norm that is diagnostic of mixed halite-dissolving primitive-recharge fluid. The uppermost Magenta water, on the other hand, is dilute (6,100 mg/l), with the thenardite-aphthitalite pair and 23.7 percent halite in the norm. This is characteristic of an anhydrite-resolution-recharge fluid that has picked up little primitive brine, and has dissolved only minor amounts of halite.

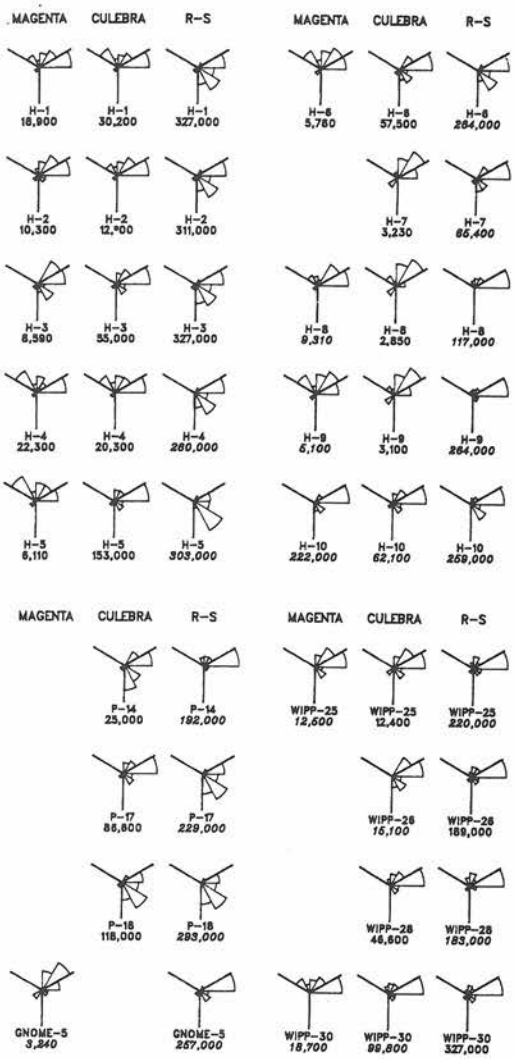

FIG. 13. Simple-salt rose diagrams comparing waters from the Magenta, Culebra, and Rustler-Salado Formation contact aquifers for those sites in the WIPP-site area with analyzed samples from more than one horizon (the samples plotted are identified in Tables 7, 9, and 11 with an asterisk). The criteria for interpreting rose diagrams are presented in Figs. 2 and 3.

Although about half the Rustler waters do not

strictly follow both these trends, a number of the anomalies, particularly when comparing dilute fluids, are minor, and reflect only small differences in the proportion of recharge-primitive solutes, halite dissolution, and/or extent and character of silicate hydrolysis effected by the recharge fluid. Those sequences that deviate markedly from the general trend, H-10, P-14, WIPP-25, and WIPP-26, were discussed earlier.

Salt norm variations with time

LAMBERT and ROBINSON (1984) discussed in detail the extended chemical instability in the sampling of brines from the drill holes in Nash Draw. A significant portion of this chemical change can exceed analytical error and is most readily attributed to mixing of brines from different parts of the sampling interval. Thus a comparison of salt norms for analyses taken at different times can highlight compositional changes suggestive of variable solute source and perhaps flow path. The great majority of and largest time interval for these comparisons resulted from recent systematic recollection and analysis of brines in the Culebra Dolomite Member of the Rustler Formation that were provided to us by Sandia Laboratories (ROBINSON and LAMBERT, written communication, 1987).

Three samples from the Rustler-Salado contact aquifer in Nash Draw (WIPP-25, 29, and 30) were recollected and analyzed in different laboratories at a four month interval with significant increases in salinity, but without an essential change in chemical character (Table 7, nos. 22–23, nos. 31–32, and nos. 33–34, respectively). A substantial dilution and sulfate increase contrast with an increase in alkaline-earth chloride in the only example of recollection and analysis after a long interval (slightly over 8 years) in the Magenta dolomite aquifer (H-3 in Table 10, nos. 3–4). These results suggest increased mixing of gypsum dissolution with residual solutes such as found in the Culebra at P-14.

Compositional variation in the Culebra brines with time of collection can be separated into four basic types. These types assist in categorizing variation in chemical composition with degree of evaporite dissolution or leaching with respect to area, stratigraphic interval, and/or time. A shift in the normative assemblage toward increased alkaline-earth chloride indicates a greater fraction of primitive-diagenetic brine, and characterizes the slight change in TDS over 4 years in H-6 (Table 9, nos. 15–16), over 6 years in WIPP-25 (Table 9, nos. 38–39), and over 5 years in WIPP-26 (Table 9, nos. 41–42). The largest shift of this type is seen in P-14 over 9 years (Table 9, nos. 30–31; we are somewhat puzzled by and suspicious of the data for potassium, only 37.9 mg/l, reported for the 2/26/86 sample, no. 31), but the total salinity actually decreased by 25 percent. This decrease might reflect a smaller proportion of halite-resolution brine. A second type of normative compositional change is the increase of NaCl, probably associated with an increase in salinity, as illustrated by H-2 collection over a 9-year interval (Table 9, no. 2–3). This may be related either to simple resolution of halite or to titration of an alkaline-earth chloride component of the brine by sodium carbonate, with precipitation of secondary calcite. A change in the salt norm toward increased alkaline-earth sulfate alone, the third type, can accompany either a slight increase in salinity, as represented by H-4 and H-5 (Table 9, nos. 7–8 and nos. 11–12), or a slight decrease in salinity, as shown by H-9, and P-17 (Table 9, nos. 24–25 and nos. 33–34), and probably reflects gypsum resolution or titration of a calcium chloride component by sodium sulfate, with precipitation of gypsum (or anhydrite). Finally, an increase in normative alkali sulfate should be expected to accompany further dilution of a Culebra fluid by sodium carbonate-bearing recharge waters, such as the WIPP-15 water from Pleistocene sediment (Table 11, no. 4), and additional precipitation of secondary calcite. The only slight, but rather inconclusive indication of this process is given in the comparison of the H-9 analyses (Table 9, nos. 24–25) separated by a 5 year interval.

In conclusion, however, it should be re-emphasized that the changes in chemical composition for well samples over extended intervals of time are just as likely to be due to sampling techniques and well condition as to the time itself.

SUMMARY AND CONCLUSIONS

The salt norms and derivative simple-salt assemblages calculated for 124 water analyses from the three aquifer units of the Ochoan (Permian) Rustler Formation (plus 4 analyses from overlying strata) at or near the Waste Isolation Pilot Plant (WIPP) in Southeastern New Mexico indicate that Rustler waters range from hypersaline, marine-like, primitive-diagenetic fluids to dilute meteoric recharge waters. The chemical compositions of these waters can be attributed to variable mixing of solutes from the following sources: 1) the intergranular or fluid inclusion retention of primary seawater-evaporative bitterns; 2) diagenetic reaction of brines with pre-

cursor carbonate or silicate sediments, principally the exchange of Ca for Mg; 3) influx of meteoric water, with and without a significant solute-weathering component; and 4) dissolution of evaporite minerals, primarily halite and anhydrite.

The Rustler Formation fluids can be classified according to principal normative component into four basic types, generally in order of decreasing salinity and depth: 1) primitive-diagenetic fluids, characterized by alkaline-earth chloride; 2) NaCl-rich resolution brines; 3) calcium sulfate-dominated recharge waters; 4) alkali carbonate-bearing recharge waters. The recharge waters have entered the Rustler aquifers through overlying strata or laterally. Their norms reflect negligible to extensive resolution of Rustler or Salado halite, pervasive resolution of calcium sulfate in the Rustler Formation throughout the region, and silicate hydrolysis of framework minerals in clastic sediments both within and overlying the Rustler.

The primitive-diagenetic brines are most prevalent in the contact zone of the Rustler with the underlying Salado halite, particularly for samples from wells east of the central part of the WIPP site where transmissivities and flow rates in the Rustler-Salado contact zone are very low (MERCER, 1983). In fact, there is a general zonation of high chloride brines from the most alkaline-earth rich in the east to the most sodium-rich (including some sulfate) in the west. The norms of the primitive-diagenetic fluids in the Rustler are similar to those for marine hypersaline bitterns, and Cl/Br ratios are appropriately low, but tachyhydrite ($CaMg_2Cl_6$) is present rather than kieserite ($MgSO_4$). End member examples are from H-5 for maximum $MgCl_2$, and from P-18 for the most $CaCl_2$, at salinities in excess of 290 g/l. For brines from the Culebra Dolomite aquifer a minor $CaCl_2$ component is restricted to norms from four wells all within the WIPP site, though a small amount of $CaCl_2$ is also present in the norm of H-10 Magenta to the southeast of the site.

Halite resolution brines are the most common type of fluid in the Rustler Formation of the region around the WIPP site. About 70 percent of the samples from the Rustler-Salado contact zone and 30 percent from the Culebra Dolomite are dominated by an NaCl component. The abundance of normative halite in the aquifer samples is compatible, for the most part, with zones describing the extent of apparent halite dissolution observed in the principal evaporite-bearing intervals of the Rustler Formation. In some sample norms (*e.g.*, H-9 and WIPP-30 from the Rustler-Salado contact) halite exceeds 90 percent of the normative salts, and the Cl/Br ratio is five times the seawater value, as expected from the dissolution of bromine-poor halite. Most of the samples from the Culebra aquifer in the eastern part of the region appear to be variable mixtures of these resolution brines with fluids of primitive-diagenetic origin. Simple halite dissolution in itself cannot destroy the normative signatures of primitive-diagenetic brines (alkaline-earth chloride) or weathering waters (alkali sulfo-carbonate). This is seen in a number of the NaCl dominated brines, which very generally fall into two groups with salinities exceeding 100 g/l or less than 25 g/l. The former typically contain some residual primitive-diagenetic indicator (usually $MgCl_2$) and the latter commonly have excess sulfate. Complex mixtures of primitive-diagenetic brine with alkali sulfate-bearing recharge can produce halite-rich norms without halite dissolution, but they are distinguished by low Cl/Br ratios. Primitive-diagenetic residuals apparently have remained in isolated pockets where formational transmissivities are low.

In that part of the WIPP site region where halite is thin, absent or has been essentially removed by dissolution, such as in Nash Draw and vicinity, the further solution of anhydrite or gypsum leads to ground-water norms dominated by calcium sulfate. Culebra aquifer samples from Nash Draw appear to result from extensive dilution of primitive-diagenetic residuals by $CaSO_4$ dissolution waters. Norms with more than 50 percent $CaSO_4$ are common for samples from the Culebra aquifer to the south and west of the WIPP site area, where the most dilute of the Culebra waters are found. As with halite, the simple dissolving of anhydrite or gypsum will not obliterate a primitive-diagenetic or weathering solute-signature, but the mixing of alkaline-earth chloride and alkali sulfate components will generate added Ca and Mg sulfates in the norm. Similarly, Na or Mg carbonate from silicate hydrolysis mixed with dissolved $CaSO_4$ will result in normative Na-Mg sulfates, as in the case for some central WIPP-site Culebra, and more especially, a number of Magenta aquifer waters. The norm for H-8 Culebra exceeds 90 percent alkaline-earth sulfate, whereas the sample of the Culebra water from the Windmill well south of the WIPP site has mixed sulfates comprising 80 percent of the norm, almost matched by the 75 percent for H-9 Magenta. Indeed, an increased sodium sulfate component appears to correlate with a greater continental sediment fraction upward in the stratigraphic section. The maximum Na_2SO_4 percentage is in the norm for a sample from the Triassic Santa Rosa Formation (H-5). For the WIPP-15 water from Cenozoic deposits,

straightforward feldspar and mafic mineral weathering is seen in the dominant Na-Mg carbonate components in the norm.

Nearly all the salt norms for waters from the shallowest of the Rustler Formation aquifers, the Magenta Dolomite, illustrate the dominance of $CaSO_4$ dissolution. The Magenta is dry at several locations in north central Nash Draw and has been removed by erosion to the south. Normative indications of halite dissolution are low in most samples, except for the most saline Magenta fluid, as might be expected, from the eastern edge of the area. Many of the Magenta norms contain sodium sulfate salts, which appear to correlate with the presence of overlying continental (siliciclastic) strata. In two uncontaminated Magenta norms, a small CaMgCl primitive-diagenetic signature remains, and even in the two norms from wells in the overlying Triassic Dewey Lake Redbeds a $MgCl_2$ residuum is present.

The large variation in hydrologic properties of the Culebra Dolomite, the most extensively considered of the Rustler Formation aquifers, is emphasized by the diversity in normative results. In addition, the flow field simulations presented by DAVIES (1989) are reflected in the areal distribution of normative compositions. The increase in flow velocities of the model from east to west across the region fits the distribution of concentrated primitive-diagenetic brines in the eastern part of area, halite-dominated waters thru the central part of the region, and dilute $CaSO_4$-type solutions to the west and south. For the WIPP site in detail, the highest flow velocity in the northwest, the high permeability zone in the center-south of the site, and the complex, relatively high flow conditions in the area some distance south and west of the site are in agreement with the normative interpretations. The predominant north to south flow direction (or even northwest to southeast, south of the WIPP site) is clearly consistent with normative inference. This is also compatible with the idea of paleo-recharge to the Rustler aquifers from the Nash Draw area (LAMBERT and HARVEY, 1987). More equivocal is the amount of vertical influx first correlated with the alkali sulfate content of some of the norms. The small shifts in flow direction predicted by DAVIES (1989) for a vertical flux ranging from negligible to a maximum of 25 percent of the total ground-water flow cannot be resolved with existing normative data.

Acknowledgements—We greatly appreciate Shirley L. Rettig for the careful analysis of many of these waters. We also thank Peter Davies and Steven Richey for providing us with the WIPP boundary and sampling site coordinates that are plotted on the many maps as well as for their willing help in locating analytical data and their enthusiastic interest and support of this work. We are very grateful to Steven Lambert, Malcom Siegel, Jerry Mercer, Karen Robinson, and Carol Stein of the Sandia Laboratories in Albuquerque for providing us with unpublished data and considerable discussion. We thank George Garcia for several of the illustrations. Walter Dean and Peter Davies reviewed the manuscript and made many helpful suggestions. Marge Shapira helped very much with manuscript preparation.

REFERENCES

ANDERSON R. Y. (1978) Deep dissolution of salt, northern Delaware Basin, New Mexico. Rept. to Sandia Laboratories, Albuquerque, NM, 106p.

ANDERSON R. Y. (1983) Deformation-dissolution potential of bedded salt, Waste Isolation Pilot Plant site, Delaware Basin, NM. Fifth International Sympos. Scientific Basis of Radioactive Waste Management, Berlin, (West) Germany, 7–10 June, 1982, 10p.

BACHMAN G. O. (1980) Regional geology and Cenozoic history of the Pecos region, southeastern New Mexico. U.S. Geol. Surv. Open-File Rept. 80-1099.

BACHMAN G. O. (1985) Assessment of near-surface dissolution at and near the Waste Isolation Pilot Plant (WIPP), southeastern New Mexico. Sandia Labs. Rept. SAND 86-7078, 33p.

BODINE M. W. JR. (1978) Clay-mineral assemblages from drill core of Ochoan evaporites, Eddy County, New Mexico. In *Geology and mineral deposits of Ochoan rocks in Delaware Basin and adjacent areas.* (ed. G. S. AUSTIN), pp. 21–31. Mexico Bur. Mines Min. Res. Circ. 159.

BODINE M. W. JR. and JONES B. F. (1986) The salt norm: A quantitative chemical-mineralogical characterization of natural waters. U.S. Geol. Surv. Water Res. Inv. Rept. 86-4086.

BRAITSCH O. (1971) *Salt Deposits, Their Origin and Composition.* 297pp. Springer-Verlag.

CROSS C. W., IDDINGS J. P., PIRSSON L. V. and WASHINGTON H. S. (1902) A quantitative chemico-mineralogical classification and nomenclature of igneous rocks. *J. Geol.* **10,** 555–690.

DAVIES P. B. (1989) Variable-density ground-water flow and paleohydrology in the Waste Isolation Pilot Plant (WIPP) region, Southeastern New Mexico. U.S. Geol. Surv. Open-File Rept. 88-490.

EUGSTER H. P., HARVIE C. E. and WEARE J. H. (1980) Mineral equilibria in the six-component sea water system, Na-K-Mg-SO_4-Cl-H_2O, at 25°C. *Geochim. Cosmochim. Acta* **44,** 1335–1348.

EUGSTER H. P. and JONES B. F. (1979) Behavior of major solutes during closed-basin brine evolution. *Amer. J. Sci.* **279,** 609–631.

FRAPE S. K. and FRITZ P. (1982) The chemistry and isotope composition of saline groundwaters from the Sudbury Basin, Ontario. *Canadian J. Earth Sci.* **19,** 645–661.

FRAPE S. K., FRITZ P. and MCNUTT R. H. (1984) Water-rock interaction and chemistry of groundwaters from the Canadian Shield. *Geochim. Cosmochim. Acta* **48,** 1617–1627.

GONZALEZ D. D. (1981) Hydrological data. In *Basic data report for drillhole WIPP 15 (Waste Isolation Pilot Plant—WIPP).* Sandia National Labs, SAND 79-0274 24–29.

HEM J. D. (1970) Study and interpretation of the chemical characteristics of natural waters. U.S. Geol. Surv. Water-Supply Paper 1473.

HERRMANN A. G., KNAKE D., SCHNEIDER J. and PETERS H. (1973) Geochemistry of modern seawater and brines from salt pans. Main components and bromine distribution. *Contrib. Mineral. Petrol.* **40,** 1–24.

HOLT R. M. and POWERS D. W. (1988) Facies variability and post-depositional alteration within the Rustler Formation in the vicinity of the Waste Isolation Pilot Plant, southeastern New Mexico. U.S. Department of Energy Report DOE/WIPP-88-004.

KUNKLER J. L. (1980) Evaluation of the Malaga Bend salinity alleviation project. U.S. Geol. Surv. Open-File Rept. 80-1111.

LAMBERT S. J. (1978) Geochemistry of Delaware Basin ground waters. In *Geology and mineral deposits of Ochoan rocks in Delaware Basin and adjacent areas.* (ed. G. S. AUSTIN), pp. 33–38. New Mexico Bur. Mines Min. Res. Circ. 159.

LAMBERT S. J. and HARVEY D. M. (1987) Stable-isotope geochemistry of groundwaters in the Delaware Basin of southeastern New Mexico. Sandia National Labs., SAND 87-0138, 258p.

LAMBERT S. J. and ROBINSON K. L. (1984) Field geochemical studies of groundwaters in Nash Draw, southeastern New Mexico. Sandia National Labs., SAND 83-1122, 38p.

LAPPIN A. R. and HUNTER R. L. eds. (1989) Systems analysis, long-term radionuclide transport, and dose assessments, Waste Isolation Pilot Plant (WIPP), southeastern New Mexico; March, 1989. Sandia National Labs., SAND 89-0462, 632p.

LEVY Y. (1977) The origin and evolution of brine in coastal sabkhas, northern Sinai. *J. Sed. Petrol.* **47,** 451–462.

MANN A. W. (1983) Hydrogeochemistry and weathering on the Yilgarn Block, Western Australia—ferrolysis and heavy metals in continental brines. *Geochim. Cosmochim. Acta* **47,** 181–190.

MCCAFFREY M. A., LAZAR B. and HOLLAND H. D. (1987) The evaporation path of seawater and the coprecipitation of Br^- and K^+ with halite. *J. Sed. Petrol.* **57,** 928–937.

MCGOWEN J. H., GRANATA G. E. and SENI S. J. (1979) Depositional framework of the lower Dockum Group (Triassic) Texas Panhandle. University of Texas Bur. Econ. Geol., Rept Inv. 97.

MERCER J. W. (1983) Geohydrology of the proposed Waste Isolation Pilot Plant site, Los Medanos area, southeastern New Mexico. U.S. Geol. Surv. Water Res. Inv. Rept. 83-4016.

POWERS D. W., LAMBERT S. J., SHAFFER S. E., HILL L. R. and WEART W. D. (editors) (1978) Geological characterization report, Waste Isolation Pilot Plant (WIPP) site, southeastern New Mexico. Sandia National Labs. Contractor Rept., SAND 78-1596, 2 vols.

RANKAMA K. and SAHAMA T. G. (1950) *Geochemistry.* 912pp. University of Chicago Press.

RICHEY S. F. (1989) Geologic and hydrologic data for the Rustler Formation near the Waste Isolation Pilot Plant, southeastern New Mexico. U.S. Geol. Surv. Open-File Rept. 89-32.

RILEY J. P. and CHESTER R. (1971) *Introduction to Marine Chemistry.* 465pp. Academic Press.

ROBINSON T. W. and LANG W. B. (1938) Geology and ground-water conditions of the Pecos River valley in the vicinity of Laguna Grande de la Sal, New Mexico. In *12th and 13th Biennial Reports.* New Mexico State Engineer, p. 77–100.

SNYDER R. P. (1985) Dissolution of halite and gypsum, and hydration of anhydrite to gypsum, Rustler Formation, in the vicinity of the Waste Isolation Pilot Plant, southeastern New Mexico. U.S. Geol. Surv. Open-File Rept. 85-229.

UHLAND D. W. and RANDALL W. S. (1986) 1986 annual water quality data report for the Waste Isolation Pilot Plant. Technology Development Dept., Waste Isolation Pilot Plant Project, Westinghouse Electric Corporation, Carlsbad, New Mexico, DOE-WIPP-86-006.

UHLAND D. W., RANDALL W. S. and CARRASCO R. C. (1987) 1987 annual water quality data report for the Waste Isolation Pilot Plant. Engineering and Repository Technology, Westinghouse Electric Corp., Carlsbad, New Mexico, DOE-WIPP-87-006.

WHITE D. E., HEM J. D. and WARING G. A. (1963) Chemical composition of subsurface waters. In *Data of Geochemistry* [6th edition]. (ed M. FLEISCHER), U.S. Geol. Surv. Prof. Paper 440-F.

ZHEREBTSOVA I. K. and VOLKOVA N. N. (1966) Experimental study of behavior of trace elements in the process of natural solar evaporation of Black Sea water and Sasyk-Sivash brine. *Geochem. Int.* **3,** 656–670.